



In the quest of the optimal collagen type II source for articular cartilage engineering

**A thesis submitted to the National University of Ireland Galway for the degree of
Doctor of Philosophy**

By

Zhuning Wu

Research Supervisor: Prof. Dimitrios I. Zeugolis

August 2021

**Regenerative, Modular & Developmental Engineering Laboratory, REMODEL
Science Foundation Ireland Centre for Research in Medical Devices, SFI CÚRAM
National University of Ireland Galway, NUI Galway, Galway, Ireland**

Table of contents

Table of contents	II
Table of figures	VIII
Table of tables	X
Plagiarism statement	XI
List of abbreviations	XII
Acknowledgements	XVI
Abstract	XVII
Chapter 1 - Introduction	1
1.1. Introduction	2
1.2. Cartilage development, cellular and extracellular composition and organisation.....	3
1.3. Collagen type II biosynthesis, extraction and synthesis via recombinant technologies	10
1.4. Collagen type II scaffolds in cartilage engineering	13
1.5. Project phases and hypotheses	25
1.6. References	27
Chapter 2 – In the quest of the optimal tissue source (porcine male and female articular, tracheal and auricular cartilage) for the development of collagen sponges for articular cartilage	56
2.1. Introduction	57
2.2. Materials and Methods	59
2.2.1. Materials	59
2.2.2. Type II collagen isolation	59
2.2.3. Sodium dodecyl sulphate poly-acrylamide gel electrophoresis	60

2.2.4. Collagen crosslinking and scaffold fabrication	60
2.2.5. Ultrastructural assessment	61
2.2.6. Biomechanical assessment.....	61
2.2.7. Denaturation temperature assessment.....	62
2.2.8. Free amines assessment	62
2.2.9. Resistance to enzymatic degradation assessment	62
2.2.10. Cell culture.....	63
2.2.11. Cell viability assessment	64
2.2.12. Cell proliferation assessment.....	64
2.2.13. Cell metabolic activity assessment	64
2.2.14. Sulphated glycosaminoglycan assessment	65
2.2.15. Histology assessment.....	65
2.2.16. RNA isolation	66
2.2.17. Quantitative real-time PCR	67
2.2.18. Statistical analysis.....	71
2.3. Results.....	72
2.3.1. Purity assessment.....	72
2.3.2. Ultrastructural assessment	74
2.3.3. Biomechanical assessment.....	77
2.3.4. Thermal properties assessment	77
2.3.5. Free amines assessment	77
2.3.6. Resistance to enzymatic degradation assessment	80
2.3.7. Basic cellular function assessment	82
2.3.8. Chondrogenic potential assessment.....	85
2.4. Discussion	91
2.5. Conclusions.....	96
2.6. References	97
Chapter 3 – In the quest of the optimal chondrichthyan for the development of collagen sponges for articular cartilage	109
3.1. Introduction.....	110
3.2. Materials and Methods.....	112

3.2.1. Materials	112
3.2.2. Collagen type II extraction and purification	112
3.2.3. Sodium dodecyl sulphate poly-acrylamide gel electrophoresis	113
3.2.4. Scaffold fabrication and physicochemical properties assessment ..	113
3.2.5. Ultrastructural assessment	114
3.2.6. Biomechanical assessment.....	114
3.2.7. Denaturation temperature assessment.....	115
3.2.8. Free amine content assessment.....	115
3.2.9. Resistance to enzymatic degradation assessment	115
3.2.10. Cell culture and scaffolds' basic cellular function assessment.....	116
3.2.11. Cell viability assessment	117
3.2.12. Cell proliferation assessment.....	117
3.2.13. Cell metabolic activity assessment	117
3.2.14. Histology assessment.....	118
3.2.15. Scaffolds' chondrogenic potential assessment (sulphated glycosaminoglycan assessment)	118
3.2.16. Scaffolds' chondrogenic potential assessment (gene expression assessment)	119
3.2.17. Statistical analysis.....	123
3.3. Results	124
3.3.1. Collagen preparations purity assessment.....	124
3.3.2. Scaffolds' physicochemical properties assessment	125
3.3.3. Scaffolds' chondrogenic potential assessment	133
3.4. Discussion	137
3.5. Conclusions.....	141
3.6. References	142
Chapter 4 – The influence of bloom index, endotoxin levels and polyethylene glycol succinimidyl glutarate crosslinking on the physicochemical and biological properties of gelatin biomaterials.....	150
4.1. Introduction.....	151
4.2. Materials and Methods.....	153

4.2.1. Materials	153
4.2.2. Purity assessment.....	155
4.2.3. Fabrication and crosslinking of gelatin hydrogels and films.....	155
4.2.4. Biomechanical assessment.....	155
4.2.5. Free amines assessment	156
4.2.6. Resistance to enzymatic degradation assessment	156
4.2.7. Cell culture.....	157
4.2.8. Cell viability assessment	157
4.2.9. Cell proliferation assessment.....	157
4.2.10. Cell metabolic activity assessment	158
4.2.11. Cell morphology assessment	158
4.2.12. Statistical analysis.....	158
4.3. Results.....	160
4.3.1. Purity assessment.....	160
4.3.2. Biomechanical and free amine assessment.....	161
4.3.3. Resistance to enzymatic degradation assessment	163
4.3.4. Macrophage viability, proliferation and metabolic activity assessment.....	165
4.3.5. Macrophage morphology assessment	167
4.4. Discussion	168
4.5. Conclusions	170
4.6. References	171
Chapter 5 – Conclusions and future studies.....	178
5.1. Conclusions.....	179
5.2. Future studies	180
5.2.1. Engineering and assessing an optimally functionalised collagen type II sponge	180
5.2.2. Engineering and assessing an optimally functionalised gelatin material	180
5.3. References	181
Appendices: protocols and research outputs.....	184

A.	Protocols	185
A.1.	Collagen type II isolation	188
A.2.	Collagen sponge fabrication and crosslinking	189
A.3.	Gelatin hydrogel fabrication and crosslinking	190
A.4.	Gelatin film fabrication and crosslinking.....	190
A.5.	Sodium dodecyl sulphate-polyacrylamide gel electrophoresis	191
A.6.	Silver staining of SDS-PAGE gels.....	195
A.7.	TNBSA assay	196
A.8.	Collagenase	197
A.9.	Scanning electron microscopy (SEM)	198
A.10.	Denaturation temperature assessment.....	198
A.11.	Biomechanical assessment – Compression test	199
A.12.	Cell thawing and expansion, freezing (human adipose derived stem cells)	200
A.13.	Cell seeding and differentiation in collagen sponges (human adipose derived stem cells)	201
A.14.	Cell expansion and differentiation (human THP-1 monocytes)	202
A.15.	Cell metabolic activity assay using alamarBlue™	203
A.16.	Cell proliferation assay using Quant-it™ Picogreen®	204
A.17.	Cell viability assay using Live/Dead staining.....	206
A.18.	Fixation and embedding of collagen sponges	206
A.19.	Alcian blue staining	207
A.20.	Haematoxylin & Eosin staining	208
A.21.	Sulphated glycosaminoglycan (sGAG) assessment.....	209
A.22.	RNA isolation	210
A.23.	cDNA synthesis.....	212

A.24. Quantitative real-time PCR.....	213
B. Research outputs	215
B.1. Published manuscripts.....	215
B.2. Submitted manuscripts	216
B.3. Book chapters	216
B.4. Conferences podium presentations.....	216
B.5. Conferences poster presentations	217

Table of figures

Figure 1.1: Sequential stem cell differentiation to chondrocytes and associated ECM changes (A). Chondrocyte secreted ECM and interactions (B). Chondrocyte cellular (left) and extracellular (right) organisation (C).....	5
Figure 1.2: Genomic structure and subdomain organisation of the exons coding for the N-propeptide of the collagen type I, II and III.	7
Figure 1.3: Collagen type II extraction flow chart from cartilage tissues and electrophoretic mobility of collagen type I and collagen type II	12
Figure 2.1: SDS-PAGE analysis of collagen preparations extracted from porcine cartilage tissues.	72
Figure 2.2: SEM and complementary pore size (μm) and porosity (%) analyses of the produced scaffolds.	75
Figure 2.3: Resistance to collagenase digestion analysis of the produced scaffolds.	81
Figure 2.4: hADSC viability (A), DNA concentration (B), metabolic activity (C) and infiltration and ECM synthesis (D) as a function of tissue and biological sex for up to 21 days in culture (longest timepoint assessed).	84
Figure 2.5: Alcian blue staining (A) and sGAG quantification (B) analyses as a function of tissue and biological sex for up to 21 days in culture.	86
Figure 2.6: Gene expression analysis after 21 days of chondrogenic induction.	89
Figure 3.1: SDS-PAGE analysis of collagen preparations extracted from the chondrichthyes.	124
Figure 3.2: Morphology, pore size and % porosity analyses of the produced scaffolds as a function of fish species and crosslinking.....	126
Figure 3.3: Resistance to collagenase digestion analysis of the produced scaffolds as a function of fish species and crosslinking.....	129
Figure 3.4: hADSC viability (a), DNA concentration (b), metabolic activity (c) and infiltration and ECM synthesis (d) as a function of fish species for up to 21 days in culture.	131

Figure 3.5: Alcian blue staining (**a**) and sGAG quantification (**b**) as a function of fish species for up to 21 days in culture.134

Figure 3.6: Gene expression analysis after 21 days as a function of fish species.136

Figure 4.1: SDS-PAGE analysis of gelatin samples used in this study.....160

Figure 4.2: Resistance to enzymatic degradation analysis of non-crosslinked (-PEG-4SG) and crosslinked (+PEG-4SG) gelatin samples used in this study..164

Figure 4.3: Macrophage viability (**A, B**), DNA concentration (**C**) and metabolic activity (**D**) analyses.166

Figure 4.4: Macrophage morphology (**A**) and cell number (**B**) analyses.167

Table of tables

Table 1.1: Indicative examples of mammalian, marine and recombinant collagen type II scaffolds that have been shown to maintain and/or induce chondrogenic phenotype <i>in vitro</i>	15
Table 1.2: Indicative examples of mammalian, marine and recombinant collagen type II scaffolds in preclinical models.	20
Table 2.1: Genes and their primer 1 (forward), probe, and primer 2 (reverse) sequences.	68
Table 2.2: Mechanical properties, denaturation temperature and free amine content of the produced scaffolds as a function of tissue, biological sex and crosslinking.	78
Table 3.1: Genes and their primer 1 (forward), probe, and primer 2 (reverse) sequences.	121
Table 3.2: Mechanical properties, denaturation temperature and free amine content of the produced scaffolds as a function of fish species and crosslinking.	128
Table 4.1: Properties of gelatin samples used in this study.	154
Table 4.2: Mechanical properties and free amine content of non-crosslinked (-PEG-4SG) and crosslinked (+PEG-4SG) gelatin samples used in this study..	162
Table A.1: List of reagents and respective suppliers	185
Table A.2: 5 % separating gel for 1mm thickness mini gel (Protean II Bio-Rad).	194
Table A.3: 3 % stacking gel for 1mm thickness mini gel (Protean II Bio-Rad).	194
Table A.4: Silver staining method step by step. Volumes are indicated per gel.	195
Table A.5: Detailed preparation of the DNA standard curve.....	205
Table A.6: Reaction setup for a single cDNA synthesis reaction.	212
Table A.7: TaqMan® Gene Expression MasterMasterMix setup for a 15 µl qPCR run.....	215

Plagiarism statement

I certify that this thesis is all my own work and I have not obtained a degree in this University or elsewhere on the basis of this work.

Zhuning Wu

List of abbreviations

µg: microgram

µm: micrometre

µl: microliter

-PEG-4SG: no crosslinked groups

+PEG-4SG: crosslinked groups

ADSC: adipose derived stem cell

APS: ammonium persulphate

ACAN: aggrecan

ADAMTS: a disintegrin and metalloproteinase with thrombospondin motifs

alpha-MEM: alpha Minimum Essential Medium

BSA: bovine serum albumin

BMP: bone morphogenetic protein

BMSC: bone marrow stem cell

BR: blonde ray

COL1A1: collagen type I α 1

COL2A1: collagen type II α 1

COL3A1: collagen type III α 1

COL10A1: collagen type X α 1

COMP: cartilage oligomeric matrix protein

CS: chondroitin sulphate

CaCl₂: calcium chloride

CR: cuckoo ray

CCL2: monocyte chemoattractant protein-1 ?

D: day

DMEM: Dulbecco's modified Eagle's medium

DMSO: dimethyl sulfoxide

DNA: deoxyribonucleic acid

DPX: distyrene-dibutyl phthalate-xylene

DSC: differential scanning calorimeter

ECM: extracellular matrix

EDTA: ethylenediaminetetraacetic acid

EDC-NHS: 1-ethyl-3-(3-dimethylaminopropyl) carbodiimide-sulfo-N-hydroxy-succinimide

EIF2B1: eukaryotic translation initiation factor 2B subunit alpha

FARC: female articular cartilage

FTRC: female tracheal cartilage

FAUC: female auricular cartilage

FBS: foetal bovine serum

FGF: fibroblast growth factor

FDA: food and drug administration

FITC: fluorescein isothiocyanate

GAG: Glycosaminoglycan

GUSB: glucuronidase beta

HA: hyaluronan

HBSS: Hanks' balanced salt solution

H&E: haematoxylin and eosin

HPRT1: hypoxanthine phosphoribosyltransferase 1

HCl: hydrogen chloride

ITS: insulin-transferrin-selenium

IGF-1: insulin-like growth factor-1

IL6: interleukin-6

LSD: lesser spotted dogfish

MARC: male articular cartilage

MTRC: male tracheal cartilage

MAUC: male auricular cartilage

MMP: matrix metalloproteinase

M: mole

mRNA: messenger RNA

mm: millimeter

mg: milligram

NC4: non-collagenous domainsxxxx

NaOH: sodium hydroxide

NaCl: sodium chloride

N: newton

NRQs: normalised relative quantities

OA: osteoarthritis

OCT: optimal cutting temperature

PBS: phosphate buffered saline

PFA: paraformaldehyde

PG: proteoglycan

PEG-4SG: polyethylene glycol succinimidyl glutarate

PMA: phorbol 12-myristate 13-acetate

PUM1: pumilio homolog 1

RNA: ribonucleic acid

RUNX2: runt-related transcription factor 2

RT-PCR: real-time polymerase chain reaction

RPLP0: ribosomal protein lateral stalk subunit P0

RPMI-1640: Rosewell Park Memorial Institute 1640 medium

SDS-PAGE: Sodium dodecyl sulphate polyacrylamide gel electrophoresis

SEM: scanning electron microscopy

SOX9: SRY-box 9

STD I: Standard collagen type I

STD II: Standard collagen type II

TCP: tissue culture plastic

TEMED: tetramethylethylenediamine

TGF- β : transforming growth factor- β

TBR: thorn back ray

TNBSA: 2,4,6-trinitrobenzene sulfonic acid

TBP: TATA-box binding protein

THP-1: human-derived leukemic monocyte cells

V: volt

Acknowledgements

First of all, I would like to express my sincere gratitude to my esteemed supervisor, Prof. Dimitrios Zeugolis, for giving me the opportunity to work in his lab and for his valuable supervision, patience, support and encouragement during my PhD study. I have learned so much from you, not only research skills but also communication strategy. It has been a precious experience to work with you.

I would like to acknowledge Dr. Anne Maria Mullen and Teagasc Walsh Fellowship (grant agreement No. 2014045) and the ReValueProtein Research Project (grant agreement No. 11/F/043) for the financial support.

A special thanks goes to Dr. Stefanie Korntner for her treasured support which was really influential in critiquing my experiment methods and results.

I would like to thank my Graduate Research Committee (GRC), Prof. Abhay Pandit, Dr. Manus Biggs for their support and helpful feedback over the years. I would like to thank Dr. Oliver Carrol for his technical assistance in daily laboratory work.

I would like to extend my thanks to all REMODEL members – Anna, Andrea, Christina, Diana, Dimitrios, Eugenia, Hector, Ignacio, João, Kieran, Kyriakos, Luis, Meletis, Naledi, Shubhasmin, Sofia, Stefanie, Valeria, for a cherished time spent together in the lab, and in social settings. It has been a pleasure to work with all of them. Additionally, a special thanks goes to my friend Mr. Xinyu Yang for his encouragement and help even at difficult moments.

Last but not the least, I would like to sincerely thank my parents, Weiping Zhu and Bangmin Wu, for bringing me to the world and supporting me spiritually throughout my life.

Abstract

Articular cartilage is a specialised connective tissue of joints, which lacks blood vessels, lymphatics and nerves. The limited capability of articular cartilage to self-repair renders its regeneration a formidable challenge. Collagen-based biomaterials are frequently used in cartilage engineering, however, most of them are focused on collagen type I scaffolds. In the quest of the ideal material for scaffold fabrication for cartilage engineering, the use of collagen type II has been advocated, as it is the major constituent of cartilage tissue. However, its optimal source still remains elusive.

In the first phase of this thesis, we ventured to assess the influence of biological sex (male, female) and tissue (articular, tracheal, auricular) on the biophysical, biochemical and biological properties of pepsin extracted porcine collagen type II sponges. Articular cartilage resulted in pure collagen type II preparations, whilst tracheal and auricular cartilage preparations were contaminated with collagen type I. Pore size, porosity and denaturation temperature were not affected ($p > 0.05$) as a function of tissue and biological sex. Articular cartilage derived sponges exhibited significantly ($p < 0.05$) higher resistance to enzymatic degradation and biomechanical properties in comparison to tracheal and auricular cartilage sponges. Biological analysis using human adipose derived stem cells revealed no significant ($p > 0.05$) differences between the groups in cell viability, DNA concentration, metabolic activity and Alcian blue staining. The articular cartilage groups induced the highest ($p < 0.05$) sulphated glycosaminoglycans synthesis, and aggrecan and collagen type II mRNA expression (fold change ≥ 2.0). Our data indicate a tissue memory of collagen type II and indicate that for cartilage engineering, articular cartilage derived collagen type II scaffolds may be more suitable for effective chondrogenesis.

In the second phase of this thesis, the extensive use of antibiotics, religious tenets and the potential for interspecies disease transmission may restrict the use of mammalian derived collagens. In this regard, marine species derived collagen offers an opportunity as a safe, sustainable and environmentally friendly alternative to mammalian species derived collagen. Thus, herein it is

hypothesised that there is an optimal chondrichthyan (cartilaginous fish) species [lesser spotted dogfish (*Scyliorhinus canicula*), thorn back ray (*Raja clavata*), cuckoo ray (*Leucoraja naevus*) and blonde ray (*Raja brachyuran*)] for pure collagen type II extraction and maximum chondrogenic induction of human adipose derived stem cells. Pure collagen type II preparations were obtained from all four Chondrichthyes, as revealed by gel electrophoresis. Pore size, porosity, denaturation temperature, resistance to enzymatic degradation and mechanical properties of the produced sponges were not significantly ($p > 0.05$) affected as a function of species. Biological analysis using human adipose derived stem cells revealed no significant ($p > 0.05$) differences between the groups in cell viability, DNA concentration, metabolic activity, Alcian blue staining and sulphated glycosaminoglycans synthesis. Human adipose derived stem cells seeded on fish-derived scaffolds expressed lower mRNA levels of COL1A1 (fold change ≥ 2.0) and COL3A1 (apart from lesser spotted dogfish; fold change < 2.0) and higher mRNA levels of COL10A1 (fold change ≥ 2.0), COMP (fold change ≥ 2.0), SOX9 (fold change ≥ 2.0), and ACAN (apart from cuckoo ray; fold change < 2.0) than cells grown on tissue culture plastic (TCP). Our data suggest that chondrichthyes derived collagen type II has the potential to be used in cartilage engineering.

In the third phase of this thesis, bloom index and residual endotoxins in gelatin preparations were investigated, as they are crucial regulators of the product's physicochemical and biological properties. Herein, gelatin preparations with variable bloom index and endotoxin level were used to fabricate crosslinked gelatin scaffolds, the physicochemical and biological properties of which were subsequently assessed. Gelatin preparations with low bloom index resulted in hydrogels with significantly lower compression stress ($p < 0.05$), elastic modulus ($p < 0.05$) and resistance to enzymatic degradation ($p < 0.05$) and higher free amine content ($p < 0.05$) than gelatin preparations with high bloom index. Gelatin preparations with high endotoxin levels resulted in films that induced significantly ($p < 0.05$) higher macrophage fusion than gelatin preparations with

low endotoxin level. For various reasons, the chondrogenic potential of gelatin preparations was not assessed.

Chapter 1 - Introduction

This chapter has been submitted for publication:

Collagen type II: From biosynthesis to advanced biomaterials for cartilage engineering

Z Wu, SH Korntner, AM Mullen, DI Zeugolis. Submitted to Biomaterials and Biosystems

Authors' contribution: Z.W. wrote the manuscript; S.H.K. reviewed and commented the manuscript; A.M.M. provided the funding; D.I.Z. contributed the concept, reviewed and edited the manuscript, provided the funding; all authors reviewed and approved the manuscript.

1.1. Introduction

Articular cartilage is a specialised connective tissue of the joints (1, 2). Hyaline cartilage provides a smooth and lubricated surface for articulation and facilitates the transmission of loads with low frictional coefficient (3, 4). As articular cartilage lacks blood vessels, lymphatics and nerves, it has limited capacity for intrinsic healing and repair (5, 6). Articular cartilage injuries are frequently caused by sports and recreational activities and, if left untreated, articular cartilage lesions form fibrocartilage and lead to osteoarthritis (OA).

OA is a whole joint disease, involving structural alterations in the hyaline articular cartilage, subchondral bone, ligaments, capsule synovium and periarticular muscles (7). OA affects over 250 million people worldwide (8) and financially drains healthcare systems. For example, medical costs account for 1.0 % to 2.5 % of gross domestic product of high-income countries (9) and in USA alone, the annual insurer spending for OA-related medical care is estimated to be US\$ 185.5 billion (10). OA, due to the imbalance between the repair and the damage of joint cartilage, leads to structural destruction and failure of the synovial joint (11). The pathogenesis of OA involves compositional changes and structural / integrity losses of cartilage (12). Initially, disruption, caused by physical forces, happens at the cartilage surface and is followed by the expansion of the calcified zone into the radial zone. Then, the hypertrophic chondrocytes synthesise extracellular matrix (ECM) degradation products and proinflammatory mediators. Subsequently, the bone turnover is increased in the subchondral bone and vascular invasion takes place towards the cartilage region (13). Clinically, the knee, hip, hand, spine and foot are the most common sites of OA, followed by the wrists, shoulders and ankles (14). OA incidents gradually increase over the years, due to the combined effects of ageing, obesity and heavy work activities (15-17). In fact, by 2032, the proportion of the population aged >45 with any doctor-diagnosed OA is estimated to increase from 26.6 % to 29.5 % (18). OA is more prevalent in women than in men, with female-to-male ratio ranging from 1.5 to 4.0 (19). Exercise, weight loss (in the case of overweight patients) and walking aids are widely recommended to improve daily activities

of OA patients (20, 21). Pharmacological agents (22-29), surgical procedures (30-33) and advanced therapy medicinal products (34-37) have shown variable degree of efficiency and effectiveness, considering their complexity, cost of goods and regulatory hurdles. To this end, biomaterial-based therapies are continuously gaining pace, especially for large defects (38-41).

Herein, we provide a brief description of cartilage's development, cellular and extracellular composition and organisation and then focus on collagen type II biosynthesis, extraction protocols, scaffold fabrication and *in vitro*, *in vivo* data, in light of recent studies that demonstrate the inability of collagen type I scaffolds to yield functional therapeutic outcomes (42, 43).

1.2. Cartilage development, cellular and extracellular composition and organisation

Cartilage morphogenesis (44-48) is a complex and well-orchestrated sequence of numerous intracellular and extracellular spatiotemporal events, responsible for the tissue composition and structure (**Figure 1.1**). Articular cartilage and long bones are formed by endochondral ossification that is initiated from the lateral growth plate that contains mesenchymal stem cells that secrete hyaluronan and collagen type I. As these stem cells move towards the centre of the limb, they aggregate; stop proliferating and expressing collagen type I; and start expressing N-cadherin, tenascin-C and cell adhesion molecules. Formation of tight aggregates marks the start of the condensation processes that involves stem cell aggregation and increased hyaluronidase activity that in turn decreases hyaluronan and cell movement and increases cell-cell interactions. These increased cell-cell interactions trigger signalling pathways responsible for the initiation of chondrogenic differentiation. An array of small proteoglycans (PGs, e.g. versican, perlecan), growth factors (e.g. fibroblast growth factors, FGF; bone morphogenetic proteins, BMPs; transforming growth factor- β , TGF- β), transcription factors (e.g. Sox5, Sox6, Sox9), signalling molecules (e.g. sonic hedgehog, Indian hedgehog) and ECM molecules (e.g. matrilins, fibronectin)

contribute in chondrogenic differentiation and cartilage formation. Subsequently, the cells cease the expression of adhesion molecules, resume proliferation via action of growth hormone, parathyroid hormone-related peptide and insulin-like growth factor-1 (IGF-1), initiate ECM synthesis (e.g. collagen types II, IX, X and XI; aggrecan; decorin; annexin II, V and VI; tenascins; thrombospondins; cartilage oligomeric matrix protein) and decrease production of fibronectin. A series of maturation steps then takes place for the differentiation of committed chondrocytes to pre-hypertrophic, hypertrophic and matrix-mineralising chondrocytes. Hypertrophic chondrocytes increase in size, start to synthesise calcified matrix rich in collagen type X and alkaline phosphatase, synthesise an array of terminal differentiation molecules (e.g. matrix metalloproteinase-13; Runx2, Runx3, BMP-6, BMP-2, BMP-7, aggrecan, hyaluronan) and cease to synthesise others (e.g. Sox9, collagen type II).

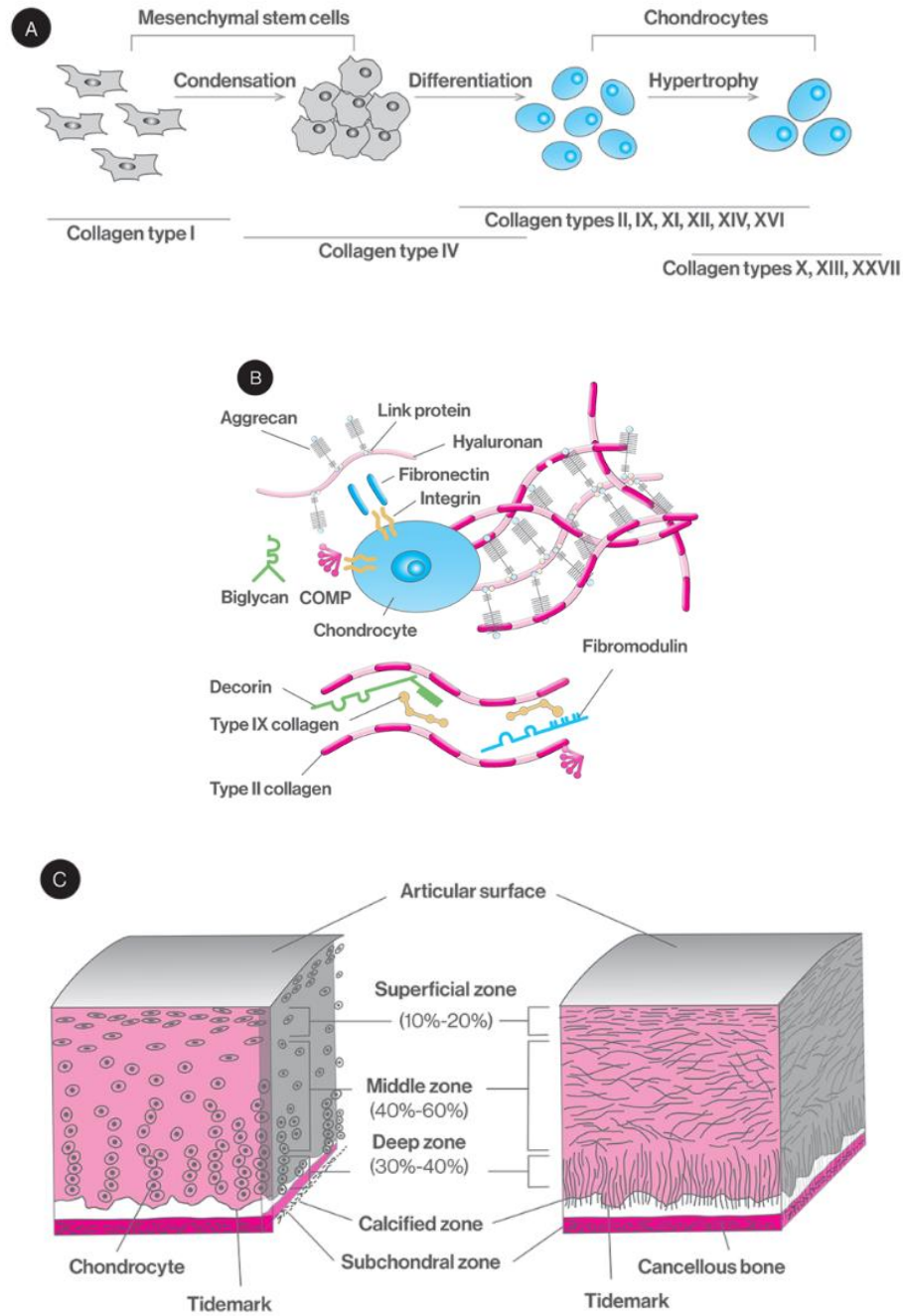


Figure 1.1: Sequential stem cell differentiation to chondrocytes and associated ECM changes (A). Chondrocyte secreted ECM and interactions (B). Chondrocyte cellular (left) and extracellular (right) organisation (C).

Articular cartilage contains a highly specialised cell population, the chondrocytes, which is responsible for the production, organisation and maintenance of the cartilage ECM (49, 50). It also contains a small number of mesenchymal progenitor cells, the number of which increases in osteoarthritic articular cartilage (51, 52). A diverse range of collagen types are encountered in cartilage with distinct functions (53-56). For example, collagen type II is the predominant component of the cartilage ECM, forms a fibrillar network primarily responsible for the mechanical integrity of the tissue and plays a significant role in chondrocyte differentiation and hypertrophy during normal cartilage development and OA pathogenesis (57, 58). Loss of collagen type II has been shown to accelerate chondrocyte hypertrophy and OA progression, through the BMP-SMAD1 pathway (59). Collagen type III is extensively crosslinked to collagen type II and regulates collagen fibrillar structure and biomechanics in cartilage tissue (60, 61). Collagen type VI is expressed in both healthy and OA cartilage tissues, is the major component of the chondrocyte pericellular matrix and enhances cartilage regeneration via stimulation of chondrocyte proliferation (62, 63). Collagen type IX covalently crosslinks to collagen type II with the collagenous (called COL3) and the non-collagenous (called NC4) domains of the molecules projecting at periodic distances away from the surface of the fibril. These projections allow it to interact with numerous components of cartilage tissue (e.g. cartilage oligomeric protein, heparin, fibromodulin), ultimately stabilising and organising the fibrillar collagen network in cartilage (64-68). Collagen type X is a short chain, non-fibril-forming collagen, primarily synthesised by hypertrophic chondrocytes, that enables endochondral ossification by regulating matrix mineralisation and is essential for mesenchymal stem cell cartilage formation and endochondral ossification (69-73). Collagen type XI interacts with various cartilage components (e.g. collagen type II, collagen type IX, perlecan, heparan sulphate) to form a meshwork that provides cartilage matrix stabilisation, mechanical resilience and homeostasis. The ratio of collagen type XI to collagen type II regulates fibre diameter, with thick fibres having more collagen type II (74-77).

Collagen type II is a homotrimer, composed of $\alpha 1(\text{II})$ chains. The human collagen type II gene is formed by 54 exons (78). The triple-helical domain consists of an uninterrupted sequence of 1014 amino acids that are coded by 44 exons. The N-propeptide domain of collagen type II is composed of 8 exons, as opposed to the 6 exons of that of collagen type I [$\alpha 1(\text{I})$ and $\alpha 2(\text{I})$] (79) and 5 exons for collagen type III [$\alpha 1(\text{III})$] (**Figure 1.2**) (80). The first exon mostly codes for the signal peptide and the second exon codes for a cysteine-rich globular domain. Exons 3-7 code for the triple-helical domain which contains 24 Gly-X-Y repeats, and the eighth exon codes for the N-telopeptide and part of the triple-helical domain (81, 82). The last four exons code for the C-propeptide domain, which facilitates the assembly of the triple helical structure for the alignment of collagen molecules.

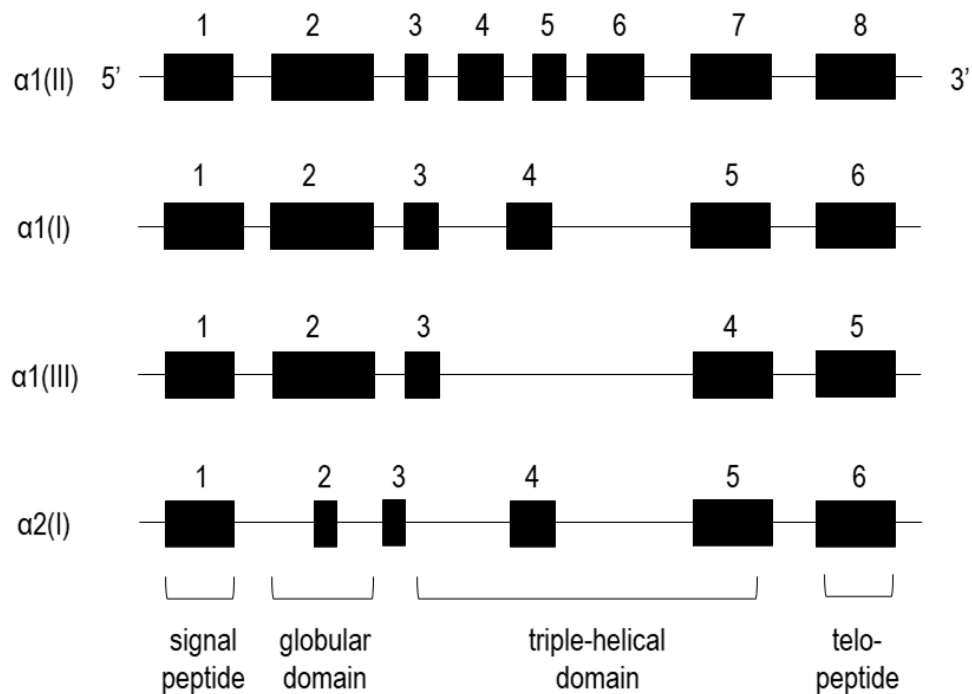


Figure 1.2: Genomic structure and subdomain organisation of the exons coding for the N-propeptide of the collagen type I, II and III. Exons (shaded boxes) are drawn approximately to scale, whereas the introns (lines) do not appear to scale.

Articular cartilage also contains a variety of PGs (e.g. aggrecan, decorin, biglycan and fibromodulin) and glycosaminoglycans (GAGs, e.g. chondroitin

sulphate, keratan sulphate and hyaluronan) that represent ~ 10 % of tissue dry weight, subject to age and disease state. PGs and GAGs play significant role in both normal tissue function and arthritis manifestation and progression (83-94). Indeed, physiological PGs and GAGs synthesis and composition contribute towards normal cartilage function and properties; control the release and protect against proteolysis of bounded cytokines, chemokines and growth factors; and modulate various signalling cascades that facilitate cell attachment and motility and cell-cell and cell-ECM interactions. For example, under physiological conditions, the major PG found in cartilage is aggrecan that interacts with hyaluronan to occupy the interfibrillar space of the cartilage ECM and provide cartilage with its osmotic properties to resist compressive loads (95). On the other hand, in arthritis, PGs and GAGs are significantly degraded by matrix metalloproteinases and their breakdown products are released into synovial fluid, eliciting an inflammatory response (96-98). Overall, ECM synthesis and degradation are regulated by the change of chondrocyte proliferation and metabolism under normal and OA conditions (99-103); the effect of hormones (104-106) and growth factors (107-109); aging (110-112); oxygen tension (113-116); and mechanical loading (117-121).

In osteoarthritic cartilage, collagen type I is increasingly synthesised along with the progression of the disease. Collagen type I and collagen type II are both fibril-forming collagens, most collagen type I is composed of $\alpha 1(I)_2$ and $\alpha 2(I)$ chains and mainly found in skin, tendon, cornea, bone and osteoarthritic cartilage. Collagen type II is composed of $\alpha 1(II)_3$ and mainly found in healthy cartilage, intervertebral disc and vitreous (122). They both present triple helices with uninterrupted Gly-X-Y structures ~ 300 nm in length (123). In general, collagen type I is associated with structural fibrils greater than 100 nm in diameter, apart from thin collagen type I fibrils found in cornea, which are lower than 30 nm in diameter; collagen type II is associated with fibrils between 10 and 30 nm in diameter and is oriented randomly in the proteoglycan matrix (124). Additionally, it has been demonstrated that collagen type II possessed lower intrinsic turbidity values and fewer free carboxylic groups than collagen type I (125). Moreover,

collagen type I has only one or two glycosylated hydroxylysine per α chain, collagen type II has around 10 glycosylated hydroxylysine per α chain (126, 127). Therefore, collagen type II chains contain a higher content of hydroxylysine as well as glucosyl and galactosyl residues which mediate the interaction with PGs to form a network-like supramolecular arrangement in cartilage. The deficiency of collagen type II results in a series of disorders, including achondrogenesis type II, hypochondrogenesis, spondyloepiphyseal dysplasia congenital, Stickler Syndrome and osteoarthritis (128). A direct correlation between the ratio of collagen type I to collagen type II in cartilage and the clinical severity of the disorder has been demonstrated, indicating that higher level of collagen type I is present in disease with more severity.

Structurally speaking, articular cartilage is divided into the superficial, transitional, radial and calcified zones from the joint surface to the subchondral bone, with distinct composition and architectural features (129-132). The superficial zone is the gliding surface of the joint; contains high concentration of collagen and low concentration of PGs; and adjoins a layer of elongated chondrocytes organised parallel to the articular surface. The transitional zone contains collagen fibres larger than those in the superficial zone, which are arranged randomly within this zone; is composed of spheroid-shaped chondrocytes; and has higher concentration of PGs compared to the superficial zone. The radial zone contains the largest collagen fibres, which are organised in a columnar pattern, perpendicularly to the joint surface; has the lowest concentration of chondrocytes; and has high PG content. Between the radial and the calcified zone, there is a wavy and irregular line, termed tidemark, that prevents the collagen fibres from being sheared of anchorage to the calcified zone. The calcified zone separates the radial zone of cartilage from subchondral bone ensuring a cohesive connection between them; has no PGs; and contains spheroid-shaped chondrocytes, which present a hypertrophic phenotype and synthesise collagen type X.

1.3. Collagen type II biosynthesis, extraction and synthesis via recombinant technologies

Collagen type II exhibits a triple stranded, coiled rod-like structure, is expressed as a homotrimer (i.e. $[\alpha 1(\text{II})]_3$) and is synthesised exclusively by chondrocytes (133, 134). During synthesis, the procollagen chains undergo proline and lysine hydroxylation by prolyl-3-hydroxylase, prolyl-4-hydroxylase and lysyl hydroxylase (135). The modification of proline and lysine hydroxylation requires ascorbic acid, iron and 2-oxo-glutarate. These steps occur prior to the formation of the triple helical structure as hydroxyproline is critical for the stabilisation of the collagen triple helix. Prolyl-4-hydroxylase triggers protein disulphide-isomerase activity, which leads to the formation of the collagen triple helix in the endoplasmic reticulum, as the association of collagen chains requires correct disulphide bond formation in the C-propeptide region of procollagen. Lysyl hydroxylase catalyses the hydroxylation of proline and lysine at both helical and non-helical regions of procollagen polypeptide chains. Moreover, some of the hydroxylysine residues then undergo glycosylation mediated by hydroxylysyl galactosyltransferase and galactosylhydroxylysyl glucosyltransferase (136, 137). Procollagen processing and crosslinking occurs in the extracellular space. The C-terminal and N-terminal non-helical propeptides of secreted procollagen molecules are removed by procollagen C-proteinases and members of the ADAMTS (a disintegrin and metalloproteinase with thrombospondin motifs) family of proteases (N-proteinases). Consequently, the removal of propeptides results in a decreased solubility of procollagen molecules, which assemble into a collagen triple helical structure with a higher organisation. Subsequent intra- and inter- molecular crosslinking enables the formation of insoluble and closely packed fibrils, able to withhold mechanical loads (138, 139).

Collagen type II is usually degraded by matrix metalloproteinases (MMP) and cysteine proteases secreted by the chondrocytes and the synoviocytes (140). MMP13 is one of the major enzymes associated with the increased collagen type II degradation in osteoarthritis. Additionally, cysteine proteases, cathepsin K and cathepsin S, also contribute to cartilage destruction with efficient capability in

degrading collagen and aggrecan, thereby destroying the integrity of cartilage network (141, 142).

Over the years, various tissues have been used and extraction protocols have been proposed to obtain collagen type II, albeit with variable degree of efficiency with respect to purity, from terrestrial and marine species. From the terrestrial species, bovine (143, 144), porcine (145) and chicken (146, 147) tissues are preferred for collagen type II extraction. With respect to marine species, squid (148), jellyfish (149, 150), amur sturgeon (151), hoki (152) and chondrichthyes (e.g. sharks (153-155), skates (156)), a diverse group of cartilaginous fish that lack true bone and exhibit a skeleton solely comprised of unmineralized cartilage, have been used for collagen type II extraction. In general, high yield, pure collagen type II preparations are produced by acid solubilisation, pepsin digestion and repeated salt precipitation / acid solubilisation and finally dialysis methods (**Figure 1.3**). Considering though the antibiotic usage in animal breeding, religious tenets and the potential for interspecies disease transmission (157-159), recombinant collagen technologies have been developed for biomedical applications (160-162). In this frontier, cells (163-165), yeast (166) and baculovirus-silkworm (167) systems have been used to express procollagen type II. Compared with the yeast expression system, the insect cell expression system has lower background interference and facilitates post-translational processing and modification (167, 168). Nonetheless, recombinant technologies are still of low yield and are primarily utilised for niche biomedicine areas (169).

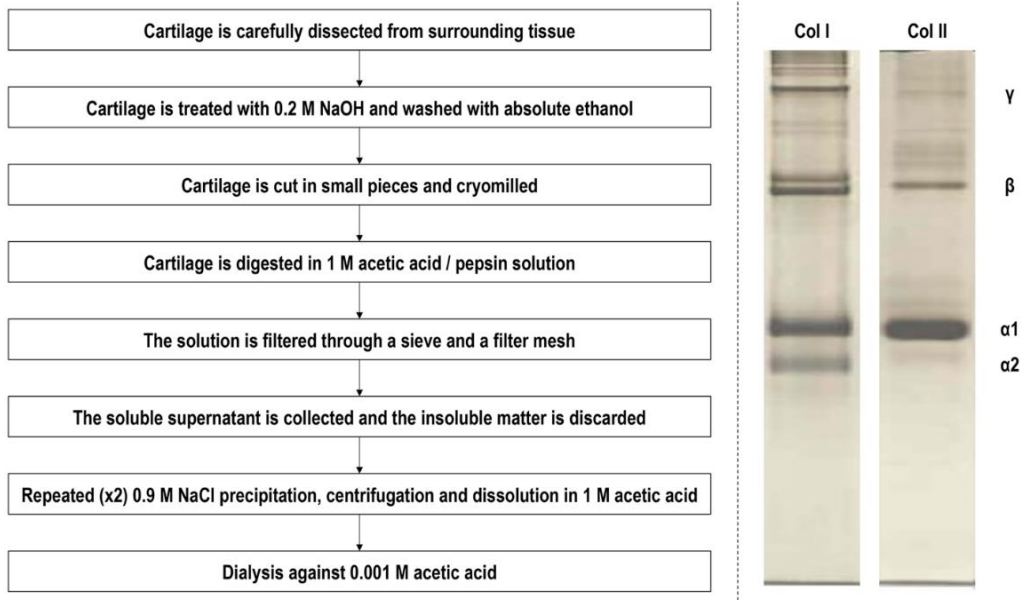


Figure 1.3: Collagen type II extraction flow chart from cartilage tissues and electrophoretic mobility of collagen type I and collagen type II (the detailed protocol can be found here (170)). Notes: As the same protocol is used to extract collagen type I (171-173), attention should be paid during dissection to remove all not cartilaginous tissues. Tissue to acetic acid / pepsin solution ratio: 1 g to 1 l. Tissue to pepsin ratio: 10 to 1 w/w. High activity pepsin (e.g. 3,200-4,500 units per mg protein) is recommended. Sieve: approximately 1,000 μm in diameter. Filter mesh: 100 μm in diameter. Centrifugation details: 20 min, 8,000 rpm, < 8 $^{\circ}\text{C}$. After the second NaCl precipitation, dissolution is conducted in minimum amount of acetic acid in order to produce a high in concentration collagen type II solution. All experiments are conducted at 4-8 $^{\circ}\text{C}$ to avoid collagen denaturation.

1.4. Collagen type II scaffolds in cartilage engineering

Mammalian, marine and recombinant collagen type II-based hydrogels and sponges (primary scaffold conformations used in cartilage engineering) have been shown to both maintain and induce chondrogenic phenotype *in vitro* (**Table 1.1**). To enhance mechanical integrity, crosslinking (e.g. poly(ethylene glycol) ether tetrasuccinimidyl glutarate (174), carbodiimide (175-177), genipin (178)) and/or blending with other polymers (e.g. polyvinyl alcohol (179), poly(L-lactide) and poly(lactide-co-glycolide) (180, 181), chitosan (182)) is traditionally employed. Although structural configurational differences between collagen type II hydrogels and sponges have been shown to induce different chondrocyte response (with respect to morphology, proliferation and gene expression), in the end, both scaffolds have been shown to stimulate comparable chondrogenesis (183). It is also worth noting that collagen type II electrospun scaffolds have also been developed (184-186), but the unavoidable denaturation of collagen prior or during the process (187, 188) has restricted their use. Advances in engineering (e.g. bioprinted collagen type II hydrogels with cell density gradient (189), alginate / collagen type II microbeads (190), hyaluronic acid / collagen type II microspheres (191)) and/or functionalisation technologies (e.g. chondroitin sulphate (192, 193), hyaluronic acid (175), glycosaminoglycan (194)) have made available elegant collagen type II scaffolds with enhanced *in vitro* chondrogenic potential. In preclinical setting, collagen type II scaffolds (with / without functional molecules and/or with / without cells) have been shown to stimulate hyaline neocartilage formation in chondral and osteochondral defects of a diverse range of animal species (**Table 1.2**).

Despite all the available data-to-date that have comprehensively shown the importance of collagen type II in chondrogenic induction or maintenance and in cartilage repair and regeneration, numerous studies still utilise collagen type I in cartilage engineering (195-198). This is surprising, as the clear superiority of collagen type II over collagen type I in cartilage engineering has been well-documented in the literature (199-202), due to a combination effect of biochemical (i.e. the lack of collagen type I and the presence of collagen type II

and other bounded cartilage-specific constituents) and biophysical (i.e. induction of round cell shape morphology, via the integrin β 1-mediated Rho A/Rock signalling pathway (203)) signals. It is also interesting to note that, to the best of our knowledge, only a handful of companies provide high purity collagen type II (e.g. porcine articular cartilage derived collagen type II, Symatase) and that no single collagen type II-based device is available, whilst numerous collagen type I devices are available for cartilage engineering (e.g. Chondro-Gide®, Geistlich Pharma AG; Novocart® Basic, TETEC AG; MeRG®, Bioteck Srl), despite the fact that collagen type I scaffolds have failed to demonstrate efficiency in healing of human osteochondral (43) and large cartilage (42) defects.

This limited technology transfer of collagen type II can be attributed to two main reasons. Firstly, we believe that commercialisation of collagen type II-based devices has been compromised by early studies that showed native collagen type II from human, chick, murine and bovine cartilage to induce inflammatory arthritis in rats (204-206) and in non-human primates (207); and antibodies of native and denatured collagen type II to be present in patients with early rheumatoid arthritis and chronic gouty arthritis (208-210). It is worth noting though that effectively crosslinked collagen type II does not induce arthritis in rats (211) and numerous studies have demonstrated collagen type II devices to promote hyaline neocartilage formation (**Table 1.2**). The second issue that may be responsible for the limited use of collagen type II in medical device development is the difficulty in producing high amounts of high purity and high yield, all in comparison to collagen type I, collagen type II preparations. Obviously, the main reason behind this is the articular cartilage tissue availability, in comparison to skin, for example, tissue. Having said, a typical cartilage defect is a lot smaller than a typical skin defect and therefore extraction of collagen type II constitutes a value for money proposition.

Table 1.1: Indicative examples of mammalian, marine and recombinant collagen type II scaffolds that have been shown to maintain and/or induce chondrogenic phenotype *in vitro*. Abbreviations: 1-ethyl-3-(3-dimethylaminopropyl) carbodiimide-sulfo-N-hydroxy-succinimide: EDC-NHS; Adipose derived stem cells: ADSCs; BMSCs: bone marrow stem cells; Cartilage oligomeric matrix protein: COMP; Chondroitin sulphate: CS; Extracellular matrix: ECM; GAG: glycosaminoglycan; Hyaluronan: HA; Matrix metalloproteinase: MMP; PG: proteoglycan

Scaffold conformation	Major findings, Reference
Bovine collagen type II, CS and HA sponges Genipin crosslinked Human chondrocytes	Chondrocytes maintained round morphology after 14 days of culture. Increased gene expression of aggrecan, collagen type II and COMP and greater accumulation of proteoglycans was seen on scaffolds with CS and HA than those without CS and HA (178)
Bovine collagen type II sponges Genipin crosslinked Human chondrocytes	The administration of GAGs to culture medium improved cell differentiation tendency to functional hyaline cartilage, as evidenced by the upregulation of GAG biosynthesis rate and gene expression of aggrecan and collagen type II after 28 days of culture (212)
Bovine collagen type II and CS sponges No crosslinker Human BMSCs	The cells produced abundant collagen type II on type II scaffolds and collagen type I on type I scaffolds, the addition of CS upregulated the gene expression of collagen type II, compared to type I and type II alone scaffolds (192)

<p>Bovine collagen type II and CS sponges</p> <p>EDC-NHS crosslinked</p> <p>Bovine chondrocytes</p>	<p>Chondrocytes maintained round morphology, the cells loaded scaffolds were surfaced with a cartilaginous-like layer, and collagen type II scaffolds contained occasionally clusters of cells inside the sponges in contrast to collagen type I sponges after 14 days of culture (213)</p>
<p>Bovine collagen type II sponges</p> <p>Ultraviolet irradiation crosslinked</p> <p>Murine chondrocytes</p>	<p>The primary chondrocytes in the scaffolds maintained chondrogenic phenotype after 3 weeks of culture. The gene expression of collagen type II, collagen type XI, and SOX9 in de-differentiated chondrocytes cultured in the scaffolds decreased when compared to that in primary chondrocytes after 4 weeks of culture (214)</p>
<p>Bovine collagen type II coated chitosan fibres</p> <p>No crosslinker</p> <p>Murine BMSCs</p>	<p>The cell number, the matrix production (dry weight, GAG quantifications), and the chondrogenic marker gene expression (aggrecan, collagen type II) were upregulated in collagen type II coated chitosan scaffolds compared to pure chitosan scaffolds and polyglycolic acid scaffolds after 21 days of culture (182)</p>
<p>Porcine collagen type II hydrogels</p> <p>No crosslinker</p> <p>Rabbit chondrocytes</p>	<p>Chondrocytes maintained chondrogenic phenotype and the cell density gradient distribution resulted in a ECM gradient distribution in the scaffolds after 3 weeks of culture (189)</p>
<p>Porcine collagen type II and CS hydrogels</p> <p>EDC-NHS crosslinked</p>	<p>Chondrocytes maintained round morphology, the collagen fibres became thicker and arranged neatly with the increase of CS in the scaffolds and displayed</p>

Rabbit chondrocytes	periodic alternation of light and shade after 7 days of culture (193)
Porcine collagen type II and GAG sheets Dehydrothermal treatment and carbodiimide crosslinked Canine chondrocytes	The addition of 5 ng/ml FGF-2 to the culture medium increased the biosynthetic activity of the cells and the accumulation of GAGs compared to the addition of 25 ng/ml FGF-2, 100 ng/ml IGF-1, 5 ng/ml FGF-2 plus 100 ng/ml IGF-1 after 2 weeks of culture (194)
Porcine collagen type II sponges EDC/NHS crosslinked Canine chondrocytes	Most of the chondrocytes were around the periphery of the sponges, the cells tend to be elongated along the periphery of the scaffolds and round inside the scaffolds. α -smooth muscle actin is present in the cytoplasm of the cells after 4 weeks of culture (215)
Porcine collagen type II sponges Ultraviolet irradiation crosslinked Canine chondrocytes	Chondrocytes maintained chondrogenic morphology and displayed less shrinkage, higher biosynthetic activity and more hyaline cartilage-like tissue formation compared to collagen type I scaffolds after 21 days of culture (216)
Porcine collagen type II and GAG sponges Ultraviolet irradiation crosslinked Canine chondrocytes	After 4 weeks of culture, a range of pore diameter from 25-257 μ m did not affect cell-mediated scaffold contraction and α -smooth muscle actin was present in the cytoplasm of the seeded chondrocytes (217)

<p>Porcine collagen type II and GAG sheets</p> <p>Dehydrothermal treatment and EDC-NHS crosslinked</p> <p>Canine chondrocytes</p>	<p>Scaffolds with low cross-link densities (dehydrothermal treatment and low EDC/NHS treatment) enhanced cell proliferation, chondrogenic maintenance and collagen type II synthesis and increased the rate of scaffold degradation compared to scaffolds with high cross-link densities (high EDC/NHS treatment) after 2 weeks of culture (218)</p>
<p>Porcine collagen type II sheets</p> <p>Dehydrothermal treatment and EDC-NHS crosslinked</p> <p>Canine chondrocytes</p>	<p>Static compressions of 50 % strain decreased the biosynthetic activity of the chondrocytes (the accumulation rate of ³H-proline-labeled protein and ³⁵S-sulfate-labeled proteoglycan over a 24-h period). Dynamic compression (3 % strain, 0.1 Hz superimposed on 10 % strain offset) upregulated protein and PG biosynthesis compared to statically compressed and uncompressed controls after 7 days of culture (219)</p>
<p>Chicken collagen type II and chondroitin sulphate sponges</p> <p>EDC-NHS crosslinked</p> <p>Rabbit chondrocytes</p>	<p>Chondrocytes maintained round morphology. The cell proliferation, the accumulation of proteoglycans and collagen type II were enhanced in collagen type II and CS scaffolds compared to pure collagen type II scaffolds after 14 days of cell culture. A cartilaginous-like layer was formed at the periphery of the scaffolds (177)</p>
<p>Chicken collagen type II hydrogels</p> <p>No crosslinker</p> <p>Rabbit chondrocytes</p>	<p>The cells in collagen type II scaffolds maintained chondrogenic phenotype and displayed increased PGs synthesis compared to the cells on polystyrene. > 50 % of the newly synthesized PGs were recovered from collagen type II scaffolds</p>

	compared to 13-16 % of those recovered from polystyrene (220)
Squid collagen type II coating No crosslinker Murine chondrocytes	Chondrocytes cultured in the conditioned medium from collagen type II treated M1 macrophages mostly maintained round morphology and displayed mild increase in the expression of MMP13, compared with those in the conditioned medium from untreated M1 macrophages (148)
Recombinant human collagen type II hydrogels No crosslinker Human BMSCs	The cells in the scaffolds displayed similar GAGs deposition and similar chondrogenic marker gene expression and upregulated gene expression of metalloproteinases compared to the high-density cell pellet after 84 days of culture (221)
Recombinant human collagen type II hydrogels No crosslinker Bovine chondrocytes	Chondrocytes maintained round morphology and the accumulation of GAGs and collagen type II increased after 4 weeks of culture. The gene expression of aggrecan and collagen type II was increased since week 1 (222)
Collagen type II (species is not mentioned) hydrogels No crosslinker Rabbit chondrocytes	The dedifferentiated auricular chondrocytes were converted to articular chondrogenic phenotype in a collagen type II coated environment after 14 days of culture. The converted auricular chondrocytes expressed similar histological and biomechanical features as articular chondrocytes in the scaffolds after 28 days of culture (223)

Table 1.2: Indicative examples of mammalian, marine and recombinant collagen type II scaffolds in preclinical models. Abbreviations: 1-ethyl-3-(3-dimethylaminopropyl) carbodiimide-sulfo-N-hydroxy-succinimide: EDC-NHS; Adipose derived stem cells: ADSCs; Bone marrow stem cells: BMSCs; Glycosaminoglycan: GAG

Scaffold conformation	Model, Major findings, Reference
Bovine collagen type II, cadherin 11 and recombinant fibronectin sponges Glutaraldehyde crosslinked Rabbit BMSCs	Rabbit chondral defect The cell loaded scaffold induced cartilage formation 12 weeks post-surgery (224)
Bovine collagen type II and chondroitin sulphate sponges Genipin crosslinked Rabbit BMSCs	Rabbit chondral defect Lacuna formation 4 weeks post-surgery and high collagen type II and aggrecan and low collagen type I gene expression 24 weeks post-surgery (225)
Bovine collagen type I and collagen type II and chondroitin sulphate sponges Carbodiimide crosslinked No cells	Rabbit chondral defect Collagen type I scaffolds attracted progenitor cells into the defect and induced fibro-cartilage repair, whilst collagen type II scaffolds attracted less cells into the defect, but the invaded cells adopted a chondrogenic phenotype and increased the amount

	of superficial cartilage-like tissue 12 weeks post-surgery (201)
<p>Bovine collagen type II hydrogels</p> <p>Pentaerythritol polyethylene glycol ether tetrasuccinimidyl glutarate crosslinked</p> <p>Rabbit chondrocytes</p>	<p>Rabbit chondral defect</p> <p>Cartilage repair was improved in cell-scaffold treated groups and collagen type I was not detected 24 weeks post-surgery (226)</p>
<p>Bovine collagen type II sponges</p> <p>Genipin crosslinked</p> <p>Rabbit BMSCs</p>	<p>Rabbit osteochondral defect</p> <p>The implanted cells became chondrocytes in the implanted area and cartilage structure, same as normal cartilage, was observed in the repair site 24 weeks post-surgery (227)</p>
<p>Porcine collagen type I, collagen type II and collagen type III blend sponges</p> <p>No crosslinker</p> <p>Autologous ovine chondrocytes</p>	<p>Ovine chondral defect</p> <p>Scaffolds with chondrocytes and with microfracture into the subchondral plate resulted in hyaline-like cartilage regeneration 16 weeks post-surgery (228)</p>
<p>Porcine collagen type II sponges</p> <p>EDC-NHS crosslinked</p> <p>Autologous chondrocytes</p>	<p>Canine chondral defect</p> <p>Scaffolds cultured with chondrocytes for 4 weeks prior implantation increased the amount of reparative hyaline cartilage tissue after 15 weeks (215)</p>

<p>Porcine collagen type II or Arg-Gly-Asp sequence with poly(L-lactide) or poly(D,L-lactide-co-glycolide) sponges</p> <p>Carbodiimide crosslinked</p> <p>Rabbit chondrocytes</p>	<p>Rabbit chondral defect</p> <p>Collagen type II prevented infiltration by host tissue and capsule formation, showed no inflammation and resulted in partial or full repair with equal cellularity and 75-80 % matrix contents of a normal rabbit articular cartilage 8 weeks post-surgery (229)</p>
<p>Porcine collagen type II sponges and films</p> <p>Ultraviolet irradiation crosslinked</p> <p>Autologous canine chondrocytes</p>	<p>Canine chondral defect</p> <p>Total defect filling ranged 56-86 %, with the greatest amount found in scaffolds with cells and microfracture compared to scaffolds alone with microfracture and microfracture alone 15 weeks post-surgery, the tissue filling the defect was predominantly fibrocartilage (230)</p>
<p>Porcine collagen type II sponges</p> <p>No crosslinker</p> <p>No cells</p>	<p>Rabbit chondral defect</p> <p>Scaffolds displayed quicker effusion absorption, greater newly formed cartilage-like areas than the empty group 18 weeks post-surgery, sporadic cartilage signals first appeared at 6 weeks in the scaffolds (231)</p>
<p>Collagen type II hydrogels</p> <p>No crosslinker</p> <p>Rabbit chondrocytes</p>	<p>Rabbit osteochondral defect</p> <p>Cells seeded collagen type II hydrogels displayed better cartilage repair compared to sham, cell pellet and scaffolds alone groups (223)</p>

<p>Collagen type II-GAG sponges reconstituted from porcine cartilage and bovine collagen type I sponges with shark chondroitin-6-sulfate</p> <p>Dehydrothermal treatment and ultraviolet irradiation crosslinked</p> <p>Autologous canine chondrocytes</p>	<p>Canine chondral defect</p> <p>Both cell-seeded scaffolds exhibited comparable cartilage regeneration potential and increased cartilaginous tissue in chondral defects and adjacent subchondral bone space compared to empty group 15 weeks post-surgery (232)</p>
<p>Chicken collagen type II and fibrin sealant hydrogels</p> <p>No crosslinker</p> <p>Human ADSCs</p>	<p>Rabbit chondral defect</p> <p>Improved overall repair of chondral defects, cellular organisation and collagen fibre alignment 12 weeks post-surgery (233)</p>
<p>Chicken collagen type II and rat collagen type I blend hydrogels</p> <p>No crosslinker</p> <p>Autologous rabbit BMSCs</p>	<p>Rabbit chondral defect</p> <p>Cell-seeded collagen type I/II scaffolds exhibited better cartilage repair outcomes in trochlear groove defects compared to pure collagen type I hydrogels and empty chondral defects 13 weeks post-surgery (234)</p>
<p>Squid collagen type II intra-articular injection</p>	<p>Suppressed pro-inflammatory macrophage phenotype, prevented hypertrophic chondrocyte</p>

<p>No crosslinker</p> <p>No cells</p>	<p>phenotype and alleviated inflammation in an OA rat model 6 weeks after OA induction (148)</p>
<p>Shark collagen type II was administered orally</p> <p>No crosslinker</p> <p>No cells</p>	<p>Facilitated recovery of articular membranes in the ankle joint and suppressed rheumatoid arthritis in a complete Freund's adjuvant-induced rheumatoid arthritis rat model 2 weeks after rheumatoid arthritis induction (235)</p>
<p>Recombinant collagen type II hydrogels</p> <p>No crosslinker</p> <p>Autologous rabbit chondrocytes</p>	<p>Rabbit osteochondral defect</p> <p>Cell-scaffold treated group exhibited a slight but insignificant improvement in cartilage repair compared to spontaneous repair group and both groups had lower modified O'Driscoll's score than intact cartilage 24 weeks post-surgery (236)</p>
<p>Recombinant collagen type II and polylactide sponges</p> <p>Carbodiimide crosslinked</p> <p>Autologous porcine chondrocytes</p>	<p>Porcine chondral defect</p> <p>Hyaline cartilage formed most frequently in the recombinant collagen type II / polylactide / cells group, which also improved biomechanically properties only over the spontaneous repair group and showed less adverse subchondral reactions than the Chondro-Gide® (a bilayer collagen type I / collagen type III membrane) / cells group, but not in comparison to the spontaneous repair group 16 weeks post-surgery (237)</p>

1.5. Project phases and hypotheses

Phase I

Considering that porcine collagen type II has been shown to maintain chondrogenic phenotype of rabbit (193), human (212) and ovine chondrocytes (228); to promote the formation of neocartilage (238); and to reduce pain in a rat osteoarthritis model when it was *per os* administered (239), porcine collagen type II may be the ideal scaffold material for cartilage tissue engineering. Considering though the inherent variability of animal-derived products, it is imperative to identify the optimal porcine collagen type II tissue source. Thus, herein it is hypothesised that there is an optimal tissue source (porcine male and female articular, tracheal and auricular cartilage) for pure collagen type II extraction for maximum chondrogenic induction.

Phase II

Extensive use of antibiotics, religious tenets and the potential for interspecies disease transmission restrict the use of mammalian derived collagens (157-159). In this regard, marine species derived collagen offers an opportunity as a safe, sustainable and environmentally friendly alternative to mammalian species derived collagen (240-243). Collagen type I / type II materials from marine species have been shown to maintain human, bovine and rat nasal chondrocyte phenotype (149, 244) and to induce chondrogenic differentiation of human mesenchymal stem cells (245, 246). Considering though that collagen type II scaffolds are more chondrogenic than collagen type I scaffolds (192, 202, 247), it is imperative to develop pure collagen type II preparations and assess their potential for cartilage engineering. Thus, herein it is hypothesised that there is an optimal chondrichthyan (cartilaginous fish) species [lesser spotted dogfish (*Scyliorhinus canicula*), thorn back ray (*Raja clavata*), cuckoo ray (*Leucoraja naevus*) and blonde ray (*Raja brachyuran*)] for pure collagen type II extraction for maximum chondrogenic induction.

Phase III

Gelatin is a mixture of hydrolysed peptides that derive from the degradation of the tertiary, secondary and to some extent, the primary structure of native collagen (248). There are two types of gelatin, type A produced through acid treatment of collagen with an isoelectric point at pH 4~5 and type B produced through alkaline hydrolytic treatment of collagen with an isoelectric point at pH 8~9 (249). In recent decades, the processing of gelatin-based products has been industrialised, resulting in increased use in the food, cosmetic and pharmaceutical sectors (250). In cartilage space, gelatin-based scaffolds have shown promising results in both *in vitro* and *in vivo* setting (251-253). Despite though the positive data that have been obtained over the years, the use of gelatin in biomedicine is somehow restricted due to its high affinity to endotoxin contamination. Endotoxins are large and complex lipopolysaccharides that are localised at the outer membrane of Gram-negative bacteria (254, 255). Although FDA has determined the acceptable level of endotoxin contamination in medical devices to be 0.5 endotoxin units/ml (256), endotoxin contamination is frequently encountered in biomedicine (256-263). It is therefore imperative to assess residual endotoxins in medical devices and especially in natural biomaterials that are prone to endotoxin contamination (264, 265). Herein, it is hypothesised that the biophysical, biochemical and biological properties of gelatin (porcine type A and bovine type B, from two different suppliers) and gelatin-based biomaterials (hydrogels for physicochemical analysis and films for biological analysis) are affected by the different levels of endotoxin content (from < 1 up to 10,370 endotoxin units per gram) and bloom index (from 220 to 355). Note: For various reasons, in the end, the chondrogenic potential of gelatin preparations was not assessed.

1.6. References

1. Kazemnejad, S., Khanmohammadi, M., Baheiraei, N., Arasteh, S. Current state of cartilage tissue engineering using nanofibrous scaffolds and stem cells. *Avicenna J Med Biotechnol.* 2017;9(2):50-65.
2. Goldberg, A., Mitchell, K., Soans, J., Kim, L., Zaidi, R. The use of mesenchymal stem cells for cartilage repair and regeneration: A systematic review. *J Orthop Surg Res.* 2017;12(1):39.
3. Sophia Fox, A. J., Bedi, A., Rodeo, S. A. The basic science of articular cartilage: Structure, composition, and function. *Sports Health.* 2009;1(6):461-8.
4. Kelly, P. A., O'connor, J. J. Transmission of rapidly applied loads through articular cartilage Part 1: Uncracked cartilage. *Proc Inst Mech Eng H.* 1996;210(1):27-37.
5. Pickett, A. M., Hensley, D. T. J. Knee cell-based cartilage restoration. *J Knee Surg.* 2019;32(02):127-33.
6. Reissis, D., Tang, Q. O., Cooper, N. C., Carasco, C. F., Gamie, Z., Mantalaris, A., Tsiridis, E. Current clinical evidence for the use of mesenchymal stem cells in articular cartilage repair. *Expert Opin Biol Ther.* 2016;16(4):535-57.
7. Poole, A. R. Osteoarthritis as a whole joint disease. *HSS J.* 2012;8(1):4-6.
8. Carlson, A. K., Rawle, R. A., Adams, E., Greenwood, M. C., Bothner, B., June, R. K. Application of global metabolomic profiling of synovial fluid for osteoarthritis biomarkers. *Biochem Biophys Res Commun.* 2018;499(2):182-8.
9. Hunter, D. J., Schofield, D., Callander, E. The individual and socioeconomic impact of osteoarthritis. *Nat Rev Rheumatol.* 2014;10(7):437-41.
10. Kotlarz, H., Gunnarsson, C. L., Fang, H., Rizzo, J. A. Insurer and out-of-pocket costs of osteoarthritis in the US: Evidence from national survey data. *Arthritis Rheum.* 2009;60(12):3546-53.
11. Fu, K., Robbins, S. R., Mcdougall, J. J. Osteoarthritis: The genesis of pain. *Rheumatology (Oxford).* 2018;57(suppl_4):iv43-iv50.

12. Horton, W. E. J., Bennion, P., Yang, L. Cellular, molecular, and matrix changes in cartilage during aging and osteoarthritis. *J Musculoskelet Neuronal Interact.* 2006;6(4):379-81.
13. Loeser, R. F., Collins, J. A., Diekman, B. O. Ageing and the pathogenesis of osteoarthritis. *Nat Rev Rheumatol.* 2016;12(7):412-20.
14. Newman, A. B., Haggerty, C. L., Goodpaster, B., Harris, T., Kritchevsky, S., Nevitt, M., Miles, T. P., Visser, M. Strength and muscle quality in a well-functioning cohort of older adults: The health, aging and body composition study. *J Am Geriatr Soc.* 2003;51(3):323-30.
15. Coggon, D., Reading, I., Croft, P., McLaren, M., Barrett, D., Cooper, C. Knee osteoarthritis and obesity. *Int J Obes Relat Metab Disord.* 2001;25(5):622-7.
16. Silverwood, V., Blagojevic-Bucknall, M., Jinks, C., Jordan, J. L., Protheroe, J., Jordan, K. P. Current evidence on risk factors for knee osteoarthritis in older adults: A systematic review and meta-analysis. *Osteoarthritis Cartilage.* 2015;23(4):507-15.
17. Harris, E. C., Coggon, D. Hip osteoarthritis and work. *Best Prac Res Clin Rheumatol.* 2015;29(3):462-82.
18. Turkiewicz, A., Petersson, I. F., Björk, J., Hawker, G., Dahlberg, L. E., Lohmander, L. S., Englund, M. Current and future impact of osteoarthritis on health care: A population-based study with projections to year 2032. *Osteoarthritis Cartilage.* 2014;22(11):1826-32.
19. Arden, N., Nevitt, M. C. Osteoarthritis: Epidemiology. *Best Prac Res Clin Rheumatol.* 2006;20(1):3-25.
20. Kolasinski, S. L., Neogi, T., Hochberg, M. C., Oatis, C., Guyatt, G., Block, J., Callahan, L., Copenhaver, C., Dodge, C., Felson, D., Gellar, K., Harvey, W. F., Hawker, G., Herzig, E., Kwoh, C. K., Nelson, A. E., Samuels, J., Scanzello, C., White, D., Wise, B., Altman, R. D., Drenzo, D., Fontanarosa, J., Girardi, G., Ishimori, M., Misra, D., Shah, A. A., Shmagel, A. K., Thoma, L. M., Turgunbaev, M., Turner, A. S., Reston, J. 2019 American College of Rheumatology/Arthritis Foundation guideline for the management of

osteoarthritis of the hand, hip, and knee. *Arthritis Care Res (Hoboken)*. 2020;72(2):149-62.

21. Nelson, A. E., Allen, K. D., Golightly, Y. M., Goode, A. P., Jordan, J. M. A systematic review of recommendations and guidelines for the management of osteoarthritis: The chronic osteoarthritis management initiative of the US bone and joint initiative. *Semin Arthritis Rheum*. 2014;43(6):701-12.

22. Da Costa, B. R., Reichenbach, S., Keller, N., Nartey, L., Wandel, S., Jüni, P., Trelle, S. Effectiveness of non-steroidal anti-inflammatory drugs for the treatment of pain in knee and hip osteoarthritis: A network meta-analysis. *Lancet*. 2017;390(10090):e21-e33.

23. Zeng, C., Wei, J., Persson, M. S. M., Sarmanova, A., Doherty, M., Xie, D., Wang, Y., Li, X., Li, J., Long, H., Lei, G., Zhang, W. Relative efficacy and safety of topical non-steroidal anti-inflammatory drugs for osteoarthritis: A systematic review and network meta-analysis of randomised controlled trials and observational studies. *Br J Sports Med*. 2018;52(10):642-50.

24. Wang, Z. Y., Shi, S. Y., Li, S. J., Chen, F., Chen, H., Lin, H. Z., Lin, J. M. Efficacy and safety of duloxetine on osteoarthritis knee pain: A meta-analysis of randomized controlled trials. *Pain Med*. 2015;16(7):1373-85.

25. Lohmander, L. S., Hellot, S., Dreher, D., Krantz, E. F., Kruger, D. S., Guermazi, A., Eckstein, F. Intraarticular sprifermin (recombinant human fibroblast growth factor 18) in knee osteoarthritis: A randomized, double-blind, placebo-controlled trial. *Arthritis Rheumatol*. 2014;66(7):1820-31.

26. Deshmukh, V., Hu, H., Barroga, C., Bossard, C., Kc, S., Dellamary, L., Stewart, J., Chiu, K., Ibanez, M., Pedraza, M., Seo, T., Do, L., Cho, S., Cahiwat, J., Tam, B., Tambiah, J. R. S., Hood, J., Lane, N. E., Yazici, Y. A small-molecule inhibitor of the Wnt pathway (SM04690) as a potential disease modifying agent for the treatment of osteoarthritis of the knee. *Osteoarthritis Cartilage*. 2018;26(1):18-27.

27. Sampson, E. R., Hilton, M. J., Tian, Y., Chen, D., Schwarz, E. M., Mooney, R. A., Bukata, S. V., O'keefe, R. J., Awad, H., Puzas, J. E., Rosier, R.

- N., Zuscik, M. J. Teriparatide as a chondroregenerative therapy for injury-induced osteoarthritis. *Sci Transl Med.* 2011;3(101):101ra93.
28. Kosloski, M. P., Goss, S., Wang, S. X., Liu, J., Loebbert, R., Medema, J. K., Liu, W., Dutta, S. Pharmacokinetics and tolerability of a dual variable domain immunoglobulin ABT-981 against IL-1 α and IL-1 β in healthy subjects and patients with osteoarthritis of the knee. *J Clin Pharmacol.* 2016;56(12):1582-90.
29. Huang, Z., Ding, C., Li, T., Yu, S. P. Current status and future prospects for disease modification in osteoarthritis. *Rheumatology (Oxford).* 2018;57(suppl_4):iv108-iv23.
30. Kraeutler, M. J., Aliberti, G. M., Scillia, A. J., Mccarty, E. C., Mulcahey, M. K. Microfracture versus drilling of articular cartilage defects: A systematic review of the basic science evidence. *Orthop J Sports Med.* 2020;8(8):2325967120945313.
31. Gao, L., Goebel, L. K. H., Orth, P., Cucchiarini, M., Madry, H. Subchondral drilling for articular cartilage repair: A systematic review of translational research. *Dis Model Mech.* 2018;11(6):dmm034280.
32. Gowd, A. K., Cvetanovich, G. L., Liu, J. N., Christian, D. R., Cabarcas, B. C., Redondo, M. L., Verma, N. N., Yanke, A. B., Cole, B. J. Management of chondral lesions of the knee: Analysis of trends and short-term complications using the national surgical quality improvement program database. *Arthroscopy.* 2019;35(1):138-46.
33. Defroda, S. F., Bokshan, S. L., Yang, D. S., Daniels, A. H., Owens, B. D. Trends in the surgical treatment of articular cartilage lesions in the United States from 2007 to 2016. *J Knee Surg.* 2020.
34. Graceffa, V., Vinatier, C., Guicheux, J., Stoddart, M., Alini, M., Zeugolis, D. I. Chasing chimeras—the elusive stable chondrogenic phenotype. *Biomaterials.* 2019;192:199-225.
35. Graceffa, V., Vinatier, C., Guicheux, J., Evans, C. H., Stoddart, M., Alini, M., Zeugolis, D. I. State of art and limitations in genetic engineering to induce stable chondrogenic phenotype. *Biotechnol Adv.* 2018;36(7):1855-69.

36. Pourakbari, R., Khodadadi, M., Aghebati-Maleki, A., Aghebati-Maleki, L., Yousefi, M. The potential of exosomes in the therapy of the cartilage and bone complications; emphasis on osteoarthritis. *Life Sci.* 2019;236:116861.
37. Confalonieri, D., Schwab, A., Walles, H., Ehlicke, F. Advanced therapy medicinal products: A guide for bone marrow-derived MSC application in bone and cartilage tissue engineering. *Tissue Eng Part B Rev.* 2018;24(2):155-69.
38. Wei, W., Ma, Y., Yao, X., Zhou, W., Wang, X., Li, C., Lin, J., He, Q., Leptihn, S., Ouyang, H. Advanced hydrogels for the repair of cartilage defects and regeneration. *Bioact Mater.* 2020;6(4):998-1011.
39. Yilmaz, E. N., Zeugolis, D. I. Electrospun polymers in cartilage engineering—State of play. *Front Bioeng Biotechnol.* 2020;8:77.
40. Armiento, A. R., Stoddart, M. J., Alini, M., Eglin, D. Biomaterials for articular cartilage tissue engineering: Learning from biology. *Acta Biomater.* 2018;65:1-20.
41. Campos, Y., Almirall, A., Fuentes, G., Bloem, H. L., Kaijzel, E. L., Cruz, L. J. Tissue engineering: An alternative to repair cartilage. *Tissue Eng Part B Rev.* 2019;25(4):357-73.
42. Schüttler, K. F., Götschenberg, A., Klasan, A., Stein, T., Pehl, A., Roessler, P. P., Figiel, J., Heyse, T. J., Efe, T. Cell-free cartilage repair in large defects of the knee: Increased failure rate 5 years after implantation of a collagen type I scaffold. *Arch Orthop Trauma Surg.* 2019;139(1):99-106.
43. Christensen, B. B., Foldager, C. B., Jensen, J., Jensen, N. C., Lind, M. Poor osteochondral repair by a biomimetic collagen scaffold: 1-to 3-year clinical and radiological follow-up. *Knee Surg Sports Traumatol Arthrosc.* 2016;24(7):2380-7.
44. Goldring, M. B., Tsuchimochi, K., Ijiri, K. The control of chondrogenesis. *J Cell Biochem.* 2006;97(1):33-44.
45. Mackie, E. J., Ahmed, Y. A., Tatarczuch, L., Chen, K. S., Mirams, M. Endochondral ossification: How cartilage is converted into bone in the developing skeleton. *Int J Biochem Cell Biol.* 2008;40(1):46-62.

46. Gadjanski, I., Spiller, K., Vunjak-Novakovic, G. Time-dependent processes in stem cell-based tissue engineering of articular cartilage. *Stem Cell Rev Rep*. 2012;8(3):863-81.
47. Tsang, K. Y., Tsang, S. W., Chan, D., Cheah, K. S. The chondrocytic journey in endochondral bone growth and skeletal dysplasia. *Birth Defects Res C Embryo Today*. 2014;102(1):52-73.
48. Chijimatsu, R., Saito, T. Mechanisms of synovial joint and articular cartilage development. *Cell Mol Life Sci*. 2019;76(20):3939-52.
49. Lotz, M., Loeser, R. F. Effects of aging on articular cartilage homeostasis. *Bone*. 2012;51(2):241-8.
50. Akkiraju, H., Nohe, A. Role of chondrocytes in cartilage formation, progression of osteoarthritis and cartilage regeneration. *J Dev Biol*. 2015;3(4):177-92.
51. Fickert, S., Fiedler, J., Brenner, R. E. Identification of subpopulations with characteristics of mesenchymal progenitor cells from human osteoarthritic cartilage using triple staining for cell surface markers. *Arthritis Res Ther*. 2004;6(5):R422-32.
52. Alsalameh, S., Amin, R., Gemba, T., Lotz, M. Identification of mesenchymal progenitor cells in normal and osteoarthritic human articular cartilage. *Arthritis Rheum*. 2004;50(5):1522-32.
53. Eyre, D. R., Weis, M. A., Wu, J. J. Articular cartilage collagen: An irreplaceable framework. *Eur Cell Mater*. 2006;12:57-63.
54. Aigner, T., Stöve, J. Collagens-major component of the physiological cartilage matrix, major target of cartilage degeneration, major tool in cartilage repair. *Adv Drug Deliv Rev*. 2003;55(12):1569-93.
55. Luo, Y., Sinkeviciute, D., He, Y., Karsdal, M., Henrotin, Y., Mobasheri, A., Önerfjord, P., Bay-Jensen, A. The minor collagens in articular cartilage. *Protein Cell*. 2017;8(8):560-72.
56. Bielajew, B. J., Hu, J. C., Athanasiou, K. A. Collagen: Quantification, biomechanics and role of minor subtypes in cartilage. *Nat Rev Mater*. 2020;5(10):730-47.

57. Yang, C. L., Rui, H., Mosler, S., Notbohm, H., Sawaryn, A., Müller, P. K. Collagen II from articular cartilage and annulus fibrosus: Structural and functional implication of tissue specific posttranslational modifications of collagen molecules. *Eur J Biochem.* 1993;213(3):1297-302.
58. Nah, H. D., Swoboda, B., Birk, D. E., Kirsch, T. Type IIA procollagen: Expression in developing chicken limb cartilage and human osteoarthritic articular cartilage. *Dev Dyn.* 2001;220(4):307-22.
59. Lian, C., Wang, X., Qiu, X., Wu, Z., Gao, B., Liu, L., Liang, G., Zhou, H., Yang, X., Peng, Y., Liang, A., Xu, C., Huang, D., Su, P. Collagen type II suppresses articular chondrocyte hypertrophy and osteoarthritis progression by promoting integrin β 1-SMAD1 interaction. *Bone Res.* 2019;7:8.
60. Wang, C., Brisson, B. K., Terajima, M., Li, Q., Hoxha, K., Han, B., Goldberg, A. M., Sherry Liu, X., Marcolongo, M. S., Enomoto-Iwamoto, M., Yamauchi, M., Volk, S. W., Han, L. Type III collagen is a key regulator of the collagen fibrillar structure and biomechanics of articular cartilage and meniscus. *Matrix Biol.* 2020;85-86:47-67.
61. Wu, J. J., Weis, M. A., Kim, L. S., Eyre, D. R. Type III collagen, a fibrillar network modifier in articular cartilage. *J Biol Chem.* 2010;285(24):18537-44.
62. Smeriglio, P., Dhulipala, L., Lai, J. H., Goodman, S. B., Drago, J. L., Smith, R. L., Maloney, W. J., Yang, F., Bhutani, N. Collagen VI enhances cartilage tissue generation by stimulating chondrocyte proliferation. *Tissue Eng Part A.* 2015;21(3-4):840-9.
63. Pullig, O., Weseloh, G., Swoboda, B. Expression of type VI collagen in normal and osteoarthritic human cartilage. *Osteoarthritis Cartilage.* 1999;7(2):191-202.
64. Müller-Glauser, W., Humbel, B., Glatt, M., Sträuli, P., Winterhalter, K. H., Bruckner, P. On the role of type IX collagen in the extracellular matrix of cartilage: Type IX collagen is localized to intersections of collagen fibrils. *J Cell Biol.* 1986;102(5):1931-9.

65. Diab, M., Wu, J. J., Eyre, D. R. Collagen type IX from human cartilage: A structural profile of intermolecular cross-linking sites. *Biochem J.* 1996;314(Pt1):327-32.
66. Parsons, P., Gilbert, S. J., Vaughan-Thomas, A., Sorrell, D. A., Notman, R., Bishop, M., Hayes, A. J., Mason, D. J., Duance, V. C. Type IX collagen interacts with fibronectin providing an important molecular bridge in articular cartilage. *J Biol Chem.* 2011;286(40):34986-97.
67. Brewton, R. G., Wright, D. W., Mayne, R. Structural and functional comparison of type IX collagen-proteoglycan from chicken cartilage and vitreous humor. *J Biol Chem.* 1991;266(8):4752-7.
68. Blumbach, K., Bastiaansen-Jenniskens, Y. M., Degroot, J., Paulsson, M., Van Osch, G. J., Zaucke, F. Combined role of type IX collagen and cartilage oligomeric matrix protein in cartilage matrix assembly: Cartilage oligomeric matrix protein counteracts type IX collagen-induced limitation of cartilage collagen fibril growth in mouse chondrocyte cultures. *Arthritis Rheum.* 2009;60(12):3676-85.
69. Von Der Mark, K., Kirsch, T., Nerlich, A., Kuss, A., Weseloh, G., Glückert, K., Stöss, H. Type X collagen synthesis in human osteoarthritic cartilage. Indication of chondrocyte hypertrophy. *Arthritis Rheum.* 1992;35(7):806-11.
70. Shen, G. The role of type X collagen in facilitating and regulating endochondral ossification of articular cartilage. *Orthod Craniofac Res.* 2005;8(1):11-7.
71. Aigner, T., Reichenberger, E., Bertling, W., Kirsch, T., Stöss, H., Von Der Mark, K. Type X collagen expression in osteoarthritic and rheumatoid articular cartilage. *Virchows Arch B Cell Pathol Incl Mol Pathol.* 1993;63(4):205-11.
72. Von Der Mark, K., Frischholz, S., Aigner, T., Beier, F., Belke, J., Erdmann, S., Burkhardt, H. Upregulation of type X collagen expression in osteoarthritic cartilage. *Acta Orthop Scand Suppl.* 1995;266:125-9.

73. Knuth, C. A., Andres Sastre, E., Fahy, N. B., Witte-Bouma, J., Ridwan, Y., Strabbing, E. M., Koudstaal, M. J., Van De Peppel, J., Wolvius, E. B., Narcisi, R., Farrell, E. Collagen type X is essential for successful mesenchymal stem cell-mediated cartilage formation and subsequent endochondral ossification. *Eur Cell Mater.* 2019;38:106-22.
74. Rodriguez, R. R., Seegmiller, R. E., Stark, M. R., Bridgewater, L. C. A type XI collagen mutation leads to increased degradation of type II collagen in articular cartilage. *Osteoarthritis Cartilage.* 2004;12(4):314-20.
75. Smith, S. M., Melrose, J. Type XI collagen-perlecan-HS interactions stabilise the pericellular matrix of annulus fibrosus cells and chondrocytes providing matrix stabilisation and homeostasis. *J Mol Histol.* 2019;50(3):285-94.
76. Lawrence, E. A., Kague, E., Aggleton, J. A., Harniman, R. L., Roddy, K. A., Hammond, C. L. The mechanical impact of *coll1a2* loss on joints; *Coll1a2* mutant zebrafish show changes to joint development and function, which leads to early-onset osteoarthritis. *Philos Trans R Soc Lond B Biol Sci.* 2018;373(1759):20170335.
77. Garofalo, S., Metsäranta, M., Ellard, J., Smith, C., Horton, W., Vuorio, E., De Crombrughe, B. Assembly of cartilage collagen fibrils is disrupted by overexpression of normal type II collagen in transgenic mice. *Proc Natl Acad Sci U S A.* 1993;90(9):3825-9.
78. Metsäranta, M., Toman, D., De Crombrughe, B., Vuorio, E. Mouse type II collagen gene. Complete nucleotide sequence, exon structure, and alternative splicing. *J Biol Chem.* 1991;266(25):16862-9.
79. D'alessio, M., Bernard, M., Pretorius, P. J., De Wet, W., Ramirez, F. Complete nucleotide sequence of the region encompassing the first twenty-five exons of the human pro α 1 (I) collagen gene (COL1A1). *Gene.* 1988;67(1):105-15.
80. Benson-Chanda, V., Ming-Wan, S., Weil, D., Mon-Li, C., Ramirez, F. Cloning and analysis of the 5' portion of the human type-III procollagen gene (COL3A1). *Gene.* 1989;78(2):255-65.

81. Kohno, K., Sullivan, M., Yamada, Y. Structure of the promoter of the rat type II procollagen gene. *J Biol Chem.* 1985;260(7):4441-7.
82. Ryan, M. C., Sieraski, M., Sandell, L. J. The human type II procollagen gene: identification of an additional protein-coding domain and location of potential regulatory sequences in the promoter and first intron. *Genomics.* 1990;8(1):41-8.
83. Eyre, D. Articular cartilage and changes in arthritis: Collagen of articular cartilage. *Arthritis Res Ther.* 2001;4(1):30-5.
84. Kuiper, N. J., Sharma, A. A detailed quantitative outcome measure of glycosaminoglycans in human articular cartilage for cell therapy and tissue engineering strategies. *Osteoarthritis Cartilage.* 2015;23(12):2233-41.
85. Watanabe, H., Cheung, S. C., Itano, N., Kimata, K., Yamada, Y. Identification of hyaluronan-binding domains of aggrecan. *J Biol Chem.* 1997;272(44):28057-65.
86. Horkay, F., Basser, P. J., Hecht, A. M., Geissler, E. Structure and properties of cartilage proteoglycans. *Macromol Symp.* 2017;372(1):43-50.
87. Vynios, D. H. Metabolism of cartilage proteoglycans in health and disease. *Biomed Res Int.* 2014;2014:452315.
88. Knudson, C. B., Knudson, W. Cartilage proteoglycans. *Semin Cell Dev Biol.* 2001;12(2):69-78.
89. Roughley, P. J., Lee, E. R. Cartilage proteoglycans: Structure and potential functions. *Microsc Res Tech.* 1994;28(5):385-97.
90. Bertrand, J., Held, A. Role of proteoglycans in osteoarthritis. *Cartilage: Springer; 2017.* p. 63-80.
91. Muir, H. Proteoglycans of cartilage. *J Clin Pathol Suppl (R Coll Pathol).* 1978;12:67-81.
92. Carney, S. L., Muir, H. The structure and function of cartilage proteoglycans. *Physiol Rev.* 1988;68(3):858-910.
93. Mankin, H. J., Lippiello, L. The glycosaminoglycans of normal and arthritic cartilage. *J Clin Invest.* 1971;50(8):1712-9.

94. Hjertquist, S. O., Lemperg, R. Identification and concentration of the glycosaminoglycans of human articular cartilage in relation to age and osteoarthritis. *Calcif Tissue Res.* 1972;10(3):223-37.
95. Han, E. H., Chen, S. S., Klisch, S. M., Sah, R. L. Contribution of proteoglycan osmotic swelling pressure to the compressive properties of articular cartilage. *Biophys J.* 2011;101(4):916-24.
96. Roughley, P. J. Articular cartilage and changes in arthritis: Noncollagenous proteins and proteoglycans in the extracellular matrix of cartilage. *Arthritis Res.* 2001;3(6):342-7.
97. Ghosh, P., Smith, M. Osteoarthritis, genetic and molecular mechanisms. *Biogerontology.* 2002;3(1-2):85-8.
98. Fosang, A. J., Last, K., Maciewicz, R. A. Aggrecan is degraded by matrix metalloproteinases in human arthritis. Evidence that matrix metalloproteinase and aggrecanase activities can be independent. *J Clin Invest.* 1996;98(10):2292-9.
99. Lippiello, L., Hall, D., Mankin, H. J. Collagen synthesis in normal and osteoarthritic human cartilage. *J Clin Invest.* 1977;59(4):593-600.
100. Nelson, F., Dahlberg, L., Lavery, S., Reiner, A., Pidoux, I., Ionescu, M., Fraser, G. L., Brooks, E., Tanzer, M., Rosenberg, L. C., Dieppe, P., Robin Poole, A. Evidence for altered synthesis of type II collagen in patients with osteoarthritis. *J Clin Invest.* 1998;102(12):2115-25.
101. Maldonado, M., Nam, J. The role of changes in extracellular matrix of cartilage in the presence of inflammation on the pathology of osteoarthritis. *Biomed Res Int.* 2013;2013:284873.
102. Goldring, M. B. Chondrogenesis, chondrocyte differentiation, and articular cartilage metabolism in health and osteoarthritis. *Ther Adv Musculoskelet Dis.* 2012;4(4):269-85.
103. Rim, Y. A., Nam, Y., Ju, J. H. The role of chondrocyte hypertrophy and senescence in osteoarthritis initiation and progression. *Int J Mol Sci.* 2020;21(7):2358.

104. Talwar, R. M., Wong, B. S., Svoboda, K., Harper, R. P. Effects of estrogen on chondrocyte proliferation and collagen synthesis in skeletally mature articular cartilage. *J Oral Maxillofac Surg.* 2006;64(4):600-9.
105. Stevens, D. A., Williams, G. R. Hormone regulation of chondrocyte differentiation and endochondral bone formation. *Mol Cell Endocrinol.* 1999;151(1-2):195-204.
106. He, H., Wang, C., Tang, Q., Yang, F., Xu, Y. Elucidation of possible molecular mechanisms underlying the estrogen-induced disruption of cartilage development in zebrafish larvae. *Toxicol Lett.* 2018;289:22-7.
107. Fortier, L. A., Barker, J. U., Strauss, E. J., Mccarrel, T. M., Cole, B. J. The role of growth factors in cartilage repair. *Clin Orthop Relat Res.* 2011;469(10):2706-15.
108. Ellman, M. B., Yan, D., Ahmadinia, K., Chen, D., An, H. S., Im, H. J. Fibroblast growth factor control of cartilage homeostasis. *J Cell Biochem.* 2013;114(4):735-42.
109. Patil, A. S., Sable, R. B., Kothari, R. M. An update on transforming growth factor- β (TGF- β): Sources, types, functions and clinical applicability for cartilage/bone healing. *J Cell Physiol.* 2011;226(12):3094-103.
110. Degroot, J., Verzijl, N., Bank, R. A., Lafeber, F. P., Bijlsma, J. W., Tekoppele, J. M. Age - related decrease in proteoglycan synthesis of human articular chondrocytes: The role of nonenzymatic glycation. *Arthritis Rheum.* 1999;42(5):1003-9.
111. Madej, W., Van Caam, A., Davidson, E. N., Hannink, G., Buma, P., Van Der Kraan, P. M. Ageing is associated with reduction of mechanically-induced activation of Smad2/3P signaling in articular cartilage. *Osteoarthritis Cartilage.* 2016;24(1):146-57.
112. Rahmati, M., Nalesso, G., Mobasheri, A., Mozafari, M. Aging and osteoarthritis: Central role of the extracellular matrix. *Ageing Res Rev.* 2017;40:20-30.

113. Fermor, B., Christensen, S. E., Youn, I., Cernanec, J. M., Davies, C. M., Weinberg, J. B. Oxygen, nitric oxide and articular cartilage. *Eur Cell Mater.* 2007;13:56-65.
114. Buckley, C. T., Vinardell, T., Kelly, D. J. Oxygen tension differentially regulates the functional properties of cartilaginous tissues engineered from infrapatellar fat pad derived MSCs and articular chondrocytes. *Osteoarthritis Cartilage.* 2010;18(10):1345-54.
115. Qu, C., Lindeberg, H., Ylärinne, J. H., Lammi, M. J. Five percent oxygen tension is not beneficial for neocartilage formation in scaffold-free cell cultures. *Cell Tissue Res.* 2012;348(1):109-17.
116. Shi, Y., Ma, J., Zhang, X., Li, H., Jiang, L., Qin, J. Hypoxia combined with spheroid culture improves cartilage specific function in chondrocytes. *Integr Biol (Camb).* 2015;7(3):289-97.
117. Bleuel, J., Zaucke, F., Brüggemann, G. P., Niehoff, A. Effects of cyclic tensile strain on chondrocyte metabolism: A systematic review. *PLoS One.* 2015;10(3):e0119816.
118. Jørgensen, A. E. M., Kjær, M., Heinemeier, K. M. The effect of aging and mechanical loading on the metabolism of articular cartilage. *J Rheumatol.* 2017;44(4):410-7.
119. Meinert, C., Schrobback, K., Hutmacher, D. W., Klein, T. J. A novel bioreactor system for biaxial mechanical loading enhances the properties of tissue-engineered human cartilage. *Sci Rep.* 2017;7(1):16997.
120. Bian, L., Fong, J. V., Lima, E. G., Stoker, A. M., Ateshian, G. A., Cook, J. L., Hung, C. T. Dynamic mechanical loading enhances functional properties of tissue-engineered cartilage using mature canine chondrocytes. *Tissue Eng Part A.* 2010;16(5):1781-90.
121. Mauck, R. L., Byers, B. A., Yuan, X., Tuan, R. S. Regulation of cartilaginous ECM gene transcription by chondrocytes and MSCs in 3D culture in response to dynamic loading. *Biomech Model Mechanobiol.* 2007;6(1-3):113-25.

122. Gelse, K., Pöschl, E., Aigner, T. Collagens-structure, function, and biosynthesis. *Adv Drug Deliv Rev.* 2003;55(12):1531-46.
123. Soroushanova, A., Delgado, L. M., Wu, Z., Shologu, N., Kshirsagar, A., Raghunath, R., Mullen, A. M., Bayon, Y., Pandit, A., Raghunath, M. The collagen suprafamily: From biosynthesis to advanced biomaterial development. *Adv Mater.* 2019;31(1):e1801651.
124. Silver, F. H., Birk, D. E. Molecular structure of collagen in solution: Comparison of types I, II, III and V. *Int J Biol Macromol.* 1984;6(3):125-32.
125. Birk, D. E., Silver, F. H. Collagen fibrillogenesis in vitro: Comparison of types I, II, and III. *Arch Biochem Biophys.* 1984;235(1):178-85.
126. Perdivara, I., Yamauchi, M., Tomer, K. Molecular characterization of collagen hydroxylysine O-glycosylation by mass spectrometry: Current status. *Aust J Chem.* 2013;66(7):760-9.
127. Bächinger, H., Mizuno, K., Vranka, J., Boudko, S. Collagen formation and structure. *Chem Mol Sci Chem Eng.* 2010;5:469-530.
128. Bateman, J. F., Boot-Handford, R. P., Lamandé, S. R. Genetic diseases of connective tissues: Cellular and extracellular effects of ECM mutations. *Nat Rev Genet.* 2009;10(3):173-83.
129. Bhosale, A. M., Richardson, J. B. Articular cartilage: structure, injuries and review of management. *Br Med Bull.* 2008;87:77-95.
130. Muir, H., Bullough, P., Maroudas, A. The distribution of collagen in human articular cartilage with some of its physiological implications. *J Bone Joint Surg Br.* 1970;52(3):554-63.
131. Chen, R., Chen, S., Chen, X. M., Long, X. Study of the tidemark in human mandibular condylar cartilage. *Arch Oral Biol.* 2011;56(11):1390-7.
132. James, C. B., Uhl, T. L. A review of articular cartilage pathology and the use of glucosamine sulfate. *J Athl Train.* 2001;36(4):413-9.
133. Shoulders, M. D., Raines, R. T. Collagen structure and stability. *Annu Rev Biochem.* 2009;78:929-58.
134. Frazer, A., Bunning, R. A., Thavarajah, M., Seid, J. M., Russell, R. G. Studies on type II collagen and aggrecan production in human articular

chondrocytes in vitro and effects of transforming growth factor- β and interleukin-1 β . *Osteoarthritis Cartilage*. 1994;2(4):235-45.

135. Kivirikko, K. I., Myllylä, R., Pihlajaniemi, T. Protein hydroxylation: Prolyl 4-hydroxylase, an enzyme with four cosubstrates and a multifunctional subunit. *FASEB J*. 1989;3(5):1609-17.

136. Prockop, D. J., Kivirikko, K. I., Tuderman, L., Guzman, N. A. The biosynthesis of collagen and its disorders. *N Engl J Med*. 1979;301(2):77-85.

137. Myllyharju, J. Prolyl 4-hydroxylases, the key enzymes of collagen biosynthesis. *Matrix Biol*. 2003;22(1):15-24.

138. Siegel, R. C. Biosynthesis of collagen crosslinks: Increased activity of purified lysyl oxidase with reconstituted collagen fibrils. *Proc Natl Acad Sci U S A*. 1974;71(12):4826-30.

139. Eyre, D. R., Paz, M. A., Gallop, P. M. Cross-linking in collagen and elastin. *Annu Rev Biochem*. 1984;53(1):717-48.

140. Mehana, E. E., Khafaga, A. F., El-Blehi, S. S. The role of matrix metalloproteinases in osteoarthritis pathogenesis: An updated review. *Life Sci*. 2019;234:116786.

141. Salminen-Mankonen, H. J., Morko, J., Vuorio, E. Role of cathepsin K in normal joints and in the development of arthritis. *Curr Drug Targets*. 2007;8(2):315-23.

142. Panwar, P., Du, X., Sharma, V., Lamour, G., Castro, M., Li, H., Brömme, D. Effects of cysteine proteases on the structural and mechanical properties of collagen fibers. *J Biol Chem*. 2013;288(8):5940-50.

143. Herbage, D., Bouillet, J., Bernengo, J. C. Biochemical and physicochemical characterization of pepsin-solubilized type-II collagen from bovine articular cartilage. *Biochem J*. 1977;161(2):303-12.

144. Bishop, P. N., Crossman, M. V., Mcleod, D., Ayad, S. Extraction and characterization of the tissue forms of collagen types II and IX from bovine vitreous. *Biochem J*. 1994;299(Pt2):497-505.

145. Eyre, D. R., Muir, H. The distribution of different molecular species of collagen in fibrous, elastic and hyaline cartilages of the pig. *Biochem J.* 1975;151(3):595-602.
146. Cao, H., Xu, S. Y. Purification and characterization of type II collagen from chick sternal cartilage. *Food Chem.* 2008;108(2):439-45.
147. Akram, A. N., Zhang, C. Extraction of collagen-II with pepsin and ultrasound treatment from chicken sternal cartilage; physicochemical and functional properties. *Ultrason Sonochem.* 2020;64:105053.
148. Dai, M., Liu, X., Wang, N., Sun, J. Squid type II collagen as a novel biomaterial: Isolation, characterization, immunogenicity and relieving effect on degenerative osteoarthritis via inhibiting stat1 signaling in pro-inflammatory macrophages. *Mater Sci Eng C Mater Biol Appl.* 2018;89:283-94.
149. Rigogliuso, S., Salamone, M., Barbarino, E., Barbarino, M., Nicosia, A., Ghersi, G. Production of injectable marine collagen-based hydrogel for the maintenance of differentiated chondrocytes in tissue engineering applications. *Int J Mol Sci.* 2020;21(16):5798.
150. Sewing, J., Klinger, M., Notbohm, H. Jellyfish collagen matrices conserve the chondrogenic phenotype in two- and three-dimensional collagen matrices. *J Tissue Eng Regen Med.* 2017;11(3):916-25.
151. Zhang, X., Adachi, S., Ura, K., Takagi, Y. Properties of collagen extracted from Amur sturgeon *Acipenser schrenckii* and assessment of collagen fibrils in vitro. *Int J Biol Macromol.* 2019;137:809-20.
152. Cumming, M. H., Hall, B., Hofman, K. Isolation and characterisation of major and minor collagens from hyaline cartilage of hoki (*Macrurus novaezelandiae*). *Mar Drugs.* 2019;17(4):223.
153. Jeevithan, E., Bao, B., Bu, Y., Zhou, Y., Zhao, Q., Wu, W. Type II collagen and gelatin from silvertip shark (*Carcharhinus albimarginatus*) cartilage: Isolation, purification, physicochemical and antioxidant properties. *Mar Drugs.* 2014;12(7):3852-73.
154. Kittiphattanabawon, P., Benjakul, S., Visessanguan, W., Shahidi, F. Isolation and characterization of collagen from the cartilages of brownbanded

bamboo shark (*Chiloscyllium punctatum*) and blacktip shark (*Carcharhinus limbatus*). *LWT-Food Sci Technol*. 2010;43(5):792-800.

155. Merly, L., Smith, S. L. Collagen type II, alpha 1 protein: A bioactive component of shark cartilage. *Int Immunopharmacol*. 2013;15(2):309-15.

156. Mizuta, S., Hwang, J. H., Yoshinaka, R. Molecular species of collagen in pectoral fin cartilage of skate (*Raja kenoi*). *Food Chem*. 2003;80:1-7.

157. Hashim, P., Mohd Ridzwan, M. S., Bakar, J., Mat Hashim, D. Collagen in food and beverage industries. *Int Food Res J*. 2015;22(1):1-8.

158. Avila Rodríguez, M. I., Rodríguez Barroso, L. G., Sánchez, M. L. Collagen: A review on its sources and potential cosmetic applications. *J Cosmet Dermatol*. 2018;17(1):20-6.

159. Silvipriya, K. S., Kumar, K. K., Bhat, A. R., Kumar, B. D., John, A., Lakshmanan, P. Collagen: Animal sources and biomedical application. *J Appl Pharm Sci*. 2015;5(3):123-7.

160. Chen, Z., Fan, D., Shang, L. Exploring the potential of the recombinant human collagens for biomedical and clinical applications: A short review. *Biomed Mater*. 2020;16(1):012001.

161. Olsen, D., Yang, C., Bodo, M., Chang, R., Leigh, S., Baez, J., Carmichael, D., Perälä, M., Hämäläinen, E. R., Jarvinen, M., Polarek, J. Recombinant collagen and gelatin for drug delivery. *Adv Drug Deliv Rev*. 2003;55(12):1547-67.

162. Fertala, A. Three decades of research on recombinant collagens: Reinventing the wheel or developing new biomedical products? *Bioengineering (Basel)*. 2020;7(4):155.

163. Fertala, A., Holmes, D. F., Kadler, K. E., Sieron, A. L., Prockop, D. J. Assembly in vitro of thin and thick fibrils of collagen II from recombinant procollagen II. The monomers in the tips of thick fibrils have the opposite orientation from monomers in the growing tips of collagen I fibrils. *J Biol Chem*. 1996;271(25):14864-9.

164. Fertala, A., Sieron, A. L., Ganguly, A., Li, S. W., Ala-Kokko, L., Anumula, K. R., Prockop, D. J. Synthesis of recombinant human procollagen II

- in a stably transfected tumour cell line (HT1080). *Biochem J.* 1994;298(Pt 1):31-7.
165. Ala-Kokko, L., Hyland, J., Smith, C., Kivirikko, K. I., Jimenez, S. A., Prockop, D. J. Expression of a human cartilage procollagen gene (COL2A1) in mouse 3T3 cells. *J Biol Chem.* 1991;266(22):14175-8.
166. Xi, C., Liu, N., Liang, F., Zhao, X., Long, J., Yuan, F., Yun, S., Sun, Y., Xi, Y. Molecular assembly of recombinant chicken type II collagen in the yeast *Pichia pastoris*. *Sci China Life Sci.* 2018;61(7):815-25.
167. Qi, Q., Yao, L., Liang, Z., Yan, D., Li, Z., Huang, Y., Sun, J. Production of human type II collagen using an efficient baculovirus-silkworm multigene expression system. *Mol Genet Genomics.* 2016;291(6):2189-98.
168. Ikonomou, L., Schneider, Y. J., Agathos, S. N. Insect cell culture for industrial production of recombinant proteins. *Appl Microbiol Biotechnol.* 2003;62(1):1-20.
169. Browne, S., Zeugolis, D. I., Pandit, A. Collagen: Finding a solution for the source. *Tissue Eng Part A.* 2013;19(13-14):1491-4.
170. Capella-Monsonís, H., Coentro, J. Q., Graceffa, V., Wu, Z., Zeugolis, D. I. An experimental toolbox for characterization of mammalian collagen type I in biological specimens. *Nat Protoc.* 2018;13(3):507-29.
171. Sorushanova, A., Skoufos, I., Tzora, A., Mullen, A. M., Zeugolis, D. I. The influence of animal species, gender and tissue on the structural, biophysical, biochemical and biological properties of collagen sponges. *J Mater Sci Mater Med.* 2021;32(1):1-12.
172. Zeugolis, D. I., Paul, R. G., Attenburrow, G. Factors influencing the properties of reconstituted collagen fibers prior to self-assembly: Animal species and collagen extraction method. *J Biomed Mater Res A.* 2008;86(4):892-904.
173. Delgado, L. M., Shologu, N., Fuller, K., Zeugolis, D. I. Acetic acid and pepsin result in high yield, high purity and low macrophage response collagen for biomedical applications. *Biomed Mater.* 2017;12(6):065009.

174. Collin, E. C., Grad, S., Zeugolis, D. I., Vinatier, C. S., Clouet, J. R., Guicheux, J. J., Weiss, P., Alini, M., Pandit, A. S. An injectable vehicle for nucleus pulposus cell-based therapy. *Biomaterials*. 2011;32(11):2862-70.
175. Taguchi, T., Ikoma, T., Tanaka, J. An improved method to prepare hyaluronic acid and type II collagen composite matrices. *J Biomed Mater Res*. 2002;61(2):330-6.
176. Yang, K., Sun, J., Wei, D., Yuan, L., Yang, J., Guo, L., Fan, H., Zhang, X. Photo-crosslinked mono-component type II collagen hydrogel as a matrix to induce chondrogenic differentiation of bone marrow mesenchymal stem cells. *J Mater Chem B*. 2017;5(44):8707-18.
177. Cao, H., Xu, S. Y. EDC/NHS-crosslinked type II collagen-chondroitin sulfate scaffold: Characterization and in vitro evaluation. *J Mater Sci Mater Med*. 2008;19(2):567-75.
178. Ko, C. S., Huang, J. P., Huang, C. W., Chu, I. M. Type II collagen-chondroitin sulfate-hyaluronan scaffold cross-linked by genipin for cartilage tissue engineering. *J Biosci Bioeng*. 2009;107(2):177-82.
179. Lan, W., Xu, M., Zhang, X., Zhao, L., Huang, D., Wei, X., Chen, W. Biomimetic polyvinyl alcohol/type II collagen hydrogels for cartilage tissue engineering. *J Biomater Sci Polym Ed*. 2020;31(9):1179-98.
180. Hsu, S. H., Tsai, C. L., Tang, C. M. Evaluation of cellular affinity and compatibility to biodegradable polyesters and type - II collagen - modified scaffolds using immortalized rat chondrocytes. *Artif Organs*. 2002;26(7):647-58.
181. Yen, H. J., Tseng, C. S., Hsu, S. H., Tsai, C. L. Evaluation of chondrocyte growth in the highly porous scaffolds made by fused deposition manufacturing (FDM) filled with type II collagen. *Biomed Microdevices*. 2009;11(3):615-24.
182. Ragetly, G., Griffon, D. J., Chung, Y. S. The effect of type II collagen coating of chitosan fibrous scaffolds on mesenchymal stem cell adhesion and chondrogenesis. *Acta Biomater*. 2010;6(10):3988-97.
183. Zhang, J., Yang, Z., Li, C., Dou, Y., Li, Y., Thote, T., Wang, D. A., Ge, Z. Cells behave distinctly within sponges and hydrogels due to differences of internal structure. *Tissue Eng Part A*. 2013;19(19-20):2166-75.

184. Shields, K. J., Beckman, M. J., Bowlin, G. L., Wayne, J. S. Mechanical properties and cellular proliferation of electrospun collagen type II. *Tissue Eng.* 2004;10(9-10):1510-7.
185. Barnes, C. P., Pemble, C. W., Brand, D. D., Simpson, D. G., Bowlin, G. L. Cross-linking electrospun type II collagen tissue engineering scaffolds with carbodiimide in ethanol. *Tissue Eng.* 2007;13(7):1593-605.
186. Matthews, J. A., Boland, E. D., Wnek, G. E., Simpson, D. G., Bowlin, G. L. Electrospinning of collagen type II: A feasibility study. *J Bioact Compat Polym.* 2003;18(2):125-34.
187. Yang, L., Fitié, C. F., Van Der Werf, K. O., Bennink, M. L., Dijkstra, P. J., Feijen, J. Mechanical properties of single electrospun collagen type I fibers. *Biomaterials.* 2008;29(8):955-62.
188. Zeugolis, D. I., Khew, S. T., Yew, E. S., Ekaputra, A. K., Tong, Y. W., Yung, L. L., Hutmacher, D. W., Sheppard, C., Raghunath, M. Electro-spinning of pure collagen nano-fibres—Just an expensive way to make gelatin? *Biomaterials.* 2008;29(15):2293-305.
189. Ren, X., Wang, F., Chen, C., Gong, X., Yin, L., Yang, L. Engineering zonal cartilage through bioprinting collagen type II hydrogel constructs with biomimetic chondrocyte density gradient. *BMC Musculoskelet Disord.* 2016;17:301.
190. Tiruvannamalai Annamalai, R., Mertz, D. R., Daley, E. L., Stegemann, J. P. Collagen type II enhances chondrogenic differentiation in agarose-based modular microtissues. *Cytherapy.* 2016;18(2):263-77.
191. Chang, S. J., Kuo, S. M., Manousakas, I., Niu, G. C., Chen, J. P. Preparation and characterization of hyaluronan/collagen II microspheres under an electrostatic field system with disc electrodes. *Acta Biomater.* 2009;5(1):101-14.
192. Tamaddon, M., Burrows, M., Ferreira, S. A., Dazzi, F., Apperley, J. F., Bradshaw, A., Brand, D. D., Czernuszka, J., Gentleman, E. Monomeric, porous type II collagen scaffolds promote chondrogenic differentiation of human bone marrow mesenchymal stem cells in vitro. *Sci Rep.* 2017;7:43519.

193. Gao, Y., Li, B., Kong, W., Yuan, L., Guo, L., Li, C., Fan, H., Fan, Y., Zhang, X. Injectable and self-crosslinkable hydrogels based on collagen type II and activated chondroitin sulfate for cell delivery. *Int J Biol Macromol.* 2018;118(Pt B):2014-20.
194. Veilleux, N., Spector, M. Effects of FGF-2 and IGF-1 on adult canine articular chondrocytes in type II collagen–glycosaminoglycan scaffolds in vitro. *Osteoarthritis Cartilage.* 2005;13(4):278-86.
195. Szychlińska, M. A., Calabrese, G., Ravalli, S., Dolcimascolo, A., Castrogiovanni, P., Fabbi, C., Puglisi, C., Lauretta, G., Di Rosa, M., Castorina, A., Parenti, R., Musumeci, G. Evaluation of a cell-free collagen type I-based scaffold for articular cartilage regeneration in an orthotopic rat model. *Materials (Basel).* 2020;13(10):2369.
196. Calabrese, G., Gulino, R., Giuffrida, R., Forte, S., Figallo, E., Fabbi, C., Salvatorelli, L., Memeo, L., Gulisano, M., Parenti, R. In vivo evaluation of biocompatibility and chondrogenic potential of a cell-free collagen-based scaffold. *Front Physiol.* 2017;8:984.
197. Yang, J., Chen, X., Yuan, T., Yang, X., Fan, Y., Zhang, X. Regulation of the secretion of immunoregulatory factors of mesenchymal stem cells (MSCs) by collagen-based scaffolds during chondrogenesis. *Mater Sci Eng C Mater Biol Appl.* 2017;70(Pt 2):983-91.
198. Cao, C., Zhang, Y., Ye, Y., Sun, T. Effects of cell phenotype and seeding density on the chondrogenic capacity of human osteoarthritic chondrocytes in type I collagen scaffolds. *J Orthop Surg Res.* 2020;15(1):120.
199. Bosnakovski, D., Mizuno, M., Kim, G., Takagi, S., Okumura, M., Fujinaga, T. Chondrogenic differentiation of bovine bone marrow mesenchymal stem cells (MSCs) in different hydrogels: Influence of collagen type II extracellular matrix on MSC chondrogenesis. *Biotechnol Bioeng.* 2006;93(6):1152-63.
200. Tao, Y., Zhou, X., Liu, D., Li, H., Liang, C., Li, F., Chen, Q. Proportion of collagen type II in the extracellular matrix promotes the differentiation of

- human adipose-derived mesenchymal stem cells into nucleus pulposus cells. *Biofactors*. 2016;42(2):212-23.
201. Buma, P., Pieper, J. S., Van Tienen, T., Van Susante, J. L., Van Der Kraan, P. M., Veerkamp, J. H., Van Den Berg, W. B., Veth, R. P., Van Kuppevelt, T. H. Cross-linked type I and type II collagenous matrices for the repair of full-thickness articular cartilage defects—a study in rabbits. *Biomaterials*. 2003;24(19):3255-63.
202. Nehrer, S., Breinan, H. A., Ramappa, A., Shortkroff, S., Young, G., Minas, T., Sledge, C. B., Yannas, I. V., Spector, M. Canine chondrocytes seeded in type I and type II collagen implants investigated in vitro. *J Biomed Mater Res*. 1997;38(2):95-104.
203. Lu, Z., Doulabi, B. Z., Huang, C., Bank, R. A., Helder, M. N. Collagen type II enhances chondrogenesis in adipose tissue-derived stem cells by affecting cell shape. *Tissue Eng Part A*. 2010;16(1):81-90.
204. Trentham, D. E., Townes, A. S., Kang, A. H. Autoimmunity to type II collagen an experimental model of arthritis. *J Exp Med*. 1977;146(3):857-68.
205. Holmdahl, R., Vingsbo, C., Malmström, V., Jansson, L., Holmdahl, M. Chronicity of arthritis induced with homologous type II collagen (CII) in rats is associated with anti-CII B-cell activation. *J Autoimmun*. 1994;7(6):739-52.
206. Ofosu-Appiah, W. A., Morgan, K., Lennox Holt, P. J. Native type II collagen-induced arthritis in the rat. III. Relationship between the cellular immune response to native type II collagen and arthritis. *Ann Rheum Dis*. 1983;42(3):331-7.
207. Cathcart, E. S., Hayes, K. C., Gonnerman, W. A., Lazzari, A. A., Franzblau, C. Experimental arthritis in a nonhuman primate. I. Induction by bovine type II collagen. *Lab Invest*. 1986;54(1):26-31.
208. Cook, A. D., Rowley, M. J., Mackay, I. R., Gough, A., Emery, P. Antibodies to type II collagen in early rheumatoid arthritis. Correlation with disease progression. *Arthritis Rheum*. 1996;39(10):1720-7.
209. Stuart, J. M., Townes, A. S., Kang, A. H. Collagen autoimmune arthritis. *Ann Rev Immunol*. 1984;2(1):199-218.

210. Kim, H. A., Seo, Y. I., Lee, J., Jung, Y. O. Detection of anti-type II collagen antibodies in patients with chronic gouty arthritis: Findings from a pilot study. *J Clin Rheumatol*. 2016;22(7):360-3.
211. Thompson, H. S., Henderson, B., Spencer, J. M., Hobbs, S. M., Peppard, J. V., Staines, N. A. Tolerogenic activity of polymerized type II collagen in preventing collagen-induced arthritis in rats. *Clin Exp Immunol*. 1988;72(1):20-5.
212. Wu, C. H., Ko, C. S., Huang, J. W., Huang, H. J., Chu, I. M. Effects of exogenous glycosaminoglycans on human chondrocytes cultivated on type II collagen scaffolds. *J Mater Sci Mater Med*. 2010;21(2):725-9.
213. Pieper, J. S., Van Der Kraan, P. M., Hafmans, T., Kamp, J., Buma, P., Van Susante, J. L. C., Van Den Berg, W. B., Veerkamp, J. H., Van Kuppevelt, T. H. Crosslinked type II collagen matrices: Preparation, characterization, and potential for cartilage engineering. *Biomaterials*. 2002;23(15):3183-92.
214. Mukaida, T., Urabe, K., Naruse, K., Aikawa, J., Katano, M., Hyon, S. H., Itoman, M. Influence of three-dimensional culture in a type II collagen sponge on primary cultured and dedifferentiated chondrocytes. *J Orthop Sci*. 2005;10(5):521-8.
215. Lee, C. R., Grodzinsky, A. J., Hsu, H. P., Spector, M. Effects of a cultured autologous chondrocyte-seeded type II collagen scaffold on the healing of a chondral defect in a canine model. *J Orthop Res*. 2003;21(2):272-81.
216. Nehrer, S., Breinan, H. A., Ramappa, A., Young, G., Shortkroff, S., Louie, L. K., Sledge, C. B., Yannas, I. V., Spector, M. Matrix collagen type and pore size influence behaviour of seeded canine chondrocytes. *Biomaterials*. 1997;18(11):769-76.
217. Lee, C. R., Breinan, H. A., Nehrer, S., Spector, M. Articular cartilage chondrocytes in type I and type II collagen-GAG matrices exhibit contractile behavior in vitro. *Tissue Eng*. 2000;6(5):555-65.
218. Vickers, S. M., Squitieri, L. S., Spector, M. Effects of cross-linking type II collagen-GAG scaffolds on chondrogenesis in vitro: Dynamic pore reduction promotes cartilage formation. *Tissue Eng*. 2006;12(5):1345-55.

219. Lee, C. R., Grodzinsky, A. J., Spector, M. Biosynthetic response of passaged chondrocytes in a type II collagen scaffold to mechanical compression. *J Biomed Mater Res A*. 2003;64(3):560-9.
220. Malesud, C. J., Stevenson, S., Mehraban, F., Papay, R. S., Purchio, A. F., Goldberg, V. M. The proteoglycan synthesis repertoire of rabbit chondrocytes maintained in type II collagen gels. *Osteoarthritis Cartilage*. 1994;2(1):29-41.
221. Muhonen, V., Narcisi, R., Nystedt, J., Korhonen, M., Van Osch, G. J., Kiviranta, I. Recombinant human type II collagen hydrogel provides a xeno-free 3D micro-environment for chondrogenesis of human bone marrow-derived mesenchymal stromal cells. *J Tissue Eng Regen Med*. 2017;11(3):843-54.
222. Pulkkinen, H. J., Tiitu, V., Valonen, P., Hamalainen, E. R., Lammi, M. J., Kiviranta, I. Recombinant human type II collagen as a material for cartilage tissue engineering. *Int J Artif Organs*. 2008;31(11):960-9.
223. Wong, C. C., Chen, C. H., Chiu, L. H., Tsuang, Y. H., Bai, M. Y., Chung, R. J., Lin, Y. H., Hsieh, F. J., Chen, Y. T., Yang, T. L. Facilitating in vivo articular cartilage repair by tissue-engineered cartilage grafts produced from auricular chondrocytes. *Am J Sports Med*. 2018;46(3):713-27.
224. Dong, S., Guo, H., Zhang, Y., Li, Z., Kang, F., Yang, B., Kang, X., Wen, C., Yan, Y., Jiang, B., Fan, Y. rFN/Cad-11-modified collagen type II biomimetic interface promotes the adhesion and chondrogenic differentiation of mesenchymal stem cells. *Tissue Eng Part A*. 2013;19(21-22):2464-77.
225. Chen, W. C., Wei, Y. H., Chu, I. M., Yao, C. L. Effect of chondroitin sulphate C on the in vitro and in vivo chondrogenesis of mesenchymal stem cells in crosslinked type II collagen scaffolds. *J Tissue Eng Regen Med*. 2013;7(8):665-72.
226. Funayama, A., Niki, Y., Matsumoto, H., Maeno, S., Yatabe, T., Morioka, H., Yanagimoto, S., Taguchi, T., Tanaka, J., Toyama, Y. Repair of full-thickness articular cartilage defects using injectable type II collagen gel embedded with cultured chondrocytes in a rabbit model. *J Orthop Sci*. 2008;13(3):225-32.

227. Chen, W. C., Yao, C. L., Wei, Y. H., Chu, I. M. Evaluating osteochondral defect repair potential of autologous rabbit bone marrow cells on type II collagen scaffold. *Cytotechnology*. 2011;63(1):13-23.
228. Dorotka, R., Windberger, U., Macfelda, K., Bindreiter, U., Toma, C., Nehrer, S. Repair of articular cartilage defects treated by microfracture and a three-dimensional collagen matrix. *Biomaterials*. 2005;26(17):3617-29.
229. Hsu, S. H., Chang, S. H., Yen, H. J., Whu, S. W., Tsai, C. L., Chen, D. C. Evaluation of biodegradable polyesters modified by type II collagen and Arg-Gly-Asp as tissue engineering scaffolding materials for cartilage regeneration. *Artif Organs*. 2006;30(1):42-55.
230. Breinan, H. A., Martin, S. D., Hsu, H. P., Spector, M. Healing of canine articular cartilage defects treated with microfracture, a type-II collagen matrix, or cultured autologous chondrocytes. *J Orthop Res*. 2000;18(5):781-9.
231. Chen, H., Yang, X., Liao, Y., Zeng, X., Liang, P., Kang, N., Tan, J., Liang, Z. MRI and histologic analysis of collagen type II sponge on repairing the cartilage defects of rabbit knee joints. *J Biomed Mater Res B Appl Biomater*. 2011;96(2):267-75.
232. Nehrer, S., Breinan, H. A., Ramappa, A., Hsu, H. P., Minas, T., Shortkroff, S., Sledge, C. B., Yannas, I. V., Spector, M. Chondrocyte-seeded collagen matrices implanted in a chondral defect in a canine model. *Biomaterials*. 1998;19(24):2313-28.
233. Lazarini, M., Bordeaux-Rego, P., Giardini-Rosa, R., Duarte, A. S. S., Baratti, M. O., Zorzi, A. R., De Miranda, J. B., Lenz Cesar, C., Luzo, Â., Olalla Saad, S. T. Natural type II collagen hydrogel, fibrin sealant, and adipose-derived stem cells as a promising combination for articular cartilage repair. *Cartilage*. 2017;8(4):439-43.
234. Kilmer, C. E., Battistoni, C. M., Cox, A., Breur, G. J., Panitch, A., Liu, J. C. Collagen type I and II blend hydrogel with autologous mesenchymal stem cells as a scaffold for articular cartilage defect repair. *ACS Biomater Sci Eng*. 2020;6(6):3464-76.

235. Chen, L., Bao, B., Wang, N., Xie, J., Wu, W. Oral administration of shark type II collagen suppresses complete Freund's adjuvant-induced rheumatoid arthritis in rats. *Pharmaceuticals (Basel)*. 2012;5(4):339-52.
236. Pulkkinen, H. J., Tiitu, V., Valonen, P., Jurvelin, J. S., Rieppo, L., Töyräs, J., Silvast, T. S., Lammi, M. J., Kiviranta, I. Repair of osteochondral defects with recombinant human type II collagen gel and autologous chondrocytes in rabbit. *Osteoarthritis Cartilage*. 2013;21(3):481-90.
237. Muhonen, V., Saloniemi, E., Haaparanta, A. M., Järvinen, E., Paatela, T., Meller, A., Hannula, M., Björkman, M., Pyhälä, T., Ellä, V., Vasara, A., Töyräs, J., Kellomäki, M., Kiviranta, I. Articular cartilage repair with recombinant human type II collagen/poly lactide scaffold in a preliminary porcine study. *J Orthop Res*. 2016;34(5):745-53.
238. Yeh, H. Y., Lin, T. Y., Lin, C. H., Yen, B. L., Tsai, C. L., Hsu, S. H. Neocartilage formation from mesenchymal stem cells grown in type II collagen-hyaluronan composite scaffolds. *Differentiation*. 2013;86(4-5):171-83.
239. Di Cesare Mannelli, L., Micheli, L., Zanardelli, M., Ghelardini, C. Low dose native type II collagen prevents pain in a rat osteoarthritis model. *BMC Musculoskelet Disord*. 2013;14:228.
240. Song, E., Yeon Kim, S., Chun, T., Byun, H. J., Lee, Y. M. Collagen scaffolds derived from a marine source and their biocompatibility. *Biomaterials*. 2006;27(15):2951-61.
241. Felician, F. F., Xia, C., Qi, W., Xu, H. Collagen from marine biological sources and medical applications. *Chem Biodivers*. 2018;15(5):e1700557.
242. Ferrario, C., Leggio, L., Leone, R., Di Benedetto, C., Guidetti, L., Coccè, V., Ascagni, M., Bonasoro, F., La Porta, C. a. M., Candia Carnevali, M. D. Marine-derived collagen biomaterials from echinoderm connective tissues. *Mar Environ Res*. 2017;128:46-57.
243. Subhan, F., Ikram, M., Shehzad, A., Ghafoor, A. Marine collagen: An emerging player in biomedical applications. *J Food Sci Technol*. 2015;52(8):4703-7.

244. Bermueller, C., Schwarz, S., Elsaesser, A. F., Sewing, J., Baur, N., Von Bomhard, A., Scheithauer, M., Notbohm, H., Rotter, N. Marine collagen scaffolds for nasal cartilage repair: Prevention of nasal septal perforations in a new orthotopic rat model using tissue engineering techniques. *Tissue Eng Part A*. 2013;19(19-20):2201-14.
245. Hoyer, B., Bernhardt, A., Lode, A., Heinemann, S., Sewing, J., Klinger, M., Notbohm, H., Gelinsky, M. Jellyfish collagen scaffolds for cartilage tissue engineering. *Acta Biomater*. 2014;10(2):883-92.
246. Pustlauk, W., Paul, B., Gelinsky, M., Bernhardt, A. Jellyfish collagen and alginate: Combined marine materials for superior chondrogenesis of hMSC. *Mater Sci Eng C Mater Biol Appl*. 2016;64:190-8.
247. Mueller, S. M., Shortkroff, S., Schneider, T. O., Breinan, H. A., Yannas, I. V., Spector, M. Meniscus cells seeded in type I and type II collagen-GAG matrices in vitro. *Biomaterials*. 1999;20(8):701-9.
248. Mariod, A. A. Extraction, purification, and modification of natural polymers. *Nat Polym: Springer*; 2016. p. 63-91.
249. Duconseille, A., Astruc, T., Quintana, N., Meersman, F., Sante-Lhoutellier, V. Gelatin structure and composition linked to hard capsule dissolution: A review. *Food Hydrocoll*. 2015;43:360-76.
250. Djagny, V. B., Wang, Z., Xu, S. Gelatin: A valuable protein for food and pharmaceutical industries: Review. *Crit Rev Food Sci Nutr*. 2001;41(6):481-92.
251. Xue, J., Feng, B., Zheng, R., Lu, Y., Zhou, G., Liu, W., Cao, Y., Zhang, Y., Zhang, W. J. Engineering ear-shaped cartilage using electrospun fibrous membranes of gelatin/polycaprolactone. *Biomaterials*. 2013;34(11):2624-31.
252. Ponticiello, M. S., Schinagl, R. M., Kadiyala, S., Barry, F. P. Gelatin-based resorbable sponge as a carrier matrix for human mesenchymal stem cells in cartilage regeneration therapy. *J Biomed Mater Res*. 2000;52(2):246-55.
253. Whu, S. W., Hung, K. C., Hsieh, K. H., Chen, C. H., Tsai, C. L., Hsu, S. H. In vitro and in vivo evaluation of chitosan-gelatin scaffolds for cartilage tissue engineering. *Mater Sci Eng C Mater Biol Appl*. 2013;33(5):2855-63.

254. Cavaillon, J. M. Exotoxins and endotoxins: Inducers of inflammatory cytokines. *Toxicon*. 2018;149:45-53.
255. Bertani, B., Ruiz, N. Function and biogenesis of lipopolysaccharides. *EcoSal Plus*. 2018;8(1):10.1128/ecosalplus.ESP-0001-2018.
256. Gorbet, M. B., Sefton, M. V. Endotoxin: The uninvited guest. *Biomaterials*. 2005;26(34):6811-7.
257. Townsend, S., Caubilla Barron, J., Loc-Carrillo, C., Forsythe, S. The presence of endotoxin in powdered infant formula milk and the influence of endotoxin and *Enterobacter sakazakii* on bacterial translocation in the infant rat. *Food Microbiol*. 2007;24(1):67-74.
258. Gorbet, M. B., Sefton, M. V. Biomaterial-associated thrombosis: Roles of coagulation factors, complement, platelets and leukocytes. *Biomaterials*. 2004;25(26):5681-703.
259. Borton, L. K., Coleman, K. P. Material-mediated pyrogens in medical devices: Applicability of the in vitro monocyte activation test. *ALTEX*. 2018;35(4):453-63.
260. Li, Y., Fujita, M., Boraschi, D. Endotoxin contamination in nanomaterials leads to the misinterpretation of immunosafety results. *Front Immunol*. 2017;8:472.
261. Wang, G., Zhang, P., Zhao, J. Endotoxin contributes to artificial loosening of prostheses induced by titanium particles. *Med Sci Monit*. 2018;24:7001-6.
262. Lieder, R., Petersen, P. H., Sigurjónsson, Ó. E. Endotoxins—The invisible companion in biomaterials research. *Tissue Eng Part B Rev*. 2013;19(5):391-402.
263. Munford, R. S. Endotoxemia—Menace, marker, or mistake? *J Leukoc Biol*. 2016;100(4):687-98.
264. Li, Y., Boraschi, D. Endotoxin contamination: A key element in the interpretation of nanosafety studies. *Nanomedicine (Lond)*. 2016;11(3):269-87.

265. Dullah, E. C., Ongkudon, C. M. Current trends in endotoxin detection and analysis of endotoxin–protein interactions. *Crit Rev Biotechnol.* 2017;37(2):251-61.

Chapter 2 – In the quest of the optimal tissue source (porcine male and female articular, tracheal and auricular cartilage) for the development of collagen sponges for articular cartilage

This chapter has been published in:

In the quest of the optimal tissue source (porcine male and female articular, tracheal and auricular cartilage) for the development of collagen sponges for articular cartilage. Z Wu, SH Korntner, AM Mullen, I Skoufos, A Tzora, DI Zeugolis. Biomedical Engineering Advances 2021

Authors' contribution: Z.W. performed all the experiments (collagen isolation, collagen purity assessment, ultrastructural assessment, biomechanical assessment, thermal properties assessment, free amines assessment, resistance to enzymatic degradation assessment, basic cellular function assessment, chondrogenic potential assessment), drafted figures and tables, wrote the manuscript; S.H.K. trained histology and qPCR methods, reviewed and commented the manuscript; A.M.M. provided the funding; I.S. and A.T. provided raw tissue materials for collagen isolation; D.I.Z. contributed the concept, reviewed and edited the manuscript, provided the funding; all authors reviewed and approved the manuscript.

2.1. Introduction

Articular cartilage is a hydrated connective tissue with low coefficient of friction that covers the bone ends of articulating joints, enabling smooth and efficient weight-bearing. Since articular cartilage is an avascular, alymphatic and aneural tissue with low metabolic activity, its self-healing capacity is minimal (1, 2). As a result of tissue degradation, due to pathophysiology or injury, osteoarthritis is manifested, which currently affects over 240 million people globally (3). Osteoarthritis is characterised as the second most expensive health condition to treat in US hospitals with total direct expenditures of US\$ 41.7 billion in 2011 (4) and is projected to increase further proportionally to the increase of population aging and obesity (5, 6). The state of the art in cartilage repair and regeneration includes microfracture (7-9), tissue grafting (10-12), scaffold or scaffold-free, autologous or allogeneic, chondrocyte or stem cell transplantation (13-15), molecular delivery (16-18) and various acellular biomaterial (19, 20) approaches. Unfortunately, there is still no widely accepted therapeutic treatment available. It is therefore imperative and timely to develop functional therapeutic interventions for cartilage repair and regeneration.

As conventional 2D monolayer cell culture systems, where cells are grown on flat surfaces, result in loss of chondrogenic phenotype, substantial research and development efforts are directed towards the development of 3D scaffolds that would mimic native cartilage tissue and therefore induce effective chondrogenesis (21-25). Among the diverse range of natural and synthetic materials, the use of collagen and in particular collagen type II (as opposed to collagen type I) has been advocated, as it constitutes the major extracellular matrix (ECM) protein of cartilage (26-28) and has shown repeatedly to maintain chondrocyte phenotype *in vitro* (29, 30). Collagen type II has also been shown to induce chondrogenic differentiation of stem cells (31) by inducing a round cell shape via the integrin β 1-mediated Rho A/Rock signalling pathway (32) and to suppresses articular chondrocyte hypertrophy and osteoarthritis progression via promotion of integrin β 1-Smad1 interactions (33). It is also worth noting that collagen type II matrices have been shown to promote superficial cartilage-like-

tissue formation in rabbit full thickness articular cartilage defects, compared to collagen type I (34), and collagen type I scaffolds have failed to demonstrate efficiency in human osteochondral repair (35) and in human large cartilage defects (36). Further, collagen type II scaffolds from porcine cartilage (with autologous articular cartilage chondrocytes) (30, 37) and from bovine trachea (with autologous rabbit bone marrow stem cells) (38) have been shown to induce hyaline neocartilage formation in chondral canine defect and osteochondral rabbit defect animal models, respectively. Considering though the inherent variability of animal-derived products, it is imperative to identify an optimal porcine collagen type II tissue source.

Herein, we ventured to assess the influence of biological sex (male, female) and tissue (articular, tracheal, auricular) on the biophysical, biochemical and biological properties of pepsin extracted porcine collagen type II scaffolds. Pepsin extraction was chosen as it has been shown to increase yield and to reduce immune responses (39-41) and 4-arm polyethylene glycol succinimidyl glutarate was selected to crosslink the produced scaffolds as its stabilisation and cytocompatibility efficiency have been demonstrated repeatedly in the literature (42-44).

2.2. Materials and Methods

2.2.1. Materials

All chemicals were of analytical grade. Porcine tissues (articular cartilage, tracheal cartilage, auricular cartilage) were obtained from a local slaughterhouse. All tissue samples were obtained freshly and stored at -20 °C until analysis. 4-arm polyethylene glycol (PEG) succinimidyl glutarate (4SG, Mw 10,000) was purchased from JenKem Technology (USA). All other materials and reagents were purchased from Sigma-Aldrich (Ireland) unless otherwise stated.

2.2.2. Type II collagen isolation

Extraction of pepsin soluble collagen was performed as previously described with slight modifications (40). The selective cleavage of the *N*- and *C*- terminal regions of the collagen molecules was achieved by enzymatic digestion with pepsin (3,200-4,500 units per mg protein, cat. no. P6887) (45). Porcine tissues were thawed at room temperature and washed thoroughly under running tap water. Cartilage was manually dissected using a surgical scalpel, incubated in 0.2 M NaOH solution for 12 h and washed with absolute ethanol. Cartilage samples were manually cut into small pieces, homogenised in liquid nitrogen using a CryoMill (SPEX SamplePrep 6870, Germany) and suspended in tissue to 1 M acetic acid ratio of 1 to 1 (g/l) under stirring for 48 h at 4 °C. Then pepsin was added at tissue to pepsin 10 to 1 (w/w) ratio at room temperature and the solutions were kept under constant stirring for 48 h at 4 °C. Collagen solution was filtered through sieve and filter mesh; insoluble matter was discarded. Purified collagen solutions were obtained after repeated [first in collagen to 1 M acetic acid ratio of 1 to 1 (g/l) and second in 1 M acetic acid at collagen to acetic acid ratio of 1.5 to 1 (g/ml)] salt precipitation (0.9 M NaCl) / centrifugation (20 min, 8,000 rpm, 4-8 °C). Both supernatants were discarded. The precipitates from the second salt precipitation were dissolved in minimum amount of 1 M acetic acid to obtain highly concentrated collagen solutions. Subsequently, the highly concentrated

collagen solutions were dialysed against 0.001 M acetic acid for 48 h at 4 °C. The final collagen solutions were stored at 4 °C until use.

2.2.3. Sodium dodecyl sulphate poly-acrylamide gel electrophoresis

To assess the purity of the extracted collagen from the various tissues, sodium dodecyl sulphate-polyacrylamide gel electrophoresis (SDS-PAGE) under non-reducing conditions was conducted (46) using a Mini-Protean 3 electrophoresis system (Bio-Rad Laboratories, UK). 3 % running gel and 5 % separation gel were used. Collagen samples were freeze dried in freezer-dryer (FreeZone Plus 4.5 Liter Console Freeze Dry System, Labconco, USA) and then dissolved at 1 mg/ml concentration in 0.5 M acetic acid. Collagen solutions were neutralised with 1 N NaOH, followed by the addition of 5x sample buffer (bromophenol blue / SDS). The sample-buffer mixture was heated at 95 °C for 5 min and a 10 µl aliquot of the mixture was loaded onto each well of the running gel. High purity soluble collagen type I (Symatase, France) was used as negative control and soluble collagen type II isolated from chicken sternal cartilage (C9301, Sigma-Aldrich) was used as positive control, both at 1 mg/ml concentration in 0.5 M acetic acid. Electrophoresis was carried out by first applying 50 V constant voltage until the samples reach the end of the running gel and then 120 V constant voltage was applied until the samples reached the end of the separation gel. The gels were silver stained using SilverQuest™ kit (Invitrogen, USA), according to the manufacturer's protocol.

2.2.4. Collagen crosslinking and scaffold fabrication

Collagen type II preparations were freeze dried, re-dissolved in 0.05 M acetic acid to form solutions of 5 mg/ml concentration, crosslinked with 1 mM 4-arm polyethylene glycol succinimidyl glutarate (PEG-4SG, Mw 10,000) in phosphate buffered saline (PBS) (43) and frozen at -80 °C for 12 h. Non-crosslinked collagens were prepared using PBS only. Frozen solutions were freeze dried to

obtain collagen type II sponges. All the collagen scaffolds were produced on the same day and under the same freeze-drying condition to avoid variabilities.

2.2.5. Ultrastructural assessment

Collagen sponges were sectioned in the dry state to expose the inner porous structure, mounted onto a carbon disk, gold sputter coated (Emitech K-550X Sputter Coater, Emitech, UK) and imaged with a Hitachi S-4700 scanning electron microscope (SEM, Hitachi, High-Technologies Europe GmbH, Germany). Three micrographs of different areas were obtained from each collagen sponge and average pore size and porosity of non-crosslinked and crosslinked collagen sponges were determined using ImageJ software (National Institutes of Health, USA). The images were binarised using thresholding procedure, a window showing pore size distribution was emerged and 80-100 pores were measured per image. The average pore size and porosity were assessed after proper thresholding (47).

2.2.6. Biomechanical assessment

The mechanical properties of the collagen sponges were assessed via uniaxial compression using a material testing machine (Z2.5, Zwick/Roell, Germany) loaded with a 10 N load cell. Uniaxial constant loading was performed on dry collagen sponges with approximately 4 mm height and 9 mm in diameter. Scaffolds were placed between two loading cells and compressed until 70 % deformation was reached, with a compression rate of 10 mm/min. Force, strain and elastic modulus were determined by plotting stress versus strain curves. Both compression strength and elastic modulus were determined within the linear area of the curves at the position of 30 % deformation and elastic modulus was calculated using the linear equation of trend-lines at the position of 30 % of the deformation (48).

2.2.7. Denaturation temperature assessment

The denaturation temperature of collagen sponges was assessed using a differential scanning calorimeter (DSC, DSC-60, Shimadzu, Japan) in wet state (49). In brief, collagen sponges were hydrated in 1x PBS for 12 h at 4 °C. The samples were then blotted with filter paper to remove excess PBS and hermetically sealed in aluminium crucibles. Collagen samples of 10-15 mg were used for DSC analysis. An empty aluminium crucible was used as reference. Heating was carried out at a constant temperature ramp of 10 °C/min with a temperature range of 20-100 °C. Thermal denaturation, the endothermic transition, was recorded as typical peak and the peak (temperature of maximum power absorption during denaturation) temperature was recorded.

2.2.8. Free amines assessment

Crosslinking efficiency was quantified using the 2,4,6-trinitrobenzene sulfonic acid (TNBSA) assay (Thermo Fisher Scientific, Ireland). Collagen free amine groups react with TNBSA to form highly chromogenic derivatives that can be measured at 335 nm. Briefly, collagen sponges (~ 3 mg) were incubated with TNBSA at 37 °C for 2 h. The reaction was stopped by adding 10 % sodium dodecyl sulphate (SDS) and 1 M hydrochloric acid. The mixtures were subsequently heated at 95 °C for 15 min in order to hydrolyse the collagen samples. The absorbance of each sample was read at 335 nm (Varioskan Flash Multimode Reader, Thermo Fisher Scientific, Ireland) and values were normalised to the standard curve, which was generated with a series of a known glycine solution at different concentrations (0.005, 0.01, 0.02, 0.03, 0.04 and 0.05 mg/ml).

2.2.9. Resistance to enzymatic degradation assessment

Enzymatic stability of the collagen sponges was quantified with the collagenase assay (50). Briefly, collagen sponges were weighed and hydrated for 2 h in 0.1 M Tris-HCl and 50 mM CaCl₂ at pH 7.4. The sponges were then incubated in 50

U/ml bacterial collagenase type II (MMP-8; Gibco, cat. no. 17101-015, Ireland). After incubation at different time points (3 h, 6 h, 9 h, 12 h and 24 h) at 37 °C, centrifugation was carried out at 10,000 g for 5 min, the supernatants were removed and the remaining collagen sponges were freeze-dried and weighed. The degree of enzymatic degradation was quantified using the weight difference approach $[(W_o - W_t) / W_o] \times 100$, where W_o is the original weight and W_t is the remaining weight.

2.2.10. Cell culture

Human adipose derived stem cells (hADSCs) from female healthy donor (cat. no. PT-5006) were purchased from Lonza (Switzerland) and cultured in alpha Minimum Essential Medium (alpha-MEM) with GlutaMAX™ (Gibco Life Technologies, Ireland) supplemented with 10 % foetal bovine serum and 1 % penicillin-streptomycin at 37 °C in 95 % humidified atmosphere of 5 % CO₂. At passages 5, cells were resuspended in fresh medium and 100 µl of cell suspension was seeded onto each collagen sponge at a density of 200,000 cells/sponge. As a negative control group, human adipose derived stem cells were cultured on tissue culture plastic (TCP) at 50,000 cells/cm². Cells were left to attach to the sponge for 2 h before the expansion medium was added. Expansion medium was changed to chondrogenic induction medium the next day to allow for the cells to attach and spread evenly throughout the scaffold. The chondrogenic induction medium was composed of high glucose Dulbecco's Modified Eagle's medium (DMEM), 100 nM dexamethasone, 50 mg/ml bovine serum albumin, 50 µg/ml ascorbic acid-2-phosphate, 5 ml insulin-transferrin-selenium (ITS) liquid media supplement, 10 ng/ml transforming growth factor beta 3 (TGF-β3, R&D Systems, USA). Cells were cultured for 7, 14 and 21 days and media were changed every 2 days.

2.2.11. Cell viability assessment

Cell viability was analysed using the Live/Dead[®] assay (Life Technologies, Ireland) as per manufacturer's protocol. Briefly, at the end of each timepoint, the collagen sponges were washed three times with Hanks' balanced salt solution (HBSS) and incubated with calcein AM and ethidium homodimer 1 solution (4 μ M calcein-AM and 2 μ M ethidium homodimer-1) in HBSS at 37 °C, 5 % CO₂ and 95 % relative humidity for 30 min. The collagen sponges were washed with fresh HBSS to remove excess dye. Subsequently, images were acquired using a Fluoroview 1000 confocal laser microscope (FV1000 Shackelton, Olympus, Japan). Live (green) and dead (red) cells were analysed using ImageJ Software (National Institutes of Health, USA).

2.2.12. Cell proliferation assessment

Cell proliferation was assessed using the Quant-iT[™] PicoGreen[®] dsDNA kit (Invitrogen, USA), according to the manufacturer's guidelines. Collagen sponges were washed three times with HBSS at the end of each timepoint, 200 μ l DNase free water was added and frozen at -80 °C until analysis. Collagen sponges were freeze-thawed at least three times in order to lyse the cells. Subsequently, PicoGreen[®] working solution was added to the collagen sponges and incubated at room temperature for 5-10 min, protected from light. Fluorescence was measured at excitation and emission wavelengths of 480 nm and 520 nm using a Varioskan[™] Flash Multimode Reader (Thermo Fisher Scientific, Ireland). The obtained values were normalised to the standard curve, which has been generated with a series of known DNA stock solutions at different concentrations (0, 5, 10, 25, 50, 100, 500 and 1,000 ng/ml).

2.2.13. Cell metabolic activity assessment

Cell metabolic activity was analysed using an alamarBlue[®] assay (Invitrogen, USA), as per manufacturer's protocol. Briefly, collagen sponges were washed

three times with HBSS at the end of each time point, 10 % alamarBlue® was added to each collagen sponge and incubated at 37 °C, 5 % CO₂ and 95 % relative humidity for 3 h. Absorbance was measured at 570 nm and 600 nm using a Varioskan™ Flash Multimode Reader (Thermo Fisher Scientific, Ireland).

2.2.14. Sulphated glycosaminoglycan assessment

The amount of sulphated glycosaminoglycans (sGAG) produced by the hADSCs was quantified using the Blyscan™ sGAG assay kit (Biocolor, UK) according to the manufacturer's protocol. Briefly, collagen sponges were washed three times with HBSS at the end of each timepoint, followed by papain extraction. Then, 1 ml Blyscan™ dye reagent was added to each sample and the samples were mixed gently using an incubated orbital shaker (Thermo Fisher Scientific, Ireland) for 30 min. The samples were then centrifuged at 17,000 g for 10 min. Unbound dye solution was carefully drained and 0.5 ml dissociation reagent was added to the remaining sGAG droplets. 200 µl of each sample was transferred to individual wells of a 96 micro well plate and the absorbance was measured at 656 nm using a Varioskan™ Flash Multimode Reader (Thermo Fisher Scientific, Ireland). Standard aliquots containing 1, 2, 3, 4 and 5 µg GAGs were used as reference standards for standard curve. The sGAG concentration of each collagen sponge was obtained after normalisation to the standard curve.

2.2.15. Histology assessment

Collagen sponges were collected at each time point, washed with 1x PBS and immersion-fixed with 4 % paraformaldehyde for 30 min at room temperature. Collagen sponges were washed with 1x PBS and cryoprotected in PBS containing 15 % and 30 % sucrose, consecutively. Collagen sponges were embedded in optimal cutting temperature compound (Tissue-Tek, USA) and cryo-sectioned using a Cryostat (Leica, CM1850, Germany). Serial sections of 5-10 µm in thickness were collected on adhesion glass slides (Superfrost Plus,

Thermo Fisher Scientific, Austria), air-dried for 1 h at room temperature and stored at -20 °C until further processing. Sections were stained using haematoxylin and eosin (H&E) stain. Nuclei were stained with Mayer's Haemalum solution (Carl Roth, Germany) for 5 min, slides were washed in 0.5 % hydrogen chloride-ethanol solution to destain the connective tissue and subsequently rinsed in 1 % acetic acid to stop the staining reaction. Samples were washed with running tap water for 10 min and sections were counterstained with an alcoholic Eosin Y solution (50 % of ethanol and 0.15 % of eosin) for 30 sec. After rinsing in 1 % acetic acid, samples were dehydrated through graded ethanol and xylene and mounted with distyrene-dibutyl phthalate-xylene (DPX) mounting medium. Images were captured under a light microscope (Olympus, Japan) and analysed using ImageJ Software (National Institutes of Health, USA).

The detection of sulphated GAGs was carried out through Alcian blue staining. Serial sections of collagen sponges were stained with 3 % Alcian blue staining solution for 30 min, followed by a rinse in 1 % acetic acid and then counterstained with nuclear fast red solution (Merck, USA) for 5 min. Then, the slides were briefly rinsed in distilled water, dehydrated with 100 % ethanol and mounted with DPX mounting medium. Images were captured under a light microscope (Olympus, Japan).

2.2.16. RNA isolation

Total RNA was isolated from hADSC-seeded collagen sponges of all groups after 21 days of *in vitro* culture in chondrogenic media and 3 collagen sponges from each group were pooled for each sample. Collagen sponges were homogenised using surgical scalpels before TRI-Reagent® was added. Two consecutive extraction steps using phenol-chloroform were performed. Total RNA was precipitated for 30 min at -20 °C with an equal volume of ice-cold isopropanol, followed by centrifugation for 30 min at 13,000 g at 4 °C. RNA pellets were washed in 75 % ethanol, air dried and resuspended in the Ambion® RNA Storage Solution (Thermo Fisher Scientific, Ireland) supplemented with

RiboSafe RNase inhibitor (Bioline, UK) and stored at -80 °C. RNA yield and purity were determined using a NanoDrop spectrophotometer (Thermo Fisher Scientific, Ireland). An OD 260/280 value between 1.8 and 2.0 was defined as pure RNA. RNA integrity was verified by the Agilent 2100 Bioanalyzer Electrophoresis System (USA). RNA with RNA quality indicator > 8 was defined as intact RNA.

2.2.17. Quantitative real-time PCR

1 µg of total RNA was reverse-transcribed using iScript™ RT-PCR Supermix (BioRad, Ireland). 5 ng cDNA per reaction were subsequently analysed by quantitative PCR using TaqMan® Gene Expression Master Mix (Applied Biosystems, Ireland) and TaqMan® PrimeTime Predesigned qPCR assays (Integrated DNA Technologies, USA) for collagen type I α1 (COL1A1), collagen type II α1 (COL2A1), collagen type III α1 (COL3A1), collagen type Xα1 (COL10A1), aggrecan (ACAN), cartilage oligomeric matrix protein (COMP), SRY-box 9 (SOX9), hypoxanthine phosphoribosyltransferase 1 (HPRT1), pumilio homolog 1 (PUM1) and ribosomal protein lateral stalk subunit P0 (RPLP0). **Table 2.1** lists the genes and the sequence of their respective primers. Default amplification conditions were as follows: 50 °C for 2 min, 95 °C for 10 min, followed by 40 cycles of 95 °C for 15 sec and 60 °C for 1 min using Applied Biosystems (Ireland) StepOnePlus™ Real Time PCR System. Cq values were analysed using qBase+ (Biogazelle, Belgium) and normalised relative quantities (NRQs) were calculated by normalising the data to the expression of 3 validated endogenous control genes (HPRT1, PUM1, RPLP0). Upregulated or downregulated mRNA expression was defined as a fold change ≥ 2.0 , no difference in mRNA expression was defined as a fold change < 2.0 .

Table 2.1: Genes and their primer 1 (forward), probe, and primer 2 (reverse) sequences.

Genes	Primer 1 (5'-3')	Probe (5'-3')	Primer 2 (5'-3')
HPRT1	GTA TTC ATT ATA GTC AAG GGC ATA TCC	/56-FAM/TGG TGA AAA /ZEN/GGA CCC CAC GAA GT/3IABkFQ/	AGA TGG TCA AGG TCG CAA G
PUM1	GAG CAG CAG AGA TGT ATC TTC C	GAC CAG GAC ATT CAC AGA CAC	GAC CAG GAC ATT CAC AGA CAC
RPLP0	CAG ACA GAC ACT GGC AAC A	/56-FAM/CCT GAA GTG /ZEN/CTT GAT ATC ACA GAG GAA ACT /3IABkFQ/	ACA TCT CCC CCT TCT CCT T

COL1A1	GGT TGA TTT CTC ATC ATA GCC AT	/56-FAM/AGG AAA CTT /ZEN/TGC TCC CCA GCT GT/3IABkFQ/	CTG GAC AGC CTG GAC TTC
COL2A1	GTT TTC CAG CTT CAC CAT CAT C	/56-FAM/TGG GAC CAG /ZEN/AGA CAC CAG GTT CA/3IABkFQ/	CCT CAA GGA TTT CAA GGC AAT
COL3A1	TTGGCATGGTTCTGGCTT	/56- FAM/TGGGAACAT/ZEN/CCTC CTTCAACAGCTTC/3IABkFQ/	CTACTTCTCGCTCTGCTT CATC
COL10A1	GTA CCT TGC TCT CCT CTT ACT G	/56-FAM/CCA AGA CAC /ZEN/AGT TCT TCA TTC CCT ACA CC/3IABkFQ/	CAT AAA AGG CCC ACT ACC CA

SOX9	CGT TCT TCA CCG ACT TCC TC	/56-FAM/AAG GGC CGC /ZEN/TTC TCG CTC T/3IABkFQ/	CTG GGC AAG CTC TGG AG
COMP	ACAGGCATCCCCTATACCAT	/56- FAM/ACCCA ACTC/ZEN/AGAC CAGAAGGACAGT/3IABkFQ/	GACCAAAAGGACACAG ACCA
ACAN	AGA TTC ACA GAA CTC CAG TGC	/56-FAM/CGA AGA ACA /ZEN/CCT CCC CCT CAA GTC /3IABkFQ/	ACC TAC GAT GTC TAC TGC TTT G

2.2.18. Statistical analysis

Numerical data are expressed as mean \pm standard deviation. Statistical analysis was performed using SPSS Statistics (USA). Analysis was performed using One-way analysis of variance (ANOVA) for multiple comparisons and 2-sample t-test for pair wise comparisons after confirming the following assumptions of parametric analysis: the distribution from which each of the samples was derived was normal (Shapiro-Wilk normality test) and the variances of the population of the samples were equal to one another (Levene's test for equal variances). Nonparametric statistics were used when either or both of the above assumptions were violated and consequently Kruskal-Wallis test for multiple comparisons or Mann-Whitney test for 2-samples were carried out. Statistical significance was accepted at $p < 0.05$.

2.3. Results

2.3.1. Purity assessment

SDS-PAGE (**Figure 2.1**) revealed a typical electrophoretic mobility of collagen type II, although collagen type I (presence of $\alpha 2$ chain) contamination was evidenced in tracheal and auricular cartilage preparations. No clear differences were observed as a function of biological sex.

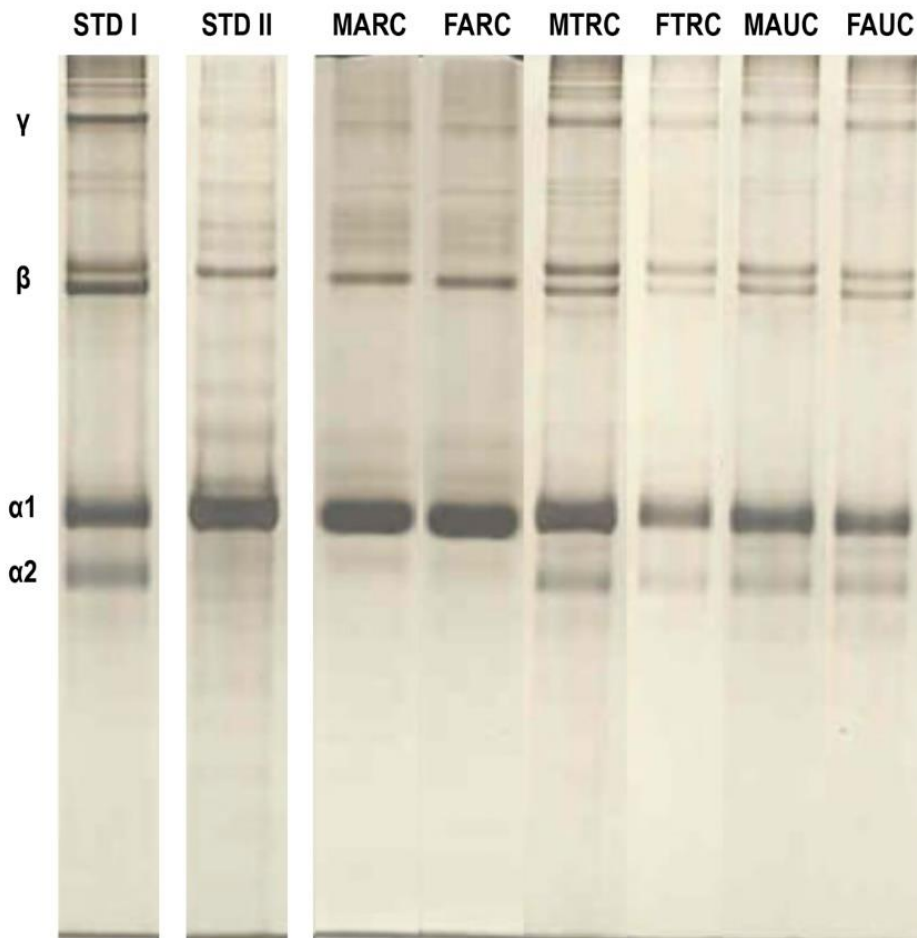


Figure 2.1: SDS-PAGE analysis of collagen preparations extracted from porcine cartilage tissues. SDS-PAGE analysis made apparent that purified collagen type II was extracted from articular cartilage tissues, but some collagen type I impurities were evidenced in tracheal and auricular cartilage preparations. STD I: Standard collagen type I. STD II: Standard collagen type II. MARC: Male

articular cartilage. FARC: Female articular cartilage. MTRC: Male tracheal cartilage. FTRC: Female tracheal cartilage. MAUC: Male auricular cartilage. FAUC: Female auricular cartilage.

2.3.2. Ultrastructural assessment

All materials exhibited a porous structure, as revealed by SEM analysis, and subsequent quantitative pore size and porosity analyses of the produced sponges revealed no apparent differences ($p > 0.05$) as function of tissue, biological sex and crosslinking (**Figure 2.2**).

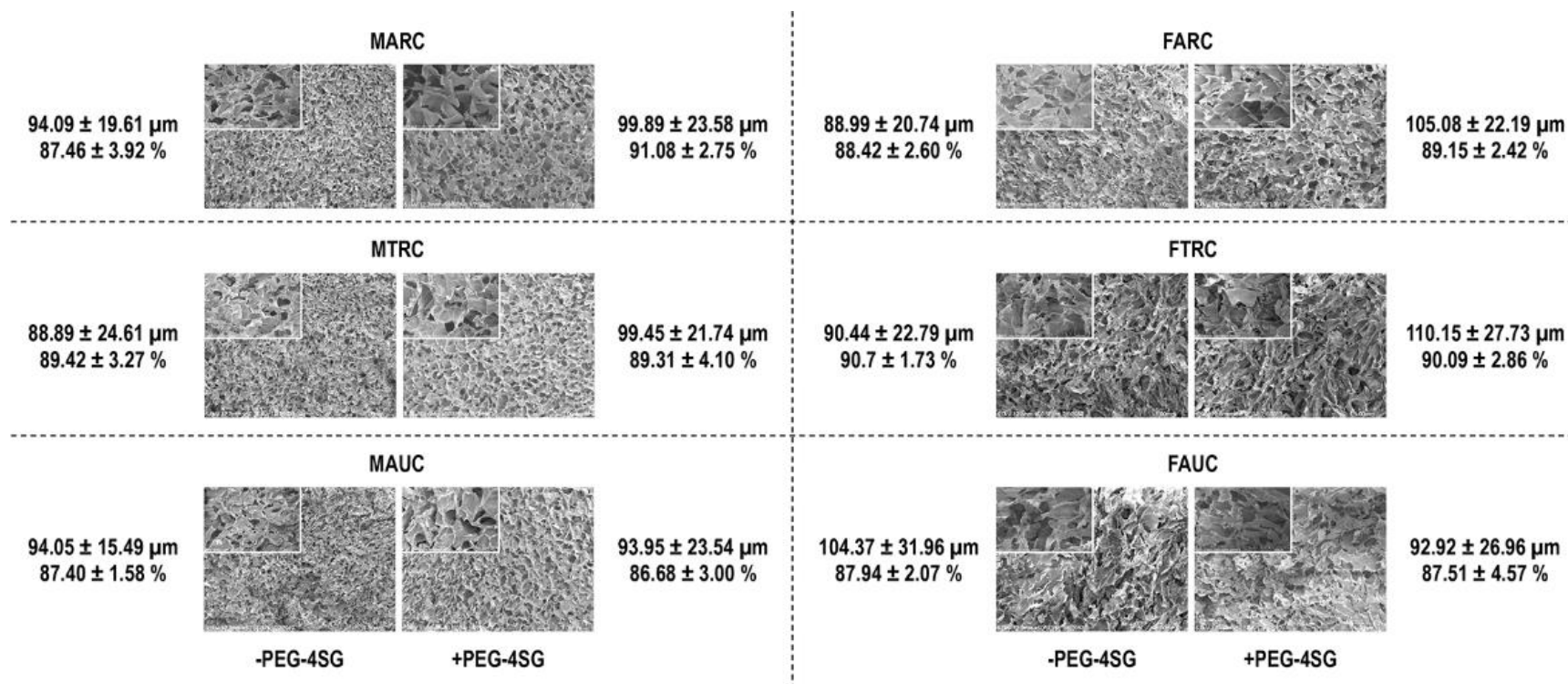


Figure 2.2: SEM and complementary pore size (μm) and porosity (%) analyses of the produced scaffolds. The analyses did not reveal any significant ($p > 0.05$) differences between the produced scaffolds. MARC: Male articular cartilage. FARC: Female articular cartilage.

MTRC: Male tracheal cartilage. FTRC: Female tracheal cartilage. MAUC: Male auricular cartilage. FAUC: Female auricular cartilage.
-PEG-4SG: No crosslinked groups. +PEG-4SG: Crosslinked groups.

2.3.3. Biomechanical assessment

Biomechanical assessment (**Table 2.2**) made apparent that among non-crosslinked and crosslinked groups, the MARC and FARC groups exhibited higher ($p < 0.005$) compression stress and elastic modulus, whilst no significant ($p > 0.05$) differences were observed as a function of biological sex within a tissue group. Crosslinking significantly ($p < 0.005$) increased the compression stress and elastic modulus in all groups.

2.3.4. Thermal properties assessment

DSC analysis (**Table 2.2**) revealed that crosslinked samples exhibited significantly ($p < 0.005$) higher denaturation temperature than their non-crosslinked counterparts and that no significant ($p > 0.05$) differences in denaturation temperature were observed as a function of tissue and biological sex within the non-crosslinked and crosslinked groups.

2.3.5. Free amines assessment

Free amine quantification (**Table 2.2**) revealed that within the male and female non-crosslinked and crosslinked groups, the MARC and FARC groups, respectively, had the highest ($p < 0.0005$) % of free amines. Crosslinking significantly ($p < 0.005$) reduced the % of free amines of each group. Within a tissue, no significant ($p > 0.05$) differences were observed in free amines as a function of biological sex.

Table 2.2: Mechanical properties, denaturation temperature and free amine content of the produced scaffolds as a function of tissue, biological sex and crosslinking. Among the non-crosslinked and crosslinked groups, the MARC and FARC groups exhibited higher ($p < 0.005$) compression stress and elastic modulus, whilst no significant ($p > 0.05$) differences were observed as a function of biological sex within a tissue group. Crosslinking significantly ($p < 0.005$) increased the compression stress and elastic modulus in all groups. Crosslinking significantly ($p < 0.005$) increased the denaturation temperature of each group and no differences ($p > 0.05$) in denaturation temperature were observed as a function of tissue and biological sex within the non-crosslinked and crosslinked groups. Articular cartilage groups ($p < 0.0005$) and non-crosslinked groups ($p < 0.005$) exhibited significantly higher % of free amines than their respectively counterparts. MARC: Male articular cartilage. FARC: Female articular cartilage. MTRC: Male tracheal cartilage. FTRC: Female tracheal cartilage. MAUC: Male auricular cartilage. FAUC: Female auricular cartilage. -PEG-4SG: No crosslinked groups. +PEG-4SG: Crosslinked groups.

	MARC		FARC		MTRC		FTRC		MAUC		FAUC	
	-PEG-	+PEG-	-PEG-	+PEG-	-PEG-	+PEG-	-PEG-	+PEG-	-PEG-	+PEG-	-PEG-	+PEG-
	4SG	4SG	4SG	4SG	4SG	4SG	4SG	4SG	4SG	4SG	4SG	4SG
Stress (kPa)	2.38 ±	4.76 ±	2.55 ±	4.75 ±	1.43 ±	3.41 ±	1.59 ±	3.44 ±	1.64 ±	3.28 ±	1.69 ±	3.36 ±
	0.26	0.5	0.21	0.37	0.4	0.61	0.08	0.42	0.21	0.31	0.22	0.28
Modulus (kPa)	7.89 ±	15.75 ±	8.41 ±	15.67 ±	4.78 ±	11.24 ±	5.25 ±	11.35 ±	5.43 ±	10.83 ±	5.58 ±	11.07 ±
	0.83	1.71	0.76	1.17	1.34	2.03	0.28	1.43	0.69	1.00	0.69	0.97
Denaturation Temperature (°C)	46.68 ±	54.27 ±	46.34 ±	53.74 ±	47.43 ±	53.55 ±	47.18 ±	53.44 ±	47.10 ±	54.26 ±	46.58 ±	53.96 ±
	0.19	1.52	0.63	0.60	0.72	1.11	0.84	1.72	0.73	0.95	0.22	0.41
Free Amines (%)	10.67 ±	7.43 ±	11.67 ±	6.59 ±	6.79 ±	4.90 ±	6.79 ±	4.83 ±	6.84 ±	5.25 ±	6.98 ±	4.93 ±
	0.64	0.29	0.69	0.98	0.16	0.25	0.32	0.34	0.37	0.55	0.44	0.19

2.3.6. Resistance to enzymatic degradation assessment

Collagenase digestion analysis (**Figure 2.3**) revealed that all non-crosslinked samples were completely degraded (< 3 % remaining mass) within 12 h of collagenase digestion, whilst crosslinked samples were more resistant to collagenase digestion (~ 30 % remaining mass after 24 h of collagenase digestion). Within the non-crosslinked male and female groups, the MARC and FARC groups were significantly ($p < 0.0005$) more resistant to collagenase digestion than the MTRC and MAUC and FTRC and FAUC groups, respectively, for the first 6 h. Within non-crosslinked tissues, no significant ($p > 0.05$) differences in susceptibility to collagenase digestion were observed as a function of biological sex. Within the crosslinked male and female groups, the MARC and FARC groups were significantly ($p < 0.005$) more resistant to collagenase digestion than the MTRC and MAUC and FTRC and FAUC groups, respectively, for the first 3 h. Crosslinking significantly ($p < 0.0005$) increased the resistance to collagenase digestion of each group.

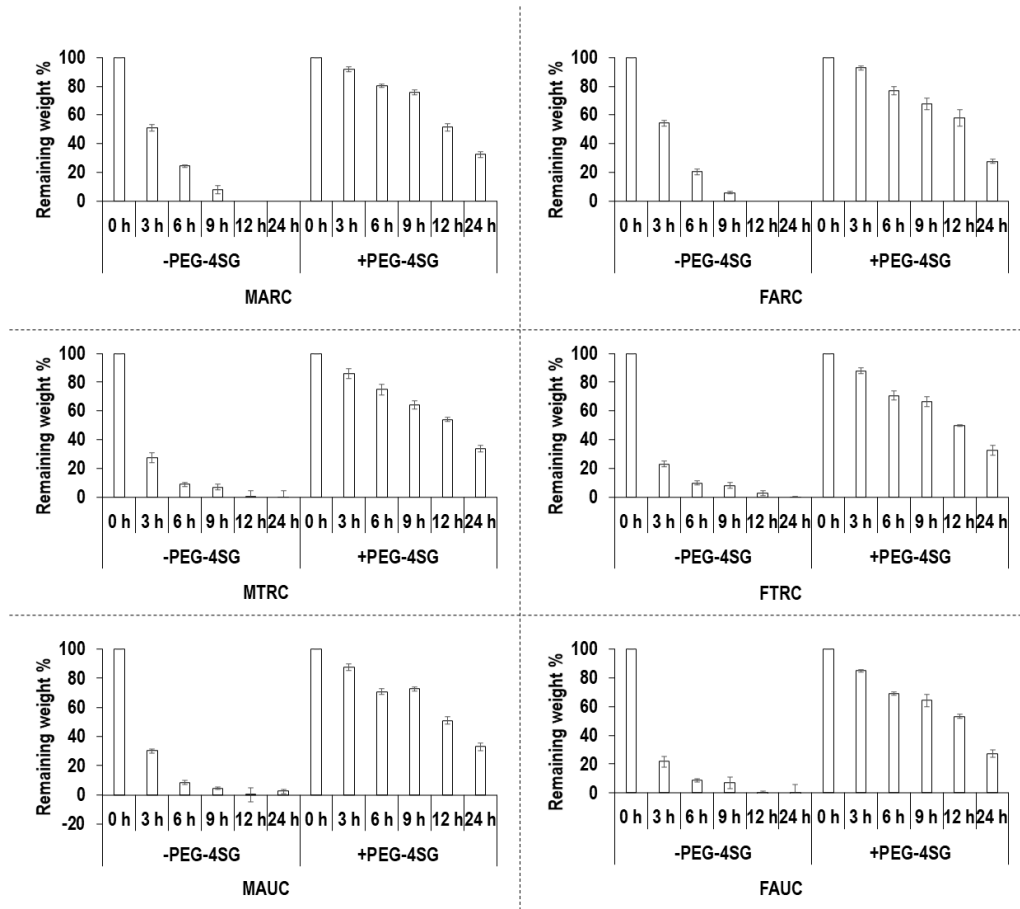


Figure 2.3: Resistance to collagenase digestion analysis of the produced scaffolds. Non-crosslinked male and female articular cartilage scaffolds were significantly ($p < 0.0005$) more resistant to enzymatic degradation than the MTRC and MAUC and FTRC and FAUC groups, respectively, for the first 6 h. No significant ($p > 0.05$) differences in susceptibility to collagenase digestion were observed as a function of biological sex within non-crosslinked tissues. Crosslinked groups MARC and FARC groups were significantly ($p < 0.005$) more resistant to collagenase digestion than the MTRC and MAUC and FTRC and FAUC groups, respectively, for the first 3 h. Crosslinking significantly ($p < 0.0005$) increased the resistance to collagenase digestion of each group. MARC: Male articular cartilage. FARC: Female articular cartilage. MTRC: Male tracheal cartilage. FTRC: Female tracheal cartilage. MAUC: Male auricular cartilage. FAUC: Female auricular cartilage. -PEG-4SG: Non-crosslinked groups. +PEG-4SG: Crosslinked groups.

2.3.7. Basic cellular function assessment

Cell viability (**Figure 2.4A**), DNA concentration (**Figure 2.4B**) and metabolic activity (**Figure 2.4C**) analyses indicated that all scaffolds equally ($p > 0.05$) supported hADSCs attachment, proliferation and growth up to 21 days in culture (longest timepoint assessed) independently of the tissue and the biological sex. Qualitative cell infiltration and ECM synthesis analysis via H&E staining (**Figure 2.4D**) revealed a homogeneous cell distribution throughout the scaffolds and increased ECM synthesis as a function of time in culture independently of the tissue and the biological sex.

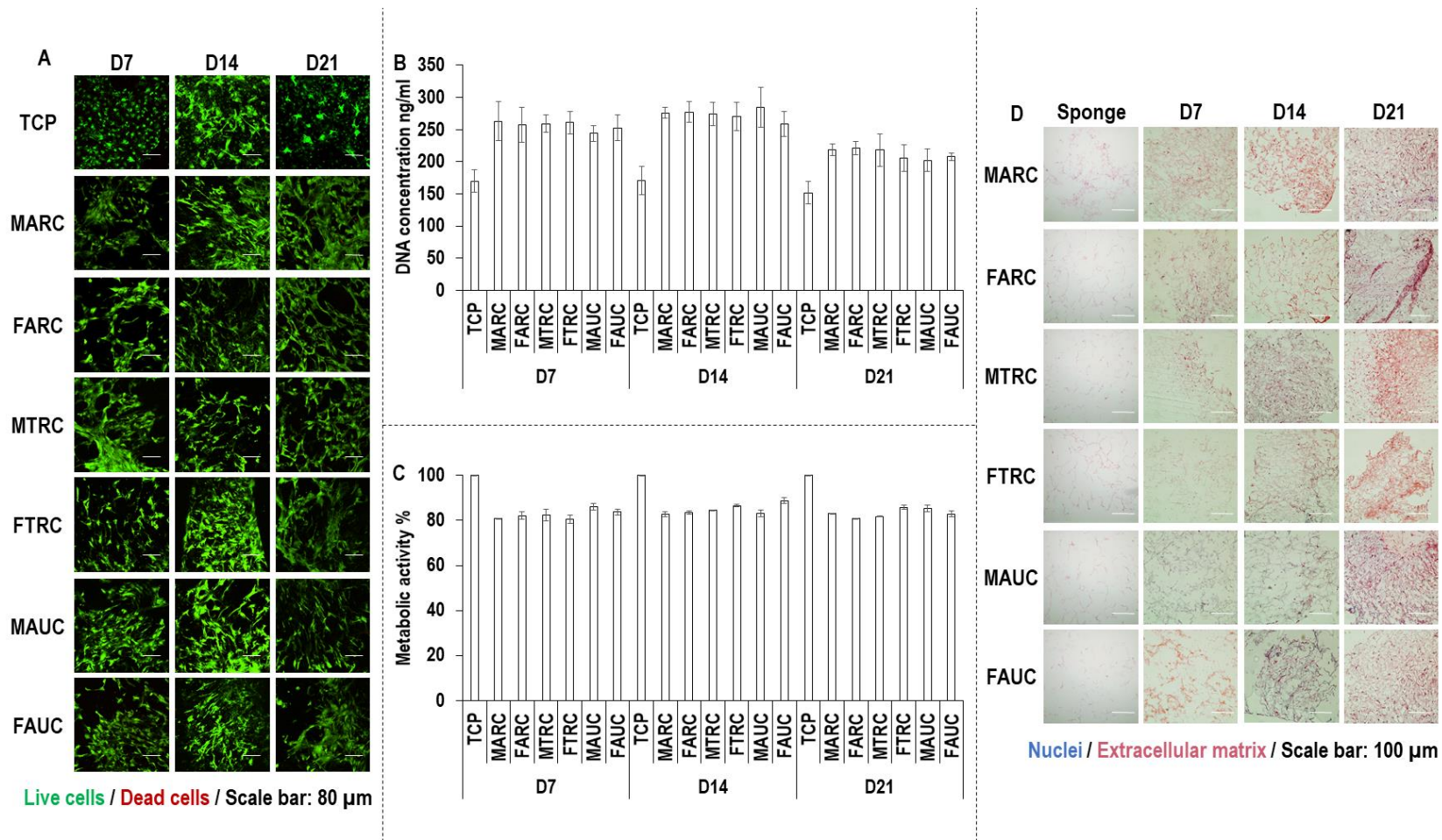


Figure 2.4: hADSC viability (**A**), DNA concentration (**B**), metabolic activity (**C**) and infiltration and ECM synthesis (**D**) as a function of tissue and biological sex for up to 21 days in culture (longest timepoint assessed). No apparent differences ($p > 0.05$) were detected. TCP: Tissue culture plastic. D: Day. MARC: Male articular cartilage. FARC: Female articular cartilage. MTRC: Male tracheal cartilage. FTRC: Female tracheal cartilage. MAUC: Male auricular cartilage. FAUC: Female auricular cartilage.

2.3.8. Chondrogenic potential assessment

Alcian blue staining (**Figure 2.5A**) and sGAG quantification (**Figure 2.5B**) revealed no differences ($p > 0.05$) as a function of biological sex at any timepoint, but a significant ($p < 0.0005$) increase in sGAG content from day 14 to day 21 for all groups, with the articular cartilage derived scaffolds to induce the highest ($p < 0.0005$) increase.

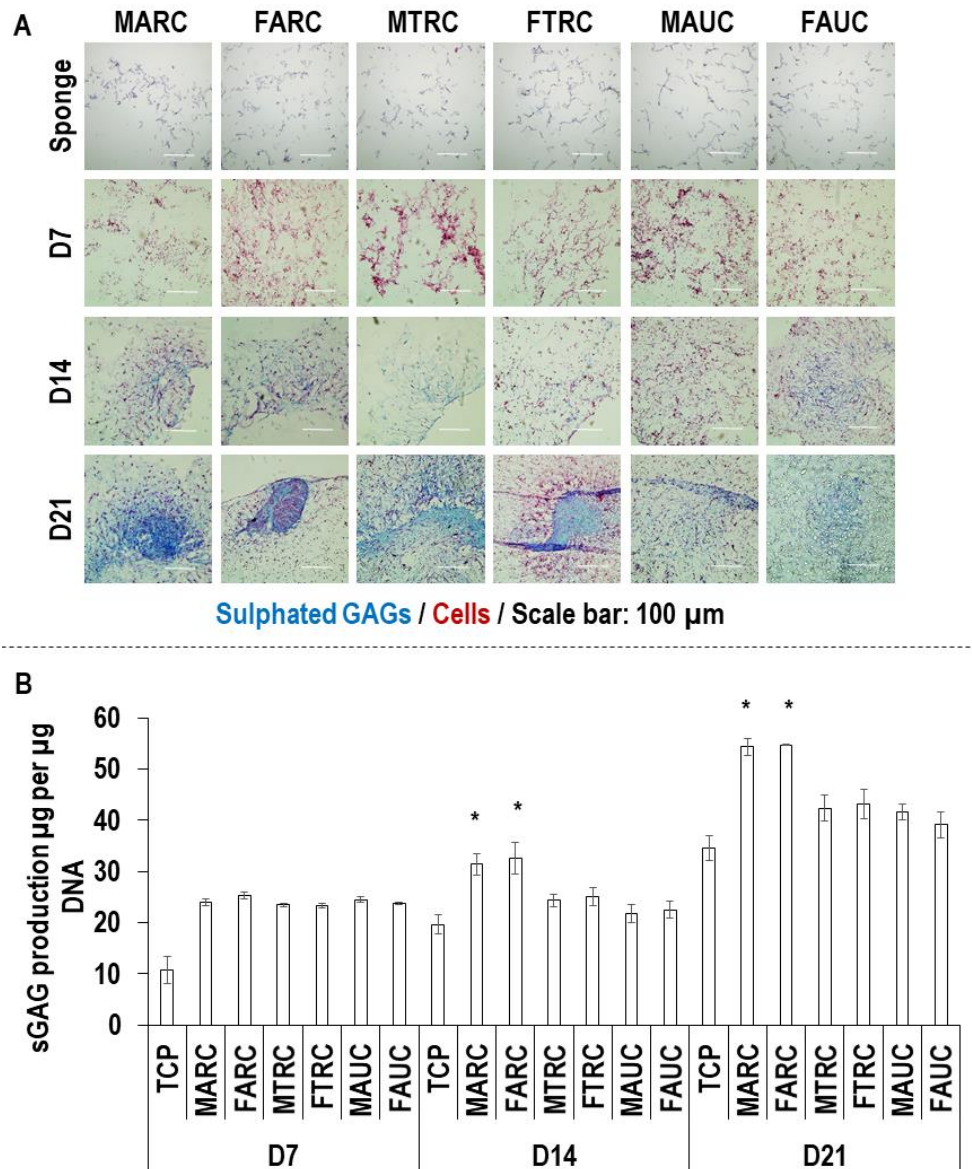


Figure 2.5: Alcian blue staining (**A**) and sGAG quantification (**B**) analyses as a function of tissue and biological sex for up to 21 days in culture. The analyses revealed that the articular cartilage derived scaffolds induce the highest ($p < 0.0005$; indicated with * in the graph) increase in sGAG content at day 14 and day 21. TCP: Tissue culture plastic. D: Day. MARC: Male articular cartilage. FARC: Female articular cartilage. MTRC: Male tracheal cartilage. FTRC:

Female tracheal cartilage. MAUC: Male auricular cartilage. FAUC: Female auricular cartilage.

Gene expression analysis after 21 days of chondrogenic induction (**Figure 2.6**) revealed no differences (fold change < 2.0) in COL1A1, COL3A1, COL10A1 and COMP mRNA levels between the experimental groups and all experimental groups showed higher (fold change ≥ 2.0) COL3A1, COL10A1 and COMP mRNA levels than TCP. With respect to SOX9 mRNA levels, the male articular cartilage showed higher (fold change ≥ 2.0) SOX9 mRNA expression compared to the female tracheal cartilage and all experimental groups showed higher (fold change ≥ 2.0) SOX9 mRNA levels than TCP. Both male and female articular cartilage derived scaffolds exhibited higher (fold change ≥ 2.0) ACAN mRNA expression compared to the female auricular cartilage scaffolds and the female articular cartilage scaffolds showed higher (fold change ≥ 2.0) ACAN mRNA expression than male and female tracheal cartilage scaffolds and TCP. COL2A1 expression was only detected in male articular cartilage, female tracheal cartilage and female auricular cartilage groups and among them, the male articular cartilage derived scaffolds showed the highest (fold change ≥ 2.0) mRNA expression of COL2A1.

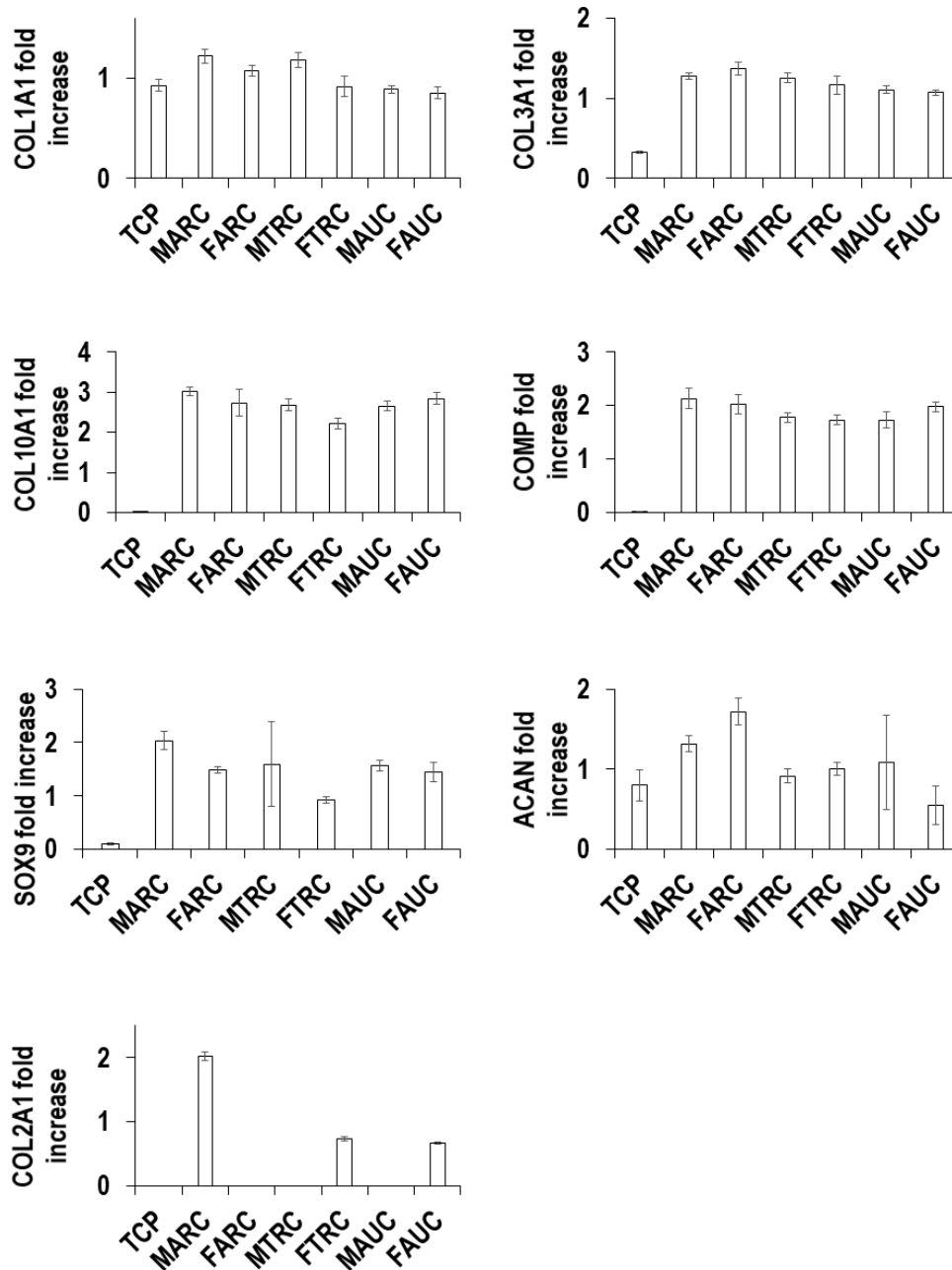


Figure 2.6: Gene expression analysis after 21 days of chondrogenic induction. The analysis revealed no difference (fold change < 2.0) in COL1A1, COL3A1, COL10A1 and COMP mRNA levels between the experimental groups. The male articular cartilage scaffold induced higher (fold change ≥ 2.0) SOX9 expression than the female tracheal cartilage scaffold. The female articular cartilage

scaffolds exhibited higher (fold change ≥ 2.0) ACAN mRNA expression than the male and female tracheal and female auricular cartilage scaffolds. The male articular cartilage scaffolds exhibited the highest (fold change ≥ 2.0) COL2A1 mRNA expression. TCP: Tissue culture plastic. MARC: Male articular cartilage. FARC: Female articular cartilage. MTRC: Male tracheal cartilage. FTRC: Female tracheal cartilage. MAUC: Male auricular cartilage. FAUC: Female auricular cartilage.

2.4. Discussion

Among the various natural and synthetic materials available for scaffold fabrication for cartilage repair and regeneration, collagen type II has shown great potential, considering that it is the main ECM component of cartilage (51) and collagen type II derived scaffolds have been shown to maintain chondrocyte phenotype (52, 53), to drive stem cells towards chondrogenic lineage (54, 55) and to induce hyaline cartilage in preclinical models (30, 56). Considering though the batch-to-batch variability of animal extracted biomolecules, it is imperative to standardise the process for consistency purposes. To this end, herein, we assessed the influence of biological sex (male, female), tissue (articular, tracheal, auricular) and crosslinking (no crosslinked and 4-arm polyethylene glycol succinimidyl glutarate crosslinked) on the biophysical, biochemical and biological properties of pepsin extracted porcine collagen type II scaffolds.

Pure collagen type II was extracted from male and female articular cartilage, as evidenced by a typical collagen type II electrophoretic mobility, corresponding to three $\alpha 1(\text{II})$ chains as has been shown before from various articular cartilage collagen type II preparations (28, 57-59). In contrast, collagen extracted from male and female tracheal and auricular cartilage presented a mixture of collagen type I and collagen type II collagen, shown by the presence of $\alpha 2(\text{I})$ chain of collagen type I (60, 61). Type I collagen contamination most probably resulted from the perichondrium surrounding tracheal and auricular cartilage, but not articular cartilage, which mainly consists of collagen type I (62).

Cartilage tissue source, biological sex and crosslinking did not significantly affect the macrostructure of the fabricated collagen type II scaffolds. All scaffolds had pore size and porosity range of 80-110 μm and 80-95 %, respectively, that has been shown to induce chondrogenic differentiation in human stem cell cultures (63-65).

Collagen scaffolds from male and female articular cartilage exhibited significantly higher stress and modulus values than their tracheal and auricular cartilage counterparts, with no significant differences as a function of biological

sex. This can be explained considering the mechanical properties of the tissue from which collagen was extracted from (modulus of porcine articular cartilage 7.2 MPa (66), tracheal cartilage 1.78 MPa (67), auricular cartilage 0.25 MPa (68)) and therefore our data suggest that collagen may retain tissue memory. It is worth noting that a previous publication showed that the addition of collagen type II to collagen type I gels significantly decreased their stiffness, but this was attributed to the reduction of the total collagen in the system (69), as opposed to the difference in mechanical properties between the different collagen types (it is also worth noting that the collagen type I was from rat tail tendon and the collagen type II was chicken sterna and therefore direct comparison cannot be conducted). In accordance with previous publications (70), crosslinking significantly increases the mechanical properties of the produced collagen sponges.

Collagen extracted from porcine male and female articular, tracheal and auricular cartilage exhibited comparable denaturation temperatures of approximately 47 °C, indicating that thermal stability is independent of tissue source and biological sex and crosslinking increased the denaturation temperature of all scaffolds to approximately 54 °C. Previous studies have shown similar denaturation temperature values for non-crosslinked collagen type II scaffolds (71, 72). The observed increase in denaturation temperature as a function of crosslinking is also well established in the literature for collagen type II scaffolds (71).

With respect to free amine content and resistance to collagenase digestion of the non-crosslinked collagen type II scaffolds, no differences were observed as function of biological sex within the different tissues and among the different tissues, the articular cartilage derived collagen type II scaffolds (the male within the male and the female within the female groups of the different tissues) had the highest free amine content and resistance to collagenase digestion. Obviously, these observations are rather contradictory, considering that higher free amine content is associated with less crosslinking and lower resistance to enzymatic degradation (73). As the tissues were from the same animals and the same

extraction and freeze-drying protocols were used for all groups, we rule out the age of the animals and the process, which can affect the crosslinking density (40, 74). We therefore speculate that the remnant collagen type I in the tracheal and auricular cartilage preparations may be the reason for these unusual results; possibly electrostatic interactions between collagen type I and collagen type II reduced the free amines, without affecting the mechanical properties. The observed differences were diminished under crosslinking and, in accordance to previous works (75), crosslinking increased the resistance to collagenase degradation and reduced the free amine content.

Biological analysis using hADSCs did not reveal any differences as a function of tissue origin, biological sex and crosslinking, which in agreement with previous publications that have been shown collagen type II scaffolds to support physiological cell growth (76) and 4-arm polyethylene glycol succinimidyl glutarate to be cytocompatible (43). Histological analysis also demonstrated equal cell and ECM distribution throughout the scaffolds independently of the tissue and the biological sex of the extracted collagen, further confirming that the pore size and porosity were suitable to allow cell migration and colonisation, as has been shown before (71). Similarly to mechanical properties, Alcian blue staining and sGAG quantification revealed a tissue (but not biological sex) dependent chondrogenesis. Specifically, both male and female articular cartilage sponges were significantly more chondrogenic than their tracheal and auricular cartilage counterparts. This can be attributed to the lack of collagen type I in the articular cartilage derived sponges. To substantiate this one should consider that a previous study has shown that collagen type I / collagen type II blends (3 to 1 ratio) had greater chondrogenic potential than pure collagen type I scaffolds (77) and other studies have shown higher chondrogenic potential of collagen type II scaffolds as opposed to collagen type I scaffolds in human bone marrow stem cells (54), bovine meniscus cells (78) and canine chondrocytes (52). With respect to gene analysis, in general all collagen scaffolds were significantly more chondrogenic than the TCP, which can be attributed to their (three-) dimensionality; it is after all well established in the field the need of a three-

dimensional environment for effective chondrogenic induction (79, 80). Between the groups, no differences were observed in mRNA levels of COL1A1, COL3A1, COL10A1 and COMP. It is interesting to note that male articular cartilage sponges induced higher SOX9 mRNA expression than female tracheal cartilage sponges, female articular cartilage sponges induced the highest ACAN mRNA expression and the male articular cartilage sponges induced the highest COL2A1 mRNA expression. Although it is clear that the male cartilage sponges follow the same trend as the mechanical properties and the histology with respect to tissue memory, we are not clear why the female articular cartilage sponges did not also follow the same trend with respect to COL2A1. One possible explanation could be the endpoint; although 21 days are traditionally used for chondrogenesis (81-83), other studies advocate longer timepoints to engineer mature cartilage-like tissue (e.g. 28 days (84-87), 42 days (88), 49 days (89), 56 days (90, 91), 84 days (92)). Of course, the high variability between donors cannot be excluded.

One should also note that despite the positive data that have been obtained over the years with collagen type II scaffolds, their commercialisation has been jeopardised by early studies that showed injections of native collagen type II from human, chick, murine and bovine cartilage to induce inflammatory arthritis in rats (93-95); native collagen type II from foetal bovine cartilage to induce arthritis in non-human primates (96); and antibodies of native and denatured collagen type II to be present in patients with early rheumatoid arthritis and chronic gouty arthritis (97-99). However, it has been shown that effectively crosslinked collagen type II, even from bovine nasal septal cartilage, does not induce arthritis in rats (100). Porcine collagen type II may be the ideal scaffold material for cartilage engineering, as *per os* administered porcine collagen type II has been shown to reduce pain in a rat osteoarthritis model (101) and porcine collagen type II scaffolds have been shown to maintain chondrogenic phenotype of rabbit (102), human (103) and ovine chondrocytes (104) and to promote the formation of neocartilage (105). Based on data obtained from this study and previous studies of our groups with collagen type I, we feel that pepsin extracted (40) and 4-arm polyethylene glycol succinimidyl glutarate (42) stabilised

articular cartilage derived collagen type II devices will have reduced immunogenicity and appropriate mechanical resilience, cytocompatibility and chondrogenic potential for cartilage engineering.

2.5. Conclusions

The use of collagen type II scaffolds for cartilage engineering has been supported, considering that cartilage is primarily comprised of collagen type II. As animal-derived products are of high variability, it is imperative to identify suitable collagen type II sources. This study suggests an extracted collagen type II memory of the tissue from which it was extracted. Specifically, our data advocate the use of male / female articular cartilage (as opposed to tracheal and auricular cartilage) derived collagen type II scaffolds for cartilage engineering applications, as judged by resistance to enzymatic degradation, biomechanical properties and chondrogenic differentiation potential.

2.6. References

1. Gomoll, A. H., Minas, T. The quality of healing: Articular cartilage. *Wound Repair Regen.* 2014;22(Suppl 1):30-8.
2. Tuan, R. S., Chen, A. F., Klatt, B. A. Cartilage regeneration. *J Am Acad Orthop Surg.* 2013;21(5):303-11.
3. Morales-Ivorra, I., Romera-Baures, M., Roman-Viñas, B., Serra-Majem, L. Osteoarthritis and the Mediterranean diet: A systematic review. *Nutrients.* 2018;10(8):1030.
4. Menon, J., Mishra, P. Health care resource use, health care expenditures and absenteeism costs associated with osteoarthritis in US healthcare system. *Osteoarthritis Cartilage.* 2018;26(4):480-4.
5. Salih, S., Sutton, P. Obesity, knee osteoarthritis and knee arthroplasty: A review. *BMC Sports Sci Med Rehabil.* 2013;5(1):25.
6. Misra, D., Fielding, R. A., Felson, D. T., Niu, J., Brown, C., Nevitt, M., Lewis, C. E., Torner, J., Neogi, T. Risk of knee osteoarthritis with obesity, sarcopenic obesity, and sarcopenia. *Arthritis Rheumatol.* 2019;71(2):232-7.
7. Williams, R. J. R., Harnly, H. W. Microfracture: Indications, technique, and results. *Instr Course Lect.* 2007;56:419-28.
8. Rodríguez-Merchán, E. C. The treatment of cartilage defects in the knee joint: Microfracture, mosaicplasty, and autologous chondrocyte implantation. *Am J Orthop (Belle Mead NJ).* 2012;41(5):236-9.
9. Becher, C., Malahias, M. A., Ali, M. M., Maffulli, N., Thermann, H. Arthroscopic microfracture vs. arthroscopic autologous matrix-induced chondrogenesis for the treatment of articular cartilage defects of the talus. *Knee Surg Sports Traumatol Arthrosc.* 2019;27(9):2731-6.
10. Desandis, B. A., Haleem, A. M., Sofka, C. M., O'malley, M. J., Drakos, M. C. Arthroscopic treatment of osteochondral lesions of the talus using juvenile articular cartilage allograft and autologous bone marrow aspirate concentration. *J Foot Ankle Surg.* 2018;57(2):273-80.
11. Vangsness, C. T. J., Higgs, G., Hoffman, J. K., Farr, J., Davidson, P. A., Milstein, F., Geraghty, S. Implantation of a novel cryopreserved viable

osteochondral allograft for articular cartilage repair in the knee. *J Knee Surg.* 2018;31(6):528-35.

12. Stone, K. R., Walgenbach, A. W., Freyer, A., Turek, T. J., Speer, D. P. Articular cartilage paste grafting to full-thickness articular cartilage knee joint lesions: A 2-to 12-year follow-up. *Arthroscopy.* 2006;22(3):291-9.

13. Wakitani, S., Nawata, M., Tensho, K., Okabe, T., Machida, H., Ohgushi, H. Repair of articular cartilage defects in the patello - femoral joint with autologous bone marrow mesenchymal cell transplantation: Three case reports involving nine defects in five knees. *J Tissue Eng Regen Med.* 2007;1(1):74-9.

14. Mumme, M., Barbero, A., Miot, S., Wixmerten, A., Feliciano, S., Wolf, F., Asnaghi, A. M., Baumhoer, D., Bieri, O., Kretzschmar, M., Pagenstert, G., Haug, M., Schaefer, D. J., Martin, I., Jakob, M. Nasal chondrocyte-based engineered autologous cartilage tissue for repair of articular cartilage defects: An observational first-in-human trial. *Lancet.* 2016;388(10055):1985-94.

15. Brittberg, M., Lindahl, A., Nilsson, A., Ohlsson, C., Isaksson, O., Peterson, L. Treatment of deep cartilage defects in the knee with autologous chondrocyte transplantation. *N Engl J Med.* 1994;331(14):889-95.

16. Holland, T. A., Mikos, A. G. Advances in drug delivery for articular cartilage. *J Control Release.* 2003;86(1):1-14.

17. Gao, X., Cheng, H., Awada, H., Tang, Y., Amra, S., Lu, A., Sun, X., Lv, G., Huard, C., Wang, B., Bi, X., Wang, Y., Huard, J. A comparison of BMP2 delivery by coacervate and gene therapy for promoting human muscle-derived stem cell-mediated articular cartilage repair. *Stem Cell Res Ther.* 2019;10(1):346.

18. Fathi-Achachelouei, M., Keskin, D., Bat, E., Vrana, N. E., Tezcaner, A. Dual growth factor delivery using PLGA nanoparticles in silk fibroin/PEGDMA hydrogels for articular cartilage tissue engineering. *J Biomed Mater Res B Appl Biomater.* 2020;108(5):2041-62.

19. Pot, M. W., Gonzales, V. K., Buma, P., Inthout, J., Van Kuppevelt, T. H., De Vries, R. B. M., Daamen, W. F. Improved cartilage regeneration by implantation of acellular biomaterials after bone marrow stimulation: A systematic review and meta-analysis of animal studies. *PeerJ.* 2016;4:e2243.

20. Sivandzade, F., Mashayekhan, S. Design and fabrication of injectable microcarriers composed of acellular cartilage matrix and chitosan. *J Biomater Sci Polym Ed.* 2018;29(6):683-700.
21. Graceffa, V., Vinatier, C., Guicheux, J., Stoddart, M., Alini, M., Zeugolis, D. I. Chasing chimeras—the elusive stable chondrogenic phenotype. *Biomaterials.* 2019;192:199-225.
22. Caron, M. M., Emans, P. J., Coolsen, M. M., Voss, L., Surtel, D. A., Cremers, A., Van Rhijn, L. W., Welting, T. J. Redifferentiation of dedifferentiated human articular chondrocytes: Comparison of 2D and 3D cultures. *Osteoarthritis Cartilage.* 2012;20(10):1170-8.
23. Kudva, A. K., Luyten, F. P., Patterson, J. Initiating human articular chondrocyte re-differentiation in a 3D system after 2D expansion. *J Mater Sci Mater Med.* 2017;28(10):156.
24. Yilmaz, E. N., Zeugolis, D. I. Electrospun polymers in cartilage engineering—State of play. *Front Bioeng Biotechnol.* 2020;8:77.
25. Kalkan, R., Nwekwo, C. W., Adali, T. The use of scaffolds in cartilage regeneration. *Crit Rev Eukaryot Gene Expr.* 2018;28(4):343-8.
26. Eyre, D. Articular cartilage and changes in arthritis: Collagen of articular cartilage. *Arthritis Res.* 2001;4(1):30.
27. Thomas, J. T., Ayad, S., Grant, M. E. Cartilage collagens: Strategies for the study of their organisation and expression in the extracellular matrix. *Ann Rheum Dis.* 1994;53(8):488-96.
28. Sorushanova, A., Delgado, L. M., Wu, Z., Shologu, N., Kshirsagar, A., Raghunath, R., Mullen, A. M., Bayon, Y., Pandit, A., Raghunath, M., Zeugolis, D. I. The collagen suprafamily: From biosynthesis to advanced biomaterial development. *Adv Mater.* 2019;31(1):e1801651.
29. Malemud, C. J., Stevenson, S., Mehraban, F., Papay, R. S., Purchio, A. F., Goldberg, V. M. The proteoglycan synthesis repertoire of rabbit chondrocytes maintained in type II collagen gels. *Osteoarthritis Cartilage.* 1994;2(1):29-41.

30. Lee, C. R., Grodzinsky, A. J., Hsu, H. P., Spector, M. Effects of a cultured autologous chondrocyte-seeded type II collagen scaffold on the healing of a chondral defect in a canine model. *J Orthop Res.* 2003;21(2):272-81.
31. Yang, K., Sun, J., Wei, D., Yuan, L., Yang, J., Guo, L., Fan, H., Zhang, X. Photo-crosslinked mono-component type II collagen hydrogel as a matrix to induce chondrogenic differentiation of bone marrow mesenchymal stem cells. *J Mater Chem B.* 2017;5(44):8707-18.
32. Lu, Z., Doulabi, B. Z., Huang, C., Bank, R. A., Helder, M. N. Collagen type II enhances chondrogenesis in adipose tissue-derived stem cells by affecting cell shape. *Tissue Eng Part A.* 2010;16(1):81-90.
33. Lian, C., Wang, X., Qiu, X., Wu, Z., Gao, B., Liu, L., Liang, G., Zhou, H., Yang, X., Peng, Y., Liang, A., Xu, C., Huang, D., Su, P. Collagen type II suppresses articular chondrocyte hypertrophy and osteoarthritis progression by promoting integrin $\beta 1$ -SMAD1 interaction. *Bone Res.* 2019;7:8.
34. Buma, P., Pieper, J. S., Van Tienen, T., Van Susante, J. L., Van Der Kraan, P. M., Veerkamp, J. H., Van Den Berg, W. B., Veth, R. P., Van Kuppevelt, T. H. Cross-linked type I and type II collagenous matrices for the repair of full-thickness articular cartilage defects—a study in rabbits. *Biomaterials.* 2003;24(19):3255-63.
35. Christensen, B. B., Foldager, C. B., Jensen, J., Jensen, N. C., Lind, M. Poor osteochondral repair by a biomimetic collagen scaffold: 1-to 3-year clinical and radiological follow-up. *Knee Surg Sports Traumatol Arthrosc.* 2016;24(7):2380-7.
36. Schüttler, K. F., Götschenberg, A., Klasan, A., Stein, T., Pehl, A., Roessler, P. P., Figiel, J., Heyse, T. J., Efe, T. Cell-free cartilage repair in large defects of the knee: Increased failure rate 5 years after implantation of a collagen type I scaffold. *Arch Orthop Trauma Surg.* 2019;139(1):99-106.
37. Nehrer, S., Breinan, H. A., Ramappa, A., Hsu, H. P., Minas, T., Shortkroff, S., Sledge, C. B., Yannas, I. V., Spector, M. Chondrocyte-seeded collagen matrices implanted in a chondral defect in a canine model. *Biomaterials.* 1998;19(24):2313-28.

38. Chen, W. C., Yao, C. L., Wei, Y. H., Chu, I. M. Evaluating osteochondral defect repair potential of autologous rabbit bone marrow cells on type II collagen scaffold. *Cytotechnology*. 2011;63(1):13-23.
39. Zeugolis, D. I., Paul, R. G., Attenburrow, G. Factors influencing the properties of reconstituted collagen fibers prior to self-assembly: Animal species and collagen extraction method. *J Biomed Mater Res A*. 2008;86(4):892-904.
40. Delgado, L. M., Shologu, N., Fuller, K., Zeugolis, D. I. Acetic acid and pepsin result in high yield, high purity and low macrophage response collagen for biomedical applications. *Biomed Mater*. 2017;12(6):065009.
41. Lynn, A. K., Yannas, I. V., Bonfield, W. Antigenicity and immunogenicity of collagen. *J Biomed Mater Res B Appl Biomater*. 2004;71(2):343-54.
42. Delgado, L. M., Fuller, K., Zeugolis, D. I. Collagen cross-linking: Biophysical, biochemical, and biological response analysis. *Tissue Eng Part A*. 2017;23(19-20):1064-77.
43. Collin, E. C., Grad, S., Zeugolis, D. I., Vinatier, C. S., Clouet, J. R., Guicheux, J. J., Weiss, P., Alini, M., Pandit, A. S. An injectable vehicle for nucleus pulposus cell-based therapy. *Biomaterials*. 2011;32(11):2862-70.
44. Wang, J., Zhang, F., Tsang, W. P., Wan, C., Wu, C. Fabrication of injectable high strength hydrogel based on 4-arm star PEG for cartilage tissue engineering. *Biomaterials*. 2017;120:11-21.
45. Rubin, A. L., Drake, M. P., Davison, P. F., Pfahl, D., Speakman, P. T., Schmitt, F. O. Effects of pepsin treatment on the interaction properties of tropocollagen macromolecules. *Biochemistry*. 1965;4(2):181-90.
46. Capella-Monsonís, H., Coentro, J. Q., Graceffa, V., Wu, Z., Zeugolis, D. I. An experimental toolbox for characterization of mammalian collagen type I in biological specimens. *Nat Protoc*. 2018;13(3):507.
47. Fuller, K. P., Gaspar, D., Delgado, L. M., Pandit, A., Zeugolis, D. I. Influence of porosity and pore shape on structural, mechanical and biological properties of poly ϵ -caprolactone electro-spun fibrous scaffolds. *Nanomedicine (Lond)*. 2016;11(9):1031-40.

48. Oliveira, S. M., Ringshia, R. A., Legeros, R. Z., Clark, E., Yost, M. J., Terracio, L., Teixeira, C. C. An improved collagen scaffold for skeletal regeneration. *J Biomed Mater Res A*. 2010;94(2):371-9.
49. Zeugolis, D. I., Raghunath, M. The physiological relevance of wet versus dry differential scanning calorimetry for biomaterial evaluation: A technical note. *Polym Int*. 2010;59(10):1403-7.
50. Helling, A. L., Tsekoura, E. K., Biggs, M., Bayon, Y., Pandit, A., Zeugolis, D. I. In vitro enzymatic degradation of tissue grafts and collagen biomaterials by matrix metalloproteinases: Improving the collagenase assay. *ACS Biomater Sci Eng*. 2017;3(9):1922-32.
51. Bhosale, A. M., Richardson, J. B. Articular cartilage: structure, injuries and review of management. *Br Med Bull*. 2008;87:77-95.
52. Nehrer, S., Breinan, H. A., Ramappa, A., Shortkroff, S., Young, G., Minas, T., Sledge, C. B., Yannas, I. V., Spector, M. Canine chondrocytes seeded in type I and type II collagen implants investigated in vitro. *J Biomed Mater Res*. 1997;38(2):95-104.
53. Mukaida, T., Urabe, K., Naruse, K., Aikawa, J., Katano, M., Hyon, S. H., Itoman, M. Influence of three-dimensional culture in a type II collagen sponge on primary cultured and dedifferentiated chondrocytes. *J Orthop Sci*. 2005;10(5):521-8.
54. Tamaddon, M., Burrows, M., Ferreira, S. A., Dazzi, F., Apperley, J. F., Bradshaw, A., Brand, D. D., Czernuszka, J., Gentleman, E. Monomeric, porous type II collagen scaffolds promote chondrogenic differentiation of human bone marrow mesenchymal stem cells in vitro. *Sci Rep*. 2017;7:43519.
55. Ng, K. K., Thatte, H. S., Spector, M. Chondrogenic differentiation of adult mesenchymal stem cells and embryonic cells in collagen scaffolds. *J Biomed Mater Res A*. 2011;99(2):275-82.
56. Funayama, A., Niki, Y., Matsumoto, H., Maeno, S., Yatabe, T., Morioka, H., Yanagimoto, S., Taguchi, T., Tanaka, J., Toyama, Y. Repair of full-thickness articular cartilage defects using injectable type II collagen gel embedded with cultured chondrocytes in a rabbit model. *J Orthop Sci*. 2008;13(3):225-32.

57. Pieper, J. S., Van Der Kraan, P. M., Hafmans, T., Kamp, J., Buma, P., Van Susante, J. L. C., Van Den Berg, W. B., Veerkamp, J. H., Van Kuppevelt, T. H. Crosslinked type II collagen matrices: Preparation, characterization, and potential for cartilage engineering. *Biomaterials*. 2002;23(15):3183-92.
58. Herbage, D., Bouillet, J., Bernengo, J. Biochemical and physiochemical characterization of pepsin-solubilized type-II collagen from bovine articular cartilage. *Biochem J*. 1977;161(2):303-12.
59. Strawich, E., Nimni, M. E. Properties of a collagen molecule containing three identical components extracted from bovine articular cartilage. *Biochemistry*. 1971;10(21):3905-11.
60. Brodsky, B., Ramshaw, J. a. M. The collagen triple-helix structure. *Matrix Biol*. 1997;15(8):545-54.
61. Shoulders, M. D., Raines, R. T. Collagen structure and stability. *Annu Rev Biochem*. 2009;78:929-58.
62. Piao, Z., Takahara, M., Harada, M., Orui, H., Otsuji, M., Takagi, M., Ogino, T. The response of costal cartilage to mechanical injury in mice. *Plast Reconstr Surg*. 2007;119(3):830-6.
63. Nehrer, S., Breinan, H. A., Ramappa, A., Young, G., Shortkroff, S., Louie, L. K., Sledge, C. B., Yannas, I. V., Spector, M. Matrix collagen type and pore size influence behaviour of seeded canine chondrocytes. *Biomaterials*. 1997;18(11):769-76.
64. Wahl, D. A., Sachlos, E., Liu, C., Czernuszka, J. T. Controlling the processing of collagen-hydroxyapatite scaffolds for bone tissue engineering. *J Mater Sci Mater Med*. 2007;18(2):201-9.
65. Katoh, K., Tanabe, T., Yamauchi, K. Novel approach to fabricate keratin sponge scaffolds with controlled pore size and porosity. *Biomaterials*. 2004;25(18):4255-62.
66. Flahiff, C. M., Narmoneva, D. A., Huebner, J. L., Kraus, V. B., Guilak, F., Setton, L. A. Osmotic loading to determine the intrinsic material properties of guinea pig knee cartilage. *J Biomech*. 2002;35(9):1285-90.

67. Wang, J. Y., Mesquida, P., Lee, T., editors. Young's modulus measurement on pig trachea and bronchial airways. *Annu Int Conf IEEE Eng Med Biol Soc*; 2011.
68. Chiu, L. L. Y., Giardini-Rosa, R., Weber, J. F., Cushing, S. L., Waldman, S. D. Comparisons of auricular cartilage tissues from different species. *Ann Otol Rhinol Laryngol*. 2017;126(12):819-28.
69. Vázquez-Portatón, N. N., Kilmer, C. E., Panitch, A., Liu, J. C. Characterization of collagen type I and II blended hydrogels for articular cartilage tissue engineering. *Biomacromolecules*. 2016;17(10):3145-52.
70. Cao, H., Xu, S. Y. EDC/NHS-crosslinked type II collagen-chondroitin sulfate scaffold: Characterization and in vitro evaluation. *J Mater Sci Mater Med*. 2008;19(2):567-75.
71. Ko, C. S., Huang, J. P., Huang, C. W., Chu, I. M. Type II collagen-chondroitin sulfate-hyaluronan scaffold cross-linked by genipin for cartilage tissue engineering. *J Biosci Bioeng*. 2009;107(2):177-82.
72. Cao, H., Xu, S. Y. Purification and characterization of type II collagen from chick sternal cartilage. *Food Chem*. 2008;108(2):439-45.
73. Grover, C. N., Gwynne, J. H., Pugh, N., Hamaia, S., Farndale, R. W., Best, S. M., Cameron, R. E. Crosslinking and composition influence the surface properties, mechanical stiffness and cell reactivity of collagen-based films. *Acta Biomater*. 2012;8(8):3080-90.
74. Coupe, C., Hansen, P., Kongsgaard, M., Kovanen, V., Suetta, C., Aagaard, P., Kjaer, M., Magnusson, S. P. Mechanical properties and collagen cross-linking of the patellar tendon in old and young men. *J Appl Physiol* (1985). 2009;107(3):880-6.
75. Yang, C. Enhanced physicochemical properties of collagen by using EDC/NHS-crosslinking. *Bull Mater Sci*. 2012;35(5):913-8.
76. Freyria, A. M., Ronziere, M. C., Cortial, D., Galois, L., Hartmann, D., Herbage, D., Mallein-Gerin, F. Comparative phenotypic analysis of articular chondrocytes cultured within type I or type II collagen scaffolds. *Tissue Eng Part A*. 2009;15(6):1233-45.

77. Kilmer, C. E., Battistoni, C. M., Cox, A., Breur, G., Panitch, A., Liu, J. C. Collagen type I and II blend hydrogel with autologous mesenchymal stem cells as a scaffold for articular cartilage defect repair. *ACS Biomater Sci Eng.* 2020;6(6):3464-76.
78. Mueller, S. M., Shortkroff, S., Schneider, T. O., Breinan, H. A., Yannas, I. V., Spector, M. Meniscus cells seeded in type I and type II collagen-GAG matrices in vitro. *Biomaterials.* 1999;20(8):701-9.
79. Tortelli, F., Cancedda, R. Three-dimensional cultures of osteogenic and chondrogenic cells: A tissue engineering approach to mimic bone and cartilage in vitro. *Eur Cell Mater.* 2009;17:1-14.
80. Estes, B. T., Guilak, F. Three-dimensional culture systems to induce chondrogenesis of adipose-derived stem cells. *Methods Mol Biol.* 2011;702:201-17.
81. Musumeci, G., Mobasher, A., Trovato, F. M., Szychlinska, M. A., Graziano, A. C., Lo Furno, D., Avola, R., Mangano, S., Giuffrida, R., Cardile, V. Biosynthesis of collagen I, II, RUNX2 and lubricin at different time points of chondrogenic differentiation in a 3D in vitro model of human mesenchymal stem cells derived from adipose tissue. *Acta Histochem.* 2014;116(8):1407-17.
82. Sekiya, I., Colter, D. C., Prockop, D. J. BMP-6 enhances chondrogenesis in a subpopulation of human marrow stromal cells. *Biochem Biophys Res Commun.* 2001;284(2):411-8.
83. Ragetly, G. R., Griffon, D. J., Lee, H. B., Fredericks, L. P., Gordon-Evans, W., Chung, Y. S. Effect of chitosan scaffold microstructure on mesenchymal stem cell chondrogenesis. *Acta Biomater.* 2010;6(4):1430-6.
84. Desancé, M., Contentin, R., Bertoni, L., Gomez-Leduc, T., Branly, T., Jacquet, S., Betsch, J. M., Batho, A., Legendre, F., Audigié, F., Galéra, P., Demoor, M. Chondrogenic differentiation of defined equine mesenchymal stem cells derived from umbilical cord blood for use in cartilage repair therapy. *Int J Mol Sci.* 2018;19(2):537.
85. Gale, A. L., Linardi, R. L., Mcclung, G., Mammone, R. M., Ortved, K. F. Comparison of the chondrogenic differentiation potential of equine synovial

membrane-derived and bone marrow-derived mesenchymal stem cells. *Front Vet Sci.* 2019;6:178.

86. Szychlinska, M. A., Calabrese, G., Ravalli, S., Parrinello, N. L., Forte, S., Castrogiovanni, P., Pricoco, E., Imbesi, R., Castorina, S., Leonardi, R., Di Rosa, M., Musumeci, G. Cycloastragenol as an exogenous enhancer of chondrogenic differentiation of human adipose-derived mesenchymal stem cells. A morphological study. *Cells.* 2020;9(2):347.

87. Rakic, R., Bourdon, B., Demoor, M., Maddens, S., Saulnier, N., Galéra, P. Differences in the intrinsic chondrogenic potential of equine umbilical cord matrix and cord blood mesenchymal stromal/stem cells for cartilage regeneration. *Sci Rep.* 2018;8(1):13799.

88. Nürnberger, S., Schneider, C., Van Osch, G. V. M., Keibl, C., Rieder, B., Monforte, X., Teuschl, A. H., Mühleder, S., Holnthoner, W., Schädli, B., Gahleitner, C., Redl, H., Wolbank, S. Repopulation of an auricular cartilage scaffold, AuriScaff, perforated with an enzyme combination. *Acta Biomater.* 2019;86:207-22.

89. Pelttari, K., Winter, A., Steck, E., Goetzke, K., Hennig, T., Ochs, B. G., Aigner, T., Richter, W. Premature induction of hypertrophy during in vitro chondrogenesis of human mesenchymal stem cells correlates with calcification and vascular invasion after ectopic transplantation in SCID mice. *Arthritis Rheum.* 2006;54(10):3254-66.

90. Sakimura, K., Matsumoto, T., Miyamoto, C., Osaki, M., Shindo, H. Effects of insulin-like growth factor I on transforming growth factor β 1 induced chondrogenesis of synovium-derived mesenchymal stem cells cultured in a polyglycolic acid scaffold. *Cells Tissues Organs.* 2006;183(2):55-61.

91. Jiang, T., Liu, W., Lv, X., Sun, H., Zhang, L., Liu, Y., Zhang, W. J., Cao, Y., Zhou, G. Potent in vitro chondrogenesis of CD105 enriched human adipose-derived stem cells. *Biomaterials.* 2010;31(13):3564-71.

92. Liu, K., Zhou, G. D., Liu, W., Zhang, W. J., Cui, L., Liu, X., Liu, T. Y., Cao, Y. The dependence of in vivo stable ectopic chondrogenesis by human

mesenchymal stem cells on chondrogenic differentiation in vitro. *Biomaterials*. 2008;29(14):2183-92.

93. Trentham, D. E., Townes, A. S., Kang, A. H. Autoimmunity to type II collagen an experimental model of arthritis. *J Exp Med*. 1977;146(3):857-68.

94. Holmdahl, R., Vingsbo, C., Malmström, V., Jansson, L., Holmdahl, M. Chronicity of arthritis induced with homologous type II collagen (CII) in rats is associated with anti-CII B-cell activation. *J Autoimmun*. 1994;7(6):739-52.

95. Ofosu-Appiah, W. A., Morgan, K., Lennox Holt, P. J. Native type II collagen-induced arthritis in the rat. III. Relationship between the cellular immune response to native type II collagen and arthritis. *Ann Rheum Dis*. 1983;42(3):331-7.

96. Cathcart, E. S., Hayes, K. C., Gonnerman, W. A., Lazzari, A. A., Franzblau, C. Experimental arthritis in a nonhuman primate. I. Induction by bovine type II collagen. *Lab Invest*. 1986;54(1):26-31.

97. Cook, A. D., Rowley, M. J., Mackay, I. R., Gough, A., Emery, P. Antibodies to type II collagen in early rheumatoid arthritis. Correlation with disease progression. *Arthritis Rheum*. 1996;39(10):1720-7.

98. Stuart, J. M., Townes, A. S., Kang, A. H. Collagen autoimmune arthritis. *Ann Rev Immunol*. 1984;2(1):199-218.

99. Kim, H. A., Seo, Y. I., Lee, J., Jung, Y. O. Detection of anti-type II collagen antibodies in patients with chronic gouty arthritis: Findings from a pilot study. *J Clin Rheumatol*. 2016;22(7):360-3.

100. Thompson, H., Henderson, B., Spencer, J., Hobbs, S., Peppard, J., Staines, N. Tolerogenic activity of polymerized type II collagen in preventing collagen-induced arthritis in rats. *Clin Exp Immunol*. 1988;72(1):20.

101. Di Cesare Mannelli, L., Micheli, L., Zanardelli, M., Ghelardini, C. Low dose native type II collagen prevents pain in a rat osteoarthritis model. *BMC Musculoskelet Disord*. 2013;14:228.

102. Gao, Y., Li, B., Kong, W., Yuan, L., Guo, L., Li, C., Fan, H., Fan, Y., Zhang, X. Injectable and self-crosslinkable hydrogels based on collagen type II

and activated chondroitin sulfate for cell delivery. *Int J Biol Macromol.* 2018;118(Pt B):2014-20.

103. Wu, C. H., Ko, C. S., Huang, J. W., Huang, H. J., Chu, I. M. Effects of exogenous glycosaminoglycans on human chondrocytes cultivated on type II collagen scaffolds. *J Mater Sci Mater Med.* 2010;21(2):725-9.

104. Dorotka, R., Windberger, U., Macfelda, K., Bindreiter, U., Toma, C., Nehrer, S. Repair of articular cartilage defects treated by microfracture and a three-dimensional collagen matrix. *Biomaterials.* 2005;26(17):3617-29.

105. Yeh, H. Y., Lin, T. Y., Lin, C. H., Yen, B. L., Tsai, C. L., Hsu, S. H. Neocartilage formation from mesenchymal stem cells grown in type II collagen–hyaluronan composite scaffolds. *Differentiation.* 2013;86(4-5):171-83.

Chapter 3 – In the quest of the optimal chondrichthyan for the development of collagen sponges for articular cartilage

This chapter has been published in:

In the quest of the optimal chondrichthyan for the development of collagen sponges for articular cartilage. Z Wu, SH Korntner, AM Mullen, DI Zeugolis. Journal of Science: Advanced Materials and Devices 2021

Authors' contribution: Z.W. performed all the experiments (collagen preparations purity assessment, scaffolds' physicochemical properties assessment, scaffolds' chondrogenic potential assessment), drafted figures and tables, wrote the manuscript; S.H.K. trained histology and qPCR methods, reviewed and commented the manuscript; A.M.M. provided the funding; D.I.Z. contributed the concept, reviewed and edited the manuscript, provided the funding; all authors reviewed and approved the manuscript.

3.1. Introduction

The absence of blood vessels, lymphatics and nerves renders cartilage with limited intrinsic healing capacity. Chondral and osteochondral lesions, caused by injury or osteoarthritis, generally lead to the degeneration of articular cartilage and formation of mechanically inferior scar tissue, ultimately resulting in progressive total joint destruction. It is predicted that by 2050, over 40 million people will be severely disabled because of osteoarthritis (OA) and over 130 million people will be suffering from OA worldwide (1). The complexity of current treatments (e.g. multiple drilling, abrasion arthroplasty, mosaicplasty and autologous chondrocyte implantation) has driven the development of scaffold-assisted cell implantation, assuming that the scaffold will be able to provide mechanical stability and promote chondrogenesis. Mammalian collagen (type I (2, 3), type II (4, 5), or combination thereof (6, 7)) derived scaffolds are used extensively in cartilage engineering, with variable degree of efficiency (8, 9). Further, extensive use of antibiotics, religious tenets and the potential for interspecies disease transmission restrict their use, hence imposing the need for alternative, yet commercially relevant, collagen sources (10, 11). In this regard, marine species derived collagen offers an opportunity as a safe, sustainable and environmentally friendly alternative to mammalian species derived collagen (12, 13).

Collagen type I/II sponges from jellyfish (*Rhopilema esculentum*) and hydrogels from jellyfish (*Rhizostoma pulmo*) have been shown to maintain human, bovine and rat nasal chondrocyte phenotype (14, 15) and to induce chondrogenic differentiation of human mesenchymal stem cells (16, 17). Considering though that collagen type II scaffolds are more chondrogenic than collagen type I scaffolds (18-20), it is imperative to develop pure collagen type II preparations and assess their potential for cartilage engineering. In this frontier, the only two studies available have demonstrated proof of principle. Specifically, collagen type II from Peru squid (*Dosidicus gigas*) has been shown to suppress pro-inflammatory macrophage phenotype, to prevent hypertrophic chondrocyte phenotype and to alleviate inflammation in an OA rat model (21). Further, oral

administration of collagen type II from blue shark (*Prionace glauca*) has been reported to facilitate recovery of articular membranes in the ankle joint and to suppress rheumatoid arthritis in a complete Freund's adjuvant-induced rheumatoid arthritis rat model (22). A systematic study is therefore required to identify marine species for collagen type II extraction for cartilage engineering.

Considering the above, herein we selected to work with chondrichthyes, which are a diverse group of cartilaginous fish (e.g. sharks, skates, rays and chimaeras (23)) that lack true bone and exhibit a skeleton solely comprised of unmineralized cartilage, predominantly built of collagen type II (24, 25), which is the main extracellular matrix (ECM) component of cartilage (26, 27). It is also worth noting that the chondrichthyes used in this study are considered non-kosher fish. Due to Torah prohibitions, non-kosher fish is recognised as religiously taboo for some populations, for example, Twelver Shia Islam and Judaism. As a result, caution should be paid when commercialising chondrichthyes-derived collagen type II biomaterials. Collagen was extracted from four chondrichthyes [lesser spotted dogfish (*Scyliorhinus canicula*), thorn back ray (*Raja clavata*), cuckoo ray (*Leucoraja naevus*) and blonde ray (*Raja brachyuran*)] using the acid/pepsin treatment that increases yield and reduces immune response (28-30). Subsequently, collagen sponges were fabricated and crosslinked with 4-arm poly(ethylene glycol) succinimidyl glutarate that has a well-established cytocompatible stabilisation capacity (31, 32). The biophysical, biochemical and biological properties of the produced sponges were then assessed.

3.2. Materials and Methods

3.2.1. Materials

All chemicals were of analytical grade. Fish products (lesser spotted dogfish (LSD), thorn back ray (TBR), cuckoo ray (CR), blonde ray (BR)) were provided from the Marine Institute (Galway, Ireland). All tissue samples were obtained fresh and stored at -20 °C until further process. 4-arm polyethylene glycol (PEG) succinimidyl glutarate (4SG, Mw 10,000) was purchased from JenKem Technology (USA). All other materials and reagents were purchased from Sigma-Aldrich (Ireland), unless otherwise stated.

3.2.2. Collagen type II extraction and purification

The cleavage of the N- and C- terminal regions of the collagen molecules was achieved by enzymatic digestion with pepsin (3,200-4,500 units per mg protein, cat. no. P6887). Fish products were thawed and washed thoroughly under running tap water. Cartilage was manually dissected from surrounding tissue using a surgical scalpel, followed by treatment with 0.2 M NaOH for 12 h and subsequently three washes with absolute ethanol. Cartilage samples were then cut into small pieces, homogenised in liquid nitrogen using a CryoMill (SPEX SamplePrep 6870, Germany) and suspended in 1 M acetic acid at tissue to 1 M acetic acid ratio of 1 to 1 (g/l) under stirring for 48 h at 4 °C. Then pepsin was added at tissue to pepsin ratio of 10 to 1 (w/w) at room temperature and the solutions were kept under constant stirring for 48 h at 4 °C. The collagen solutions were filtered through a sieve (approximately 1,000 µm in diameter) and a filter mesh (100 µm in diameter); insoluble matter was discarded. Purified acid soluble collagen solutions were obtained after repeated (twice) salt precipitation (0.9 M NaCl) / centrifugation (20 min, 8,000 rpm, 4-8 °C). Supernatants were discarded and precipitates were dissolved in 1 M acetic acid. The precipitates from the second salt precipitation were dissolved in minimum amount of 1 M acetic acid to obtain highly concentrated collagen solutions, which were

repeatedly dialysed against 0.001 mM acetic acid for 48 h at 4 °C and then stored at 4 °C until use.

3.2.3. Sodium dodecyl sulphate poly-acrylamide gel electrophoresis

To assess the purity of the extracted collagen from the various tissues, sodium dodecyl sulphate-polyacrylamide gel electrophoresis (SDS-PAGE) under non-reducing conditions was conducted using a Mini-Protean 3 electrophoresis system (Bio-Rad Laboratories, UK) (33). 3 % stacking gel and 5 % separation gel were used. Collagen samples were freeze dried (FreeZone Plus 4.5 Liter Console Freeze Dry System, Labconco, USA) and then dissolved at 1 mg/ml concentration in 0.5 M acetic acid. Collagen solutions were neutralised with 1 N NaOH, followed by the addition of 5x sample buffer (bromophenol blue / SDS). The sample-buffer mixture was heated at 95 °C for 5 min and a 10 µl aliquot of the mixture was loaded onto each well of the stacking gel. High purity soluble collagen type I (Symatase, France) was used as negative control and soluble collagen type II isolated from chicken sternal cartilage (C9301, Sigma-Aldrich) was used as positive control, both at 1 mg/ml concentration in 0.5 M acetic acid. Electrophoresis was carried out by first applying 50 V constant voltage until the samples reached the end of the stacking gel (~ 30 min) and then 120 V constant voltage was applied until the samples reached the end of the separation gel (~ 60 min). The gels were stained with the silver staining kit (SilverQuest™, Invitrogen, USA) according to the manufacturer's protocol.

3.2.4. Scaffold fabrication and physicochemical properties assessment

Collagen type II preparations were freeze dried, re-dissolved in 0.05 M acetic acid to form solutions of 5 mg/ml, crosslinked with 1 mM PEG-4SG in phosphate buffered saline (PBS) and frozen at -80 °C for 12 h. Non-crosslinked collagens were prepared using PBS only. Frozen solutions were freeze dried to obtain collagen type II sponges. All the collagens were produced on the same day and under the same freeze-drying conditions. The produced scaffolds were subjected

to ultrastructural (34), biomechanical (35), denaturation temperature (36), free amine content (33) and resistance to enzymatic degradation (37) analyses.

3.2.5. Ultrastructural assessment

Collagen sponges were sectioned in the dry state to expose the inner porous structure, mounted onto a carbon disk, gold sputter coated (Emitech K-550X Sputter Coater, Emitech, UK) and imaged with a Hitachi S-4700 scanning electron microscope (SEM, Hitachi, High-Technologies Europe GmbH, Germany). Three micrographs of different areas were obtained from each collagen sponge and the average pore size and porosity of non-crosslinked and crosslinked collagen sponges were determined using ImageJ software (NIH, USA). The images were binarised using thresholding procedure, a window showing pore size distribution was emerged and 80-100 pores were measured per image. The average pore size and porosity were assessed after proper thresholding (34).

3.2.6. Biomechanical assessment

The mechanical properties of the collagen sponges were assessed via uniaxial compression using a material testing machine (Z2.5, Zwick/Roell, Germany) loaded with a 10 N load cell. Uniaxial constant loading was performed on dry collagen sponges with approximately 4 mm in height and 9 mm in diameter. Scaffolds were placed between two loading cells and compressed until 70 % deformation was reached, with a compression rate of 10 mm/min. Force, strain and elastic modulus were determined by plotting stress versus strain curves. Both compression strength and elastic modulus were determined within the linear area of the curves at the position of 30 % deformation and elastic modulus was calculated using the linear equation of trend-lines at the position of 30 % of the deformation (35).

3.2.7. Denaturation temperature assessment

The denaturation temperature of collagen sponges was assessed using a differential scanning calorimeter (DSC-60, Shimadzu, Japan) in wet state (36). In brief, collagen sponges were hydrated in 1x PBS for 12 h at 4 °C. The samples were then blotted with filter paper to remove excess PBS and hermetically sealed in aluminium crucibles. Collagen samples of 10-15 mg were used for DSC analysis. An empty aluminium crucible was used as reference. Heating was carried out at a constant temperature ramp of 10 °C/min with a temperature range of 20-100 °C. Thermal denaturation, the endothermic transition, was recorded as typical peak and the peak (temperature of maximum power absorption during denaturation) temperature was recorded.

3.2.8. Free amine content assessment

Crosslinking efficiency was quantified using the 2,4,6-trinitrobenzene sulfonic acid (TNBSA) assay (Thermo Fisher Scientific, Ireland) (33). Collagen free amine groups react with TNBSA to form highly chromogenic derivatives that can be measured at 335 nm. Briefly, collagen sponges (~ 3 mg) were incubated with TNBSA at 37 °C for 2 h. The reaction was stopped by adding 10 % SDS and 1 M HCl. The mixtures were subsequently heated at 95 °C for 15 min in order to hydrolyse the collagen samples. The absorbance of each sample was read at 335 nm (Varioskan Flash Multimode Reader, Thermo Fisher Scientific, Ireland) and values were normalised to the standard curve, which was generated with a series of a known glycine solution at different concentrations (0.005, 0.01, 0.02, 0.03, 0.04 and 0.05 mg/ml).

3.2.9. Resistance to enzymatic degradation assessment

Enzymatic stability of the collagen sponges was quantified with the collagenase assay (37). Briefly, collagen sponges were weighed and hydrated for 2 h in 0.1 M Tris-HCl and 50 mM CaCl₂ at pH 7.4. The sponges were then incubated in 50 U/ml bacterial collagenase type II (MMP-8; Gibco, cat. no. 17101-015, Ireland).

After incubation at different time points (3 h, 6 h, 9 h, 12 h and 24 h) at 37 °C, centrifugation was carried out at 10,000 g for 5 min, the supernatants were discarded and the remaining collagen sponges were freeze dried and weighed. The degree of enzymatic degradation was quantified using the weight difference approach $[(W_o - W_t) / W_o] \times 100$, where W_o is the original weight and W_t is the remaining weight.

3.2.10. Cell culture and scaffolds' basic cellular function assessment

Human adipose derived stem cells (hADSCs) from a female healthy donor (cat. no. PT-5006) were purchased from Lonza (Switzerland) and cultured in alpha Minimum Essential Medium (a-MEM) with GlutaMAX™ (Gibco Life Technologies, Ireland) supplemented with 10 % foetal bovine serum and 1 % penicillin-streptomycin at 37 °C in 95 % humidified atmosphere of 5 % CO₂. At passages 5, cells were resuspended in fresh medium and 100 µl of cell suspension was seeded onto each collagen sponge at a density of 200,000 cells/sponge. As a negative control group, human adipose derived stem cells were cultured on tissue culture plastic (TCP) at 50,000 cells/cm². Cells were left to attach to the sponge for 2 h before the expansion medium was added. Expansion medium was changed to chondrogenic induction medium the next day to allow for the cells to attach and spread evenly throughout the scaffold. Media were changed every 2 days. The chondrogenic induction medium was composed of high glucose Dulbecco's Modified Eagle's medium (DMEM), 100 nM dexamethasone, 50 mg/ml bovine serum albumin, 50 µg/ml ascorbic acid-2-phosphate, 5 ml insulin-transferrin-selenium (ITS) liquid media supplement, 10 ng/ml transforming growth factor beta 3 (TGF-β3, R&D Systems, USA). Cell viability, proliferation and metabolic activity were assessed after 7, 14 and 21 days in culture. Cell infiltration and ECM synthesis analyses were conducted at the same timepoints, following cryosectioning and haematoxylin and eosin (H&E) staining.

3.2.11. Cell viability assessment

Cell viability was analysed using the Live/Dead[®] assay (Life Technologies, Ireland) as per manufacturer's protocol. Briefly, at the end of each timepoint, the collagen sponges were washed three times with Hanks' balanced salt solution (HBSS) and incubated with calcein AM and ethidium homodimer 1 solution (4 μ M calcein-AM and 2 μ M ethidium homodimer-1) in HBSS at 37 °C, 5 % CO₂ and 95 % relative humidity for 30 min. The collagen sponges were washed with fresh HBSS to remove excess dye. Subsequently, images were acquired using a Fluoroview 1000 confocal laser microscope (FV1000 Shackelton, Olympus, Japan). Live (green) and dead (red) cells were analysed using ImageJ Software (NIH, USA).

3.2.12. Cell proliferation assessment

Cell proliferation was assessed using the Quant-iT[™] PicoGreen[®] dsDNA kit (Invitrogen, USA), according to the manufacturer's guidelines. Collagen sponges were washed three times with HBSS at the end of each timepoint, 200 μ l DNase free water was added and frozen at -80 °C until analysis. Collagen sponges were freeze thawed at least three times in order to lyse the cells. Subsequently, PicoGreen[®] working solution was added to the collagen sponges and incubated at room temperature for 5-10 min, protected from light. Fluorescence was measured at excitation and emission wavelengths of 480 nm and 520 nm using a Varioskan[™] Flash Multimode Reader (Thermo Fisher Scientific, Ireland). The obtained values were normalised to the standard curve, which has been generated with a series of known DNA stock solutions at different concentrations (0, 5, 10, 25, 50, 100, 500 and 1,000 ng/ml).

3.2.13. Cell metabolic activity assessment

Cell metabolic activity was analysed using an alamarBlue[®] assay (Invitrogen, USA), as per manufacturer's protocol. Briefly, collagen sponges were washed

three times with HBSS at the end of each time point, 10 % alamarBlue® was added to each collagen sponge and incubated at 37 °C, 5 % CO₂ and 95 % relative humidity for 3 h. Absorbance was measured at 570 nm and 600 nm using a Varioskan™ Flash Multimode Reader (Thermo Fisher Scientific, Ireland).

3.2.14. Histology assessment

Collagen sponges were collected at each time point, washed with 1x PBS and immersion-fixed with 4 % paraformaldehyde for 30 min at room temperature. Collagen sponges were washed with 1x PBS and cryoprotected in PBS containing 15 % and 30 % sucrose, consecutively. Collagen sponges were embedded in optimal cutting temperature (OCT) compound (Tissue-Tek, USA) and cryo-sectioned using a Cryostat (Leica, CM1850, Germany). Serial sections of 5-10 µm in thickness were collected on adhesion glass slides (Superfrost Plus, Thermo Fisher Scientific, Austria), air-dried for 1 h at room temperature and stored at -20 °C until further processing. Sections were stained using haematoxylin and eosin (H&E) stain. Nuclei were stained with Mayer's Haemalum solution (Carl Roth, Germany) for 5 min, slides were washed in 0.5 % hydrogen chloride-ethanol solution to destain the connective tissue and subsequently rinsed in 1 % acetic acid to stop the staining reaction. Samples were washed with running tap water for 10 min and sections were counterstained with an alcoholic Eosin Y solution (50 % of ethanol and 0.15 % of eosin) for 30 sec. After rinsing in 1 % acetic acid, samples were dehydrated through graded ethanol and xylene and mounted with distyrene-dibutyl phthalate-xylene (DPX) mounting medium. Images were captured under a light microscope (Olympus, Japan) and analysed using ImageJ Software (NIH, USA).

3.2.15. Scaffolds' chondrogenic potential assessment (sulphated glycosaminoglycan assessment)

The amount of sulphated glycosaminoglycans (sGAG) produced by the hADSCs was qualitatively assessed via Alcian blue staining and quantitatively assessed

via the Blyscan™ sGAG (Biocolor, UK) assay kit. For the Alcian blue staining, serial sections of collagen sponges were stained with 3 % Alcian blue staining solution for 30 min, followed by a rinse in 1 % acetic acid and then counterstained with nuclear fast red solution (Merck, USA) for 5 min. Then, the slides were briefly rinsed in distilled water, dehydrated with 100 % ethanol and mounted with DPX mounting medium. Images were captured under a light microscope (Olympus, Japan). For the Blyscan™ sGAG assay, collagen sponges were washed three times with HBSS at the end of each timepoint, followed by papain extraction. Then, 1 ml Blyscan™ dye reagent was added to each sample and the samples were mixed gently using an incubated orbital shaker (Thermo Fisher Scientific, Ireland) for 30 min. The samples were then centrifuged at 17,000 g for 10 min. Unbound dye solution was carefully drained and 0.5 ml dissociation reagent was added to the remaining sGAG droplets. 200 µl of each sample was transferred to individual wells of a 96 micro well plate and the absorbance was measured at 656 nm using a Varioskan™ Flash Multimode Reader (Thermo Fisher Scientific, Ireland). Standard aliquots containing 1, 2, 3, 4 and 5 µg GAGs were used as reference standards for standard curve. The sGAG concentration of each collagen sponge was obtained after normalisation to the standard curve.

3.2.16. Scaffolds' chondrogenic potential assessment (gene expression assessment)

Quantitative gene analysis via real-time polymerase chain reaction (RT-PCR) was also conducted. Total RNA was isolated from hADSC-seeded collagen sponges of all groups after 21 days of *in vitro* culture in chondrogenic media and 3 collagen sponges from each group were pooled for each sample. Collagen sponges were homogenised using surgical scalpels before TRI-Reagent® was added. Two consecutive extraction steps using phenol-chloroform were performed. Total RNA was precipitated for 30 min at -20 °C with an equal volume of ice-cold isopropanol, followed by centrifugation for 30 min at 13,000

g at 4 °C. RNA pellets were washed in 75 % ethanol, air dried and resuspended in RNA storage solution (Thermo Fisher Scientific, Ireland) supplemented with RiboSafe RNase inhibitor (Bioline, UK) and stored at -80 °C. RNA yield and purity were determined using a NanoDrop spectrophotometer (Thermo Fisher Scientific, Ireland). Optical density (OD) 260/280 value between 1.8 and 2.0 was defined as pure RNA. RNA integrity was verified by the Agilent 2100 Bioanalyzer Electrophoresis System (USA). RNA with RNA quality indicator (RQI) > 8 was defined as intact RNA.

1 µg of total RNA was reverse-transcribed using iScript™ RT-PCR Supermix (BioRad, Ireland). 5 ng cDNA per reaction were subsequently analysed by quantitative PCR using TaqMan® Gene Expression Master Mix (Applied Biosystems, Ireland) and TaqMan® PrimeTime Predesigned qPCR assays (Integrated DNA Technologies, USA) for collagen type I α 1 (COL1A1), collagen type II α 1 (COL2A1), collagen type III α 1 (COL3A1), collagen type X α 1 (COL10A1), aggrecan (ACAN), cartilage oligomeric matrix protein (COMP), SRY-box 9 (SOX9), EIF2B1 (eukaryotic translation initiation factor 2B subunit alpha), GUSB (glucuronidase beta), TBP (TATA-box binding protein). Default amplification conditions were as the follows: 50 °C for 2 min, 95 °C for 10 min, followed by 40 cycles of 95 °C for 15 sec and 60 °C for 1 min using Applied Biosystems (Ireland) StepOnePlus™ RT-PCR System. Cq values were analysed using qBase+ (Biogazelle, Belgium) and normalised relative quantities (NRQs) were calculated by normalising the data to the expression of 3 validated endogenous control genes (EIF2B1, GUSB, TBP). Upregulated or downregulated mRNA expression was defined as a fold change ≥ 2.0 , no difference in mRNA expression was defined as a fold change < 2.0. **Table 3.1** lists the genes and the sequence of their respective primers.

Table 3.1: Genes and their primer 1 (forward), probe, and primer 2 (reverse) sequences.

Genes	Primer 1 (5'-3')	Probe (5'-3')	Primer 2 (5'-3')
EIF2B1	GGTTTCTATGGCACTGGTGAG	/56- FAM/ACCCTGGAT/ZEN/TGTCTCCCCT TTATCTCT/3IABkFQ/	GACGTTGCTGGAGTTCTTG A
GUSB	GTT TTT GAT CCA GAC CCA GAT G	/56-FAM/TGC AGG GTT /ZEN/TCA CCA GGA TCC AC/3IABkFQ/	GCC CAT TAT TCA GAG CGA GTA
TBP	CAA GAA CTT AGC TGG AAA ACC C	/56-FAM/CAC AGG AGC /ZEN/CAA GAG TGA AGA ACA GT/3IABkFQ/	GAT AAG AGA GCC ACG AAC CAC
COL1A1	GGT TGA TTT CTC ATC ATA GCC AT	/56-FAM/AGG AAA CTT /ZEN/TGC TCC CCA GCT GT/3IABkFQ/	CTG GAC AGC CTG GAC TTC
COL2A1	GTT TTC CAG CTT CAC CAT CAT C	/56-FAM/TGG GAC CAG /ZEN/AGA CAC CAG GTT CA/3IABkFQ/	CCT CAA GGA TTT CAA GGC AAT
COL3A1	TTGGCATGGTTCTGGCTT	/56- FAM/TGGGAACAT/ZEN/CCTCCTTCAA CAGCTTC/3IABkFQ/	CTACTTCTCGCTCTGCTTCA TC

Genes	Primer 1 (5'-3')	Probe (5'-3')	Primer 2 (5'-3')
COL10A1	GTA CCT TGC TCT CCT CTT ACT G	/56-FAM/CCA AGA CAC /ZEN/AGT TCT TCA TTC CCT ACA CC/3IABkFQ/	CAT AAA AGG CCC ACT ACC CA
SOX9	CGT TCT TCA CCG ACT TCC TC	/56-FAM/AAG GGC CGC /ZEN/TTC TCG CTC T/3IABkFQ/	CTG GGC AAG CTC TGG AG
COMP	ACAGGCATCCCCTATACCAT	/56- FAM/ACCCA ACTC/ZEN/AGACCAGAA GGACAGT/3IABkFQ/	GACCAAAAGGACACAGACC A
ACAN	AGA TTC ACA GAA CTC CAG TGC	/56-FAM/CGA AGA ACA /ZEN/CCT CCC CCT CAA GTC /3IABkFQ/	ACC TAC GAT GTC TAC TGC TTT G

3.2.17. Statistical analysis

Numerical data are expressed as mean \pm standard deviation. Statistical analysis was performed using SPSS Statistics (USA). Analysis was performed using One-way analysis of variance (ANOVA) for multiple comparisons and 2-sample t-test for pair wise comparisons after confirming the following assumptions of parametric analysis: the distribution from which each of the samples was derived was normal (Shapiro-Wilk normality test) and the variances of the population of the samples were equal to one another (Levene's test for equal variances). Nonparametric statistics were used when either or both of the above assumptions were violated and consequently Kruskal-Wallis test for multiple comparisons or Mann-Whitney test for 2-samples were carried out. Statistical significance was accepted at $p < 0.05$.

3.3. Results

3.3.1. Collagen preparations purity assessment

SDS-PAGE (**Figure 3.1**) revealed a typical electrophoretic mobility of collagen type II from all fish species, comprised of $\alpha 1$, β and γ bands and no $\alpha 2$ bands, which would have been indicative of collagen type I contamination. It is also worth noting that the produced collagen type II preparations, having derived from acid/pepsin extraction, repeated salt precipitation / acid solubilisation and dialysis, were of higher purity than the commercially available collagen type II preparation, as evidenced by lower amounts of high molecular weight bands.

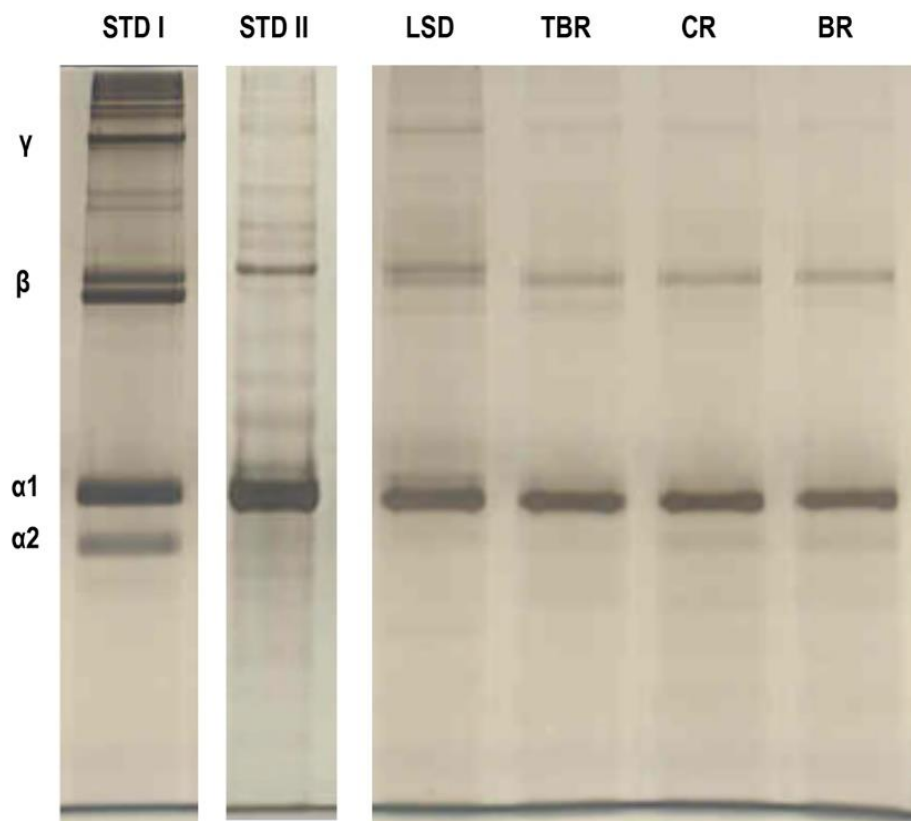


Figure 3.1: SDS-PAGE analysis of collagen preparations extracted from the chondrichthyes. STD I: Standard collagen type I. STD II: Standard collagen type II. LSD: lesser spotted dogfish. TBR: thorn back ray. CR: cuckoo ray. BR: blonde ray.

3.3.2. Scaffolds' physicochemical properties assessment

Qualitative morphology analysis via SEM made apparent that all materials exhibited a porous structure (**Figure 3.2**). Subsequent quantitative pore size and % porosity analyses revealed no apparent differences ($p > 0.05$) as function of fish species and crosslinking, as the pore size and % porosity ranged from $90.1 \pm 21.2 \mu\text{m}$ to $106.4 \pm 23.9 \mu\text{m}$ and from $88.5 \pm 3.6 \%$ to $91.4 \pm 1.5 \%$, respectively, for the non-crosslinked collagen type II sponges and from $95.9 \pm 23.0 \mu\text{m}$ to $105.3 \pm 19.2 \mu\text{m}$ and from $88.8 \pm 3.4 \%$ to $91.2 \pm 3.4 \%$, respectively, for the crosslinked collagen type II sponges.

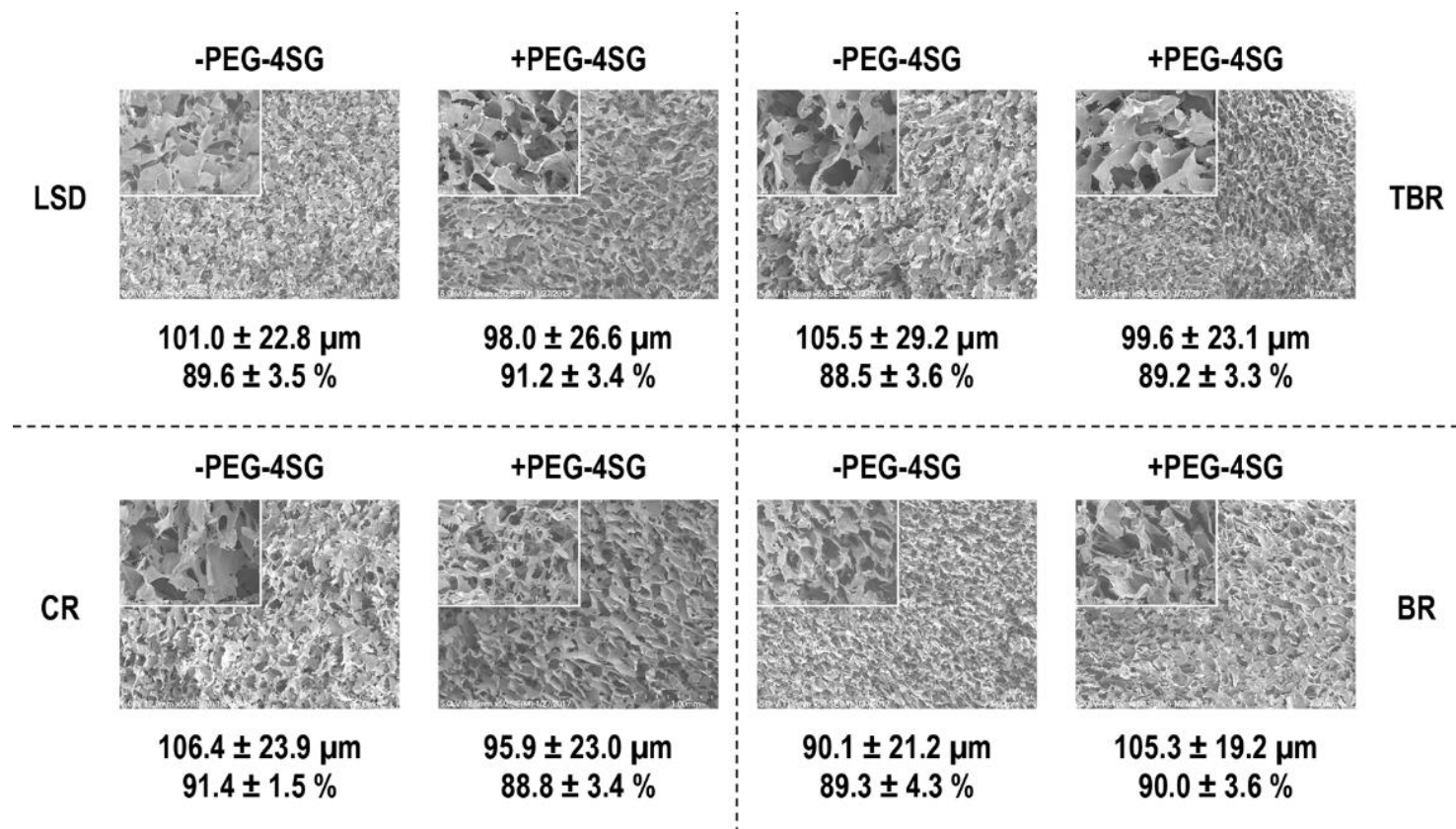


Figure 3.2: Morphology, pore size and % porosity analyses of the produced scaffolds as a function of fish species and crosslinking. LSD: lesser spotted dogfish. TBR: thorn back ray. CR: cuckoo ray. BR: blonde ray. -PEG-4SG: Non crosslinked groups. +PEG-4SG: Crosslinked groups.

Biomechanical assessment (**Table 3.2**) revealed no significant ($p > 0.05$) differences in compression stress and elastic modulus as a function of fish species and crosslinking significantly ($p < 0.05$) increased compression stress and elastic modulus in all groups (compression stress and modulus ranged from 2.4 ± 0.2 kPa to 2.5 ± 0.3 kPa and 8.1 ± 0.7 kPa to 8.3 ± 1.0 kPa, respectively, for the non-crosslinked collagen type II sponges and from 3.6 ± 0.6 kPa to 3.7 ± 0.4 kPa and 12.0 ± 1.6 kPa to 12.3 ± 1.3 kPa, respectively, for the crosslinked collagen type II sponges).

DSC analysis (**Table 3.2**) revealed no significant ($p > 0.05$) differences in denaturation temperature as a function of fish species and crosslinking significantly ($p < 0.05$) increased denaturation temperature in all groups (denaturation temperature ranged from 37.4 ± 0.3 °C to 38.6 ± 1.1 °C for the non-crosslinked collagen type II sponges and from 41.4 ± 0.3 °C to 43.9 ± 1.0 °C for the crosslinked collagen type II sponges).

Free amine quantification (**Table 3.2**) revealed no significant ($p > 0.05$) differences in free amine content as a function of fish species and crosslinking significantly ($p < 0.05$) reduced free amine content in all groups (% free amines ranged from 13.6 ± 0.2 % to 14.3 ± 0.6 % for the non-crosslinked collagen type II sponges and from 8.4 ± 0.1 % to 9.9 ± 0.3 % for the crosslinked collagen type II sponges).

Table 3.2: Mechanical properties, denaturation temperature and free amine content of the produced scaffolds as a function of fish species and crosslinking. LSD: Lesser spotted dogfish. TBR: Thorn back ray. CR: Cuckoo ray. BR: Blonde ray. -PEG-4SG: No crosslinked groups. +PEG-4SG: Crosslinked groups. * indicates significant ($p < 0.05$) difference to the non-crosslinked group, within the same fish species.

	LSD		TBR		CR		BR	
	-PEG-4SG	+PEG-4SG	-PEG-4SG	+PEG-4SG	-PEG-4SG	+PEG-4SG	-PEG-4SG	+PEG-4SG
Stress (kPa)	2.4 ± 0.2	3.7 ± 0.2*	2.5 ± 0.3	3.7 ± 0.4*	2.5 ± 0.2	3.6 ± 0.5*	2.5 ± 0.3	3.6 ± 0.6*
Modulus (kPa)	8.1 ± 0.7	12.2 ± 0.7*	8.3 ± 1.0	12.3 ± 1.3*	8.2 ± 0.5	12.0 ± 1.6*	8.2 ± 1.0	12.1 ± 2.2*
Denaturation Temperature (°C)	37.4 ± 0.3	42.5 ± 0.2*	38.6 ± 1.1	43.7 ± 1.3*	37.9 ± 0.9	43.9 ± 1.0*	37.7 ± 1.3	41.4 ± 0.3*
Free Amines (%)	13.7 ± 0.1	9.6 ± 0.9*	14.3 ± 0.6	9.9 ± 0.4*	13.8 ± 0.1	8.4 ± 0.1*	13.6 ± 0.2	9.0 ± 0.1*

Collagenase digestion analysis (**Figure 3.3**) revealed no significant ($p > 0.05$) differences in resistance to enzymatic degradation as a function of fish species. Crosslinking significantly ($p < 0.05$) increased the resistance to collagenase digestion of each group. Further, all non-crosslinked samples were completely ($< 3\%$ remaining mass) digested within 12 h of collagenase digestion, whilst crosslinked samples were more resistant to collagenase digestion ($\sim 30\%$ remaining mass after 24 h of collagenase digestion).

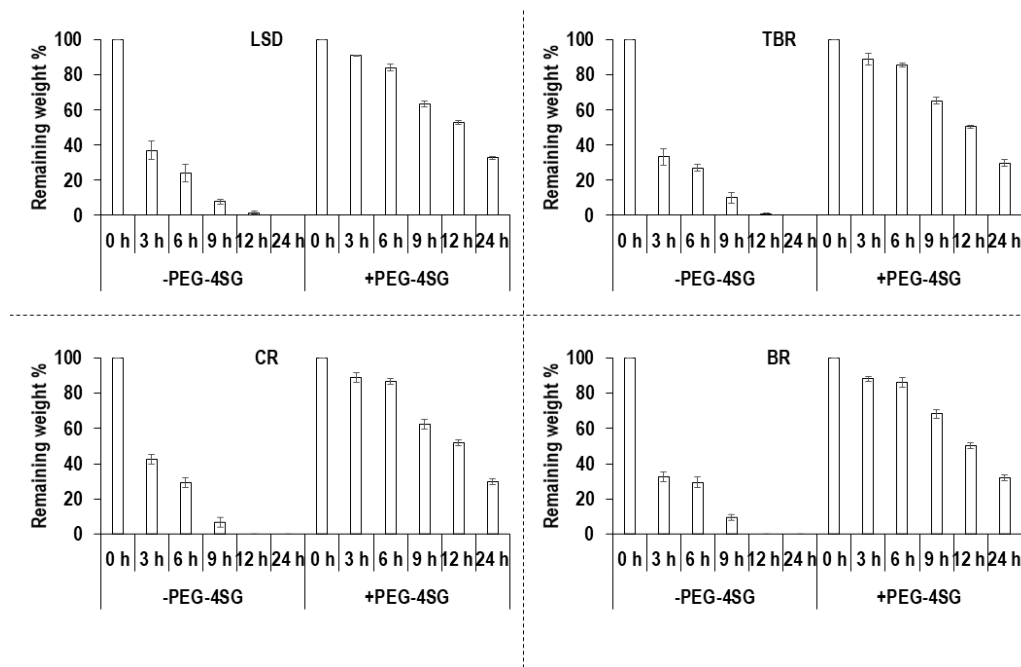


Figure 3.3: Resistance to collagenase digestion analysis of the produced scaffolds as a function of fish species and crosslinking. LSD: lesser spotted dogfish. TBR: thorn back ray. CR: cuckoo ray. BR: blonde ray. -PEG-4SG: Non crosslinked groups. +PEG-4SG: Crosslinked groups.

Cell viability (**Figure 3.4a**), DNA concentration (**Figure 3.4b**) and metabolic activity (**Figure 3.4c**) analyses indicated that all scaffolds equally ($p > 0.05$) supported hADSCs attachment, proliferation and growth up to 21 days (longest timepoint assessed) in chondrogenic media independently of the fish species. Qualitative cell infiltration and ECM synthesis analyses via H&E staining (**Figure 3.4d**) revealed a homogeneous cell distribution throughout the scaffolds and increased ECM synthesis as a function of time in culture independently of the fish species.

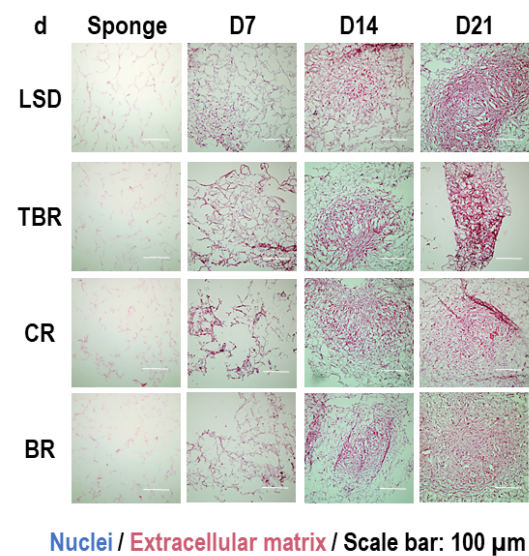
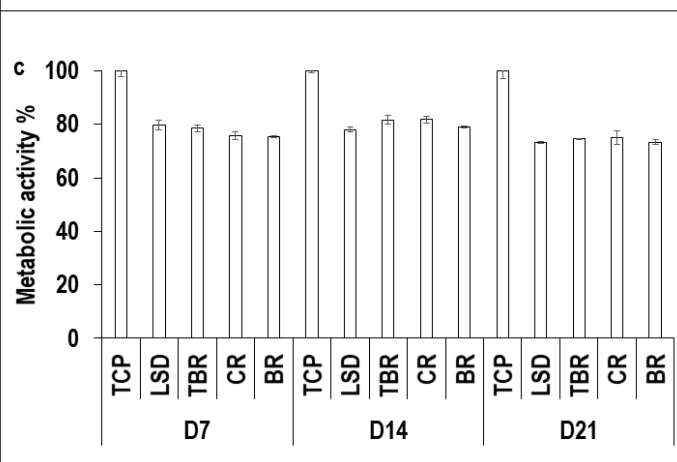
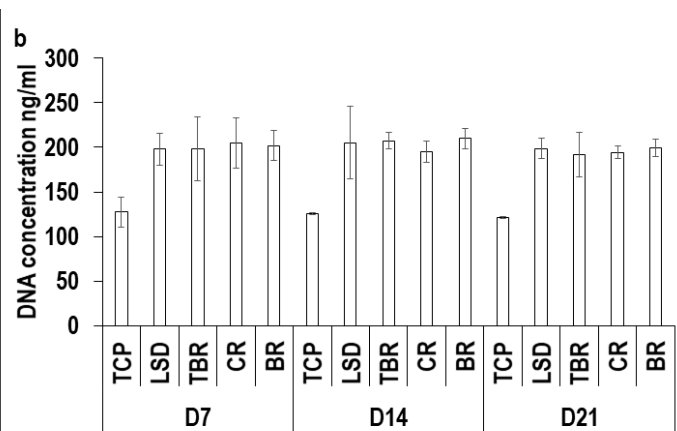
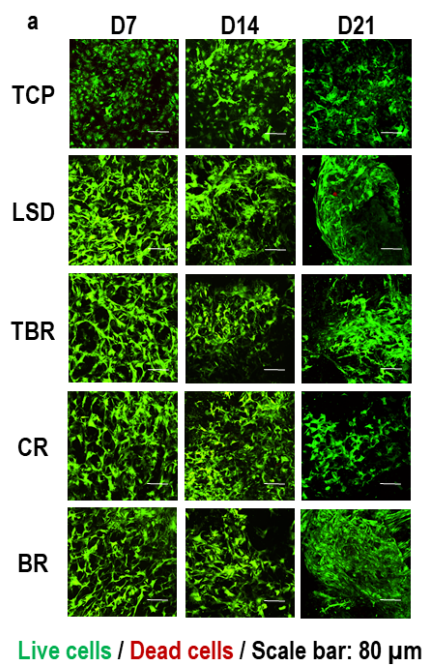


Figure 3.4: hADSC viability (**a**), DNA concentration (**b**), metabolic activity (**c**) and infiltration and ECM synthesis (**d**) as a function of fish species for up to 21 days in culture. TCP: Tissue culture plastic. D: Day. LSD: lesser spotted dogfish. TBR: thorn back ray. CR: cuckoo ray. BR: blonde ray. Note: The reduced cell number as a function of time in culture (**a**) is attributed to the migration of cells from the surface to the inner of the collagen sponges.

3.3.3. Scaffolds' chondrogenic potential assessment

Alcian blue staining (**Figure 3.5a**) and sGAG quantification (**Figure 3.5b**) revealed no significant ($p > 0.05$) differences as a function of fish species at any timepoint, sGAG content was significantly ($p < 0.05$) increased as a function of time in culture for all collagen scaffolds and at all timepoints, collagen scaffolds induced significantly ($p < 0.05$) higher sGAG content than TCP.

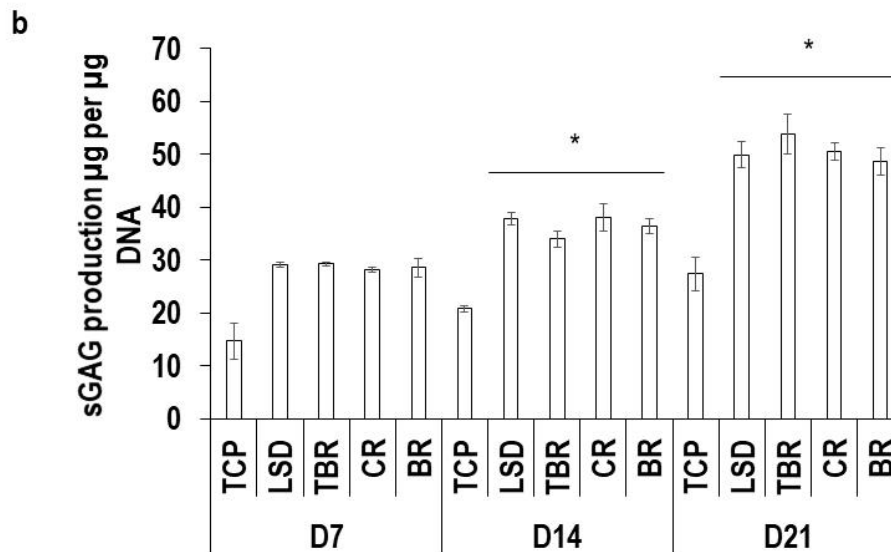
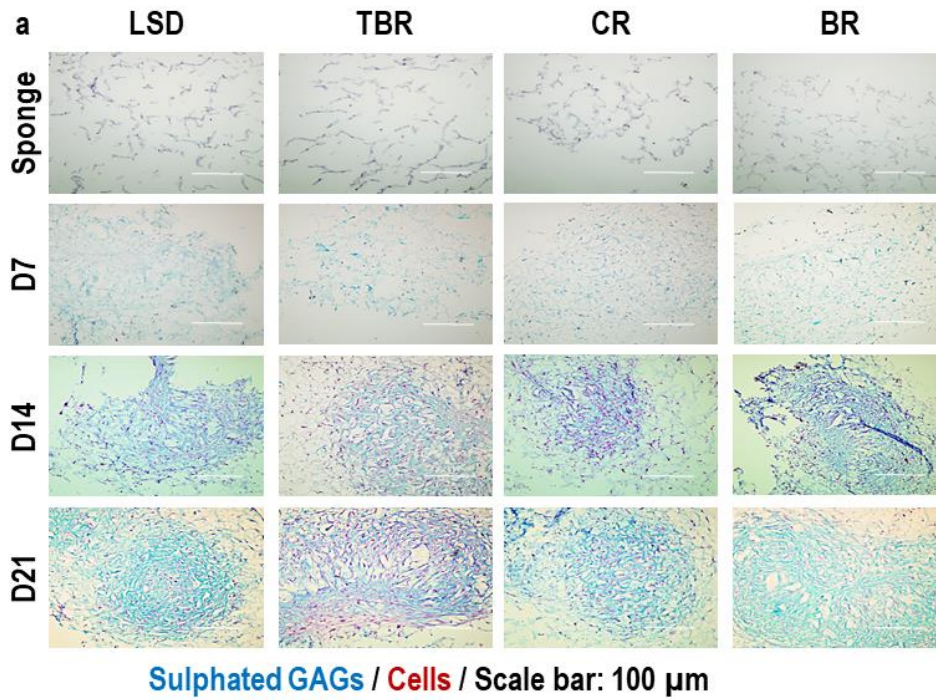


Figure 3.5: Alcian blue staining (**a**) and sGAG quantification (**b**) as a function of fish species for up to 21 days in culture. TCP: Tissue culture plastic. D: Day. LSD: lesser spotted dogfish. TBR: thorn back ray. CR: cuckoo ray. BR: blonde ray. *: indicates $p < 0.05$.

Gene expression analysis after 21 days of chondrogenic induction (**Figure 3.6**) revealed no COL2A1 gene expression in any of the groups (data not shown); the LSD group exhibited upregulated (fold change ≥ 2.0) COL1A1 mRNA levels compared to the other collagen groups and all collagen groups exhibited downregulated (fold change ≥ 2.0) COL1A1 mRNA levels compared to TCP; TCP and the LSD group showed upregulated (fold change ≥ 2.0) COL3A1 mRNA levels compared to the TBR and BR groups; all collagen groups exhibited upregulated (fold change ≥ 2.0) COL10A1 mRNA levels compared to TCP; the LSD group showed upregulated (fold change ≥ 2.0) compared to the CR and BR groups and no difference (fold change < 2.0) compared to the TBR group COMP mRNA expression and all collagen groups showed upregulated (fold change ≥ 2.0) COMP expression compared to TCP; no differences (fold change < 2.0) in SOX9 mRNA levels were observed between all collagen groups and all collagen groups exhibited upregulated (fold change ≥ 2.0) SOX9 mRNA levels compared to TCP; and the LSD, TBR and BR groups showed upregulated (fold change ≥ 2.0) ACAN mRNA expression levels compared to TCP and the CR group.

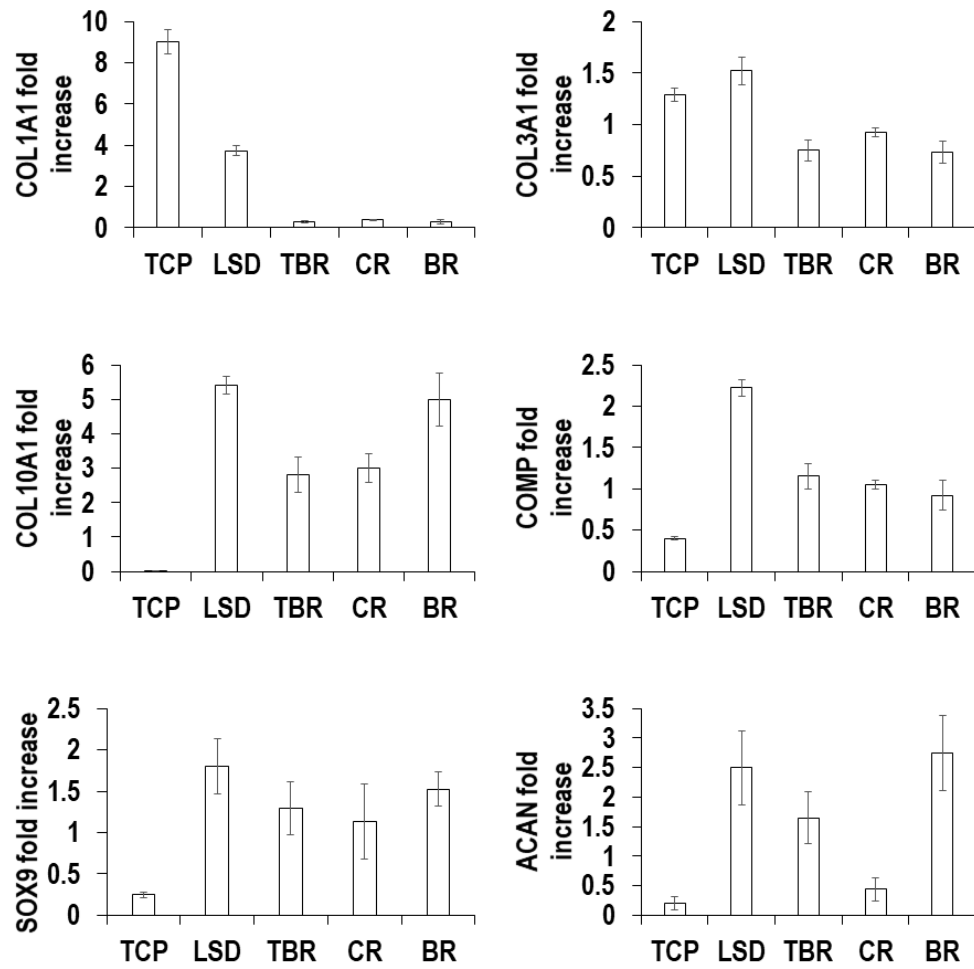


Figure 3.6: Gene expression analysis after 21 days as a function of fish species. TCP: Tissue culture plastic. LSD: lesser spotted dogfish. TBR: thorn back ray. CR: cuckoo ray. BR: blonde ray.

3.4. Discussion

Marine species derived collagen is slowly, but progressively, being considered as a viable, safe, sustainable and environmentally friendly alternative to mammalian species derived collagen. In cartilage engineering, although marine collagen has been shown to maintain chondrocyte phenotype (14, 15); suppress pro-inflammatory macrophage phenotype, prevent hypertrophic chondrocyte phenotype and alleviate inflammation in OA rats (21); and induce chondrogenic differentiation of human mesenchymal stem cells (16, 17), a systematic study to identify the optimal collagen preparation has not been published as yet. Thus, herein, we ventured to assess the potential of four chondrichthyes species [lesser spotted dogfish (*Scyliorhinus canicula*), thorn back ray (*Raja clavata*), cuckoo ray (*Leucoraja naevus*) and blonde ray (*Raja brachyuran*)] to yield collagen suitable for cartilage engineering. We selected chondrichthyes as they lack true bone and exhibit a skeleton solely comprised of unmineralized cartilage, predominantly built of collagen type II (24, 25), which is the main ECM component of cartilage (26, 27).

Pure collagen type II (no collagen type I contamination was detected, as evidenced by the absence of $\alpha 2$ chain) was extracted from all chondrichthyes, as evidenced by a typical collagen type II electrophoretic mobility, corresponding to three $\alpha 1(\text{II})$ chains. This was similar to previous studies with collagen extracted from silvertip shark (*Carcharhinus albimarginatus*) (38) and Peru squid (*Dosidicus gigas*) (21). It is worth noting that collagen extracted from brownbanded bamboo shark (*Chiloscyllium punctatum*) and blacktip shark (*Carcharhinus limbatus*) were contaminated with collagen type I (39), which may reduce the chondrogenic potential of the scaffold, as has been shown before with mammalian collagen type I / collagen type II preparations (18-20).

The three-dimensional macrostructure of the resultant collagen type II collagen sponges was not significantly affected as a function of chondrichthyes species and crosslinking. All sponges exhibited a homogenous porous structure with 70-

120 μm pore size and 80-100 % porosity, which have been shown before to induce chondrogenic differentiation of human adipose derived stem cells (40-42).

Free amine content and mechanical properties, denaturation temperature and resistance to enzymatic degradation were not affected as function of fish species and the former was significantly decreased and the latter were significantly increased as a function of crosslinking. All these observations are in accordance with previous publications, where PEG-4SG has been shown to increase mechanical properties, denaturation temperature and resistance to enzymatic degradation and to decrease free amines in collagen type I (43) and collagen type II (32) preparations. It is worth mentioning that the denaturation temperature of non-crosslinked fish derived scaffolds was $< 40\text{ }^{\circ}\text{C}$, as has been reported before for various marine collagen preparations (e.g. 33-34 $^{\circ}\text{C}$ for collagen from ray skin (44) and 35 $^{\circ}\text{C}$ for collagen from tilapia scales (45)). This low (relatively to mammalian derived collagen preparations that exhibit denaturation of $> 40\text{ }^{\circ}\text{C}$ (31, 33, 45)) can be attributed to their lower than mammalian collagen amino acid contents (proline and hydroxyproline) (46, 47).

Biological analysis revealed that all collagen preparations crosslinked with PEG-4SG supported hADSC growth, which is in agreement with previous publications that have demonstrated the cytocompatibility of PEG-4SG collagen scaffolds with both permanently differentiated (32, 48) and stem cell (49) populations. Histological analysis demonstrated equal among the different collagen preparations cell and ECM distribution. Further, cartilage-like ECM deposition was confirmed with both Alcian blue staining and sGAG quantification. These observations not only confirm that the pore size and porosity were suitable for cell and ECM migration within the three-dimensional conformation of the scaffolds, but also indicate the chondrogenic potential of the scaffolds. Again these observations are in agreement with previous work in the field, where Jellyfish (*Rhopilema esculentum*) collagen sponges with pore size of 40-200 μm (at the centre of the scaffold, the pore diameter was $74 \pm 18\text{ }\mu\text{m}$ and at superficial zones, the pore diameter was $50 \pm 20\text{ }\mu\text{m}$) (14) and bovine collagen type II

sponges with pore size of $140 \pm 30 \mu\text{m}$ (50) maintained chondrocyte phenotype and Jellyfish (*Rhopilema esculentum*) collagen sponges with porosity of $98.2 \pm 0.4 \%$ induced chondrogenic differentiation of human mesenchymal stem cells (16).

With respect to gene analysis, in general all collagen scaffolds showed a higher chondro-inductive potential compared to TCP, as evidenced by downregulated expression of COL1A1 and COL3A1 (except the LSD scaffold) and upregulated expression of COL10A1, SOX9, COMP and ACAN (except the CR scaffold). This can be attributed to the three-dimensional conformation of the scaffolds, as studies have demonstrated the important role of three-dimensional environment in effectively inducing (51) or maintaining (52) chondrogenic phenotype. Having said that, the biochemical signals of the scaffold cannot be excluded, as it has been shown previously that collagen type I and collagen type II coatings (i.e. two-dimensional culture) were more effective in maintaining chondrogenesis of human articular chondrocytes than non-coated substrates (53). Within the different collagen preparations, the LSD preparation induced the highest COL1A1, COL3A1 (in comparison to TBR and BR), COMP (in comparison to CR and BR) and ACAN (in comparison to CR) gene expression, suggesting that the LSD preparation held the highest chondrogenic induction potential. We recognise that the presence of COL1A1, COL3A1 and COL10A1 may be indicative of hypertrophy, but we believe that this is due to incomplete differentiation as opposed to established hypertrophy. To substantiate this one should consider that in chondrogenic differentiation of stem cells, collagen type I and collagen type III are frequently encountered (54-56). Further, considering that collagen type X was expressed before collagen type II, it is unlikely that in such short period of time (21 days) the stem cells became hypertrophic before becoming chondrocytes, further advocating that caution should be paid when lineage commitment is judged based on collagen type X (57). We recognise that although 21 days are customarily used for chondrogenesis (58-60), higher COL2A1 expression is expected to occur at later stages of chondrogenic differentiation and hence longer timepoints to engineer mature cartilage-like

tissue are recommended (e.g. 28 days (61), 42 days (62), 49 days (63), 56 days (64), 84 days (65)). In addition, it has been demonstrated that chondrogenic redifferentiation of chondrocytes in marine collagen scaffolds takes at least 21 days and the shift from collagen type I to collagen type II gene expression occurs after 21 days (14). We speculate that this higher chondrogenic capacity of the shark derived collagen over the ray-derived collagens may be due to their compositional materials differences (66) that may result in some form of tissue memory, as has been shown before for collagen type I sponges that were prepared from collagen preparations extracted from bovine and porcine skin and tendon tissues (67).

3.5. Conclusions

Considering that cartilage is primarily composed of collagen type II, the use of collagen type II scaffolds has been advocated for cartilage engineering approaches. Ethical and biological, albeit questionable, issues associated with mammalian collagen have triggered investigations into the potential of marine collagen in biomedicine. This study advocates the use of marine collagen type II and in particular collagen type II extracted from a marine chondrichthyan species (i.e. lesser spotted dogfish, *Scyliorhinus canicula*) for cartilage engineering.

3.6. References

1. Saccomano, S. J. Osteoarthritis treatment: Decreasing pain, improving mobility. *Nurse Pract.* 2018;43(9):49-55.
2. Szychlińska, M. A., Calabrese, G., Ravalli, S., Dolcimascolo, A., Castrogiovanni, P., Fabbi, C., Puglisi, C., Lauretta, G., Di Rosa, M., Castorina, A., Parenti, R., Musumeci, G. Evaluation of a cell-free collagen type I-based scaffold for articular cartilage regeneration in an orthotopic rat model. *Materials (Basel)*. 2020;13(10):2369.
3. Calabrese, G., Gulino, R., Giuffrida, R., Forte, S., Figallo, E., Fabbi, C., Salvatorelli, L., Memeo, L., Gulisano, M., Parenti, R. In vivo evaluation of biocompatibility and chondrogenic potential of a cell-free collagen-based scaffold. *Front Physiol.* 2017;8:984.
4. Gao, Y., Li, B., Kong, W., Yuan, L., Guo, L., Li, C., Fan, H., Fan, Y., Zhang, X. Injectable and self-crosslinkable hydrogels based on collagen type II and activated chondroitin sulfate for cell delivery. *Int J Biol Macromol.* 2018;118(Pt B):2014-20.
5. Lian, C., Wang, X., Qiu, X., Wu, Z., Gao, B., Liu, L., Liang, G., Zhou, H., Yang, X., Peng, Y., Liang, A., Xu, C., Huang, D., Su, P. Collagen type II suppresses articular chondrocyte hypertrophy and osteoarthritis progression by promoting integrin $\beta 1$ -SMAD1 interaction. *Bone Res.* 2019;7:8.
6. Vázquez-Portalatín, N. N., Kilmer, C. E., Panitch, A., Liu, J. C. Characterization of collagen type I and II blended hydrogels for articular cartilage tissue engineering. *Biomacromolecules.* 2016;17(10):3145-52.
7. Kilmer, C. E., Battistoni, C. M., Cox, A., Breur, G., Panitch, A., Liu, J. C. Collagen type I and II blend hydrogel with autologous mesenchymal stem cells as a scaffold for articular cartilage defect repair. *ACS Biomater Sci Eng.* 2020;6(6):3464-76.
8. Christensen, B. B., Foldager, C. B., Jensen, J., Jensen, N. C., Lind, M. Poor osteochondral repair by a biomimetic collagen scaffold: 1-to 3-year clinical and radiological follow-up. *Knee Surg Sports Traumatol Arthrosc.* 2016;24(7):2380-7.

9. Schüttler, K. F., Götschenberg, A., Klasan, A., Stein, T., Pehl, A., Roessler, P. P., Figiel, J., Heyse, T. J., Efe, T. Cell-free cartilage repair in large defects of the knee: Increased failure rate 5 years after implantation of a collagen type I scaffold. *Arch Orthop Trauma Surg.* 2019;139(1):99-106.
10. Avila Rodríguez, M. I., Rodríguez Barroso, L. G., Sánchez, M. L. Collagen: A review on its sources and potential cosmetic applications. *J Cosmet Dermatol.* 2018;17(1):20-6.
11. Silvipriya, K. S., Kumar, K. K., Bhat, A. R., Kumar, B. D., John, A., Lakshmanan, P. Collagen: Animal sources and biomedical application. *J Appl Pharm Sci.* 2015;5(3):123-7.
12. Felician, F. F., Xia, C., Qi, W., Xu, H. Collagen from marine biological sources and medical applications. *Chem Biodivers.* 2018;15(5):e1700557.
13. Ferrario, C., Leggio, L., Leone, R., Di Benedetto, C., Guidetti, L., Coccè, V., Ascagni, M., Bonasoro, F., La Porta, C. a. M., Candia Carnevali, M. D. Marine-derived collagen biomaterials from echinoderm connective tissues. *Mar Environ Res.* 2017;128:46-57.
14. Bermueller, C., Schwarz, S., Elsaesser, A. F., Sewing, J., Baur, N., Von Bomhard, A., Scheithauer, M., Notbohm, H., Rotter, N. Marine collagen scaffolds for nasal cartilage repair: Prevention of nasal septal perforations in a new orthotopic rat model using tissue engineering techniques. *Tissue Eng Part A.* 2013;19(19-20):2201-14.
15. Rigogliuso, S., Salamone, M., Barbarino, E., Barbarino, M., Nicosia, A., Ghersi, G. Production of injectable marine collagen-based hydrogel for the maintenance of differentiated chondrocytes in tissue engineering applications. *Int J Mol Sci.* 2020;21(16):5798.
16. Hoyer, B., Bernhardt, A., Lode, A., Heinemann, S., Sewing, J., Klinger, M., Notbohm, H., Gelinsky, M. Jellyfish collagen scaffolds for cartilage tissue engineering. *Acta Biomater.* 2014;10(2):883-92.
17. Pustlauk, W., Paul, B., Gelinsky, M., Bernhardt, A. Jellyfish collagen and alginate: Combined marine materials for superior chondrogenesis of hMSC. *Mater Sci Eng C Mater Biol Appl.* 2016;64:190-8.

18. Tamaddon, M., Burrows, M., Ferreira, S. A., Dazzi, F., Apperley, J. F., Bradshaw, A., Brand, D. D., Czernuszka, J., Gentleman, E. Monomeric, porous type II collagen scaffolds promote chondrogenic differentiation of human bone marrow mesenchymal stem cells in vitro. *Sci Rep.* 2017;7:43519.
19. Mueller, S. M., Shortkroff, S., Schneider, T. O., Breinan, H. A., Yannas, I. V., Spector, M. Meniscus cells seeded in type I and type II collagen-GAG matrices in vitro. *Biomaterials.* 1999;20(8):701-9.
20. Nehrer, S., Breinan, H. A., Ramappa, A., Shortkroff, S., Young, G., Minas, T., Sledge, C. B., Yannas, I. V., Spector, M. Canine chondrocytes seeded in type I and type II collagen implants investigated in vitro. *J Biomed Mater Res.* 1997;38(2):95-104.
21. Dai, M., Liu, X., Wang, N., Sun, J. Squid type II collagen as a novel biomaterial: Isolation, characterization, immunogenicity and relieving effect on degenerative osteoarthritis via inhibiting stat1 signaling in pro-inflammatory macrophages. *Mater Sci Eng C Mater Biol Appl.* 2018;89:283-94.
22. Chen, L., Bao, B., Wang, N., Xie, J., Wu, W. Oral administration of shark type II collagen suppresses complete Freund's adjuvant-induced rheumatoid arthritis in rats. *Pharmaceuticals (Basel).* 2012;5(4):339-52.
23. Merly, L., Smith, S. L. Collagen type II, alpha 1 protein: A bioactive component of shark cartilage. *Int Immunopharmacol.* 2013;15(2):309-15.
24. Ebert, D. A., Compagno, L. J. V. Biodiversity and systematics of skates (Chondrichthyes: Rajiformes: Rajoidei). *Environ Biol Fishes.* 2007;80:111-24.
25. Stehmann, M. F. W. Proposal of a maturity stages scale for oviparous and viviparous cartilaginous fishes (Pisces, Chondrichthyes). *Arch Fish Mar Res.* 2002;50(1):23-48.
26. Eyre, D. Articular cartilage and changes in arthritis: Collagen of articular cartilage. *Arthritis Res Ther.* 2001;4(1):30.
27. Soroushanova, A., Delgado, L. M., Wu, Z., Shologu, N., Kshirsagar, A., Raghunath, R., Mullen, A. M., Bayon, Y., Pandit, A., Raghunath, M., Zeugolis, D. I. The collagen suprafamily: From biosynthesis to advanced biomaterial development. *Adv Mater.* 2019;31(1):e1801651.

28. Zeugolis, D. I., Paul, R. G., Attenburrow, G. Factors influencing the properties of reconstituted collagen fibers prior to self-assembly: Animal species and collagen extraction method. *J Biomed Mater Res A*. 2008;86(4):892-904.
29. Delgado, L. M., Shologu, N., Fuller, K., Zeugolis, D. I. Acetic acid and pepsin result in high yield, high purity and low macrophage response collagen for biomedical applications. *Biomed Mater*. 2017;12(6):065009.
30. Lynn, A. K., Yannas, I. V., Bonfield, W. Antigenicity and immunogenicity of collagen. *J Biomed Mater Res B Appl Biomater*. 2004;71(2):343-54.
31. Delgado, L. M., Fuller, K., Zeugolis, D. I. Collagen cross-linking: Biophysical, biochemical, and biological response analysis. *Tissue Eng Part A*. 2017;23(19-20):1064-77.
32. Collin, E. C., Grad, S., Zeugolis, D. I., Vinatier, C. S., Clouet, J. R., Guicheux, J. J., Weiss, P., Alini, M., Pandit, A. S. An injectable vehicle for nucleus pulposus cell-based therapy. *Biomaterials*. 2011;32(11):2862-70.
33. Capella-Monsonís, H., Coentro, J. Q., Graceffa, V., Wu, Z., Zeugolis, D. I. An experimental toolbox for characterization of mammalian collagen type I in biological specimens. *Nat Protoc*. 2018;13(3):507.
34. Fuller, K. P., Gaspar, D., Delgado, L. M., Pandit, A., Zeugolis, D. I. Influence of porosity and pore shape on structural, mechanical and biological properties of poly ϵ -caprolactone electro-spun fibrous scaffolds. *Nanomedicine (Lond)*. 2016;11(9):1031-40.
35. Oliveira, S. M., Ringshia, R. A., Legeros, R. Z., Clark, E., Yost, M. J., Terracio, L., Teixeira, C. C. An improved collagen scaffold for skeletal regeneration. *J Biomed Mater Res A*. 2010;94(2):371-9.
36. Zeugolis, D. I., Raghunath, M. The physiological relevance of wet versus dry differential scanning calorimetry for biomaterial evaluation: A technical note. *Polym Int*. 2010;59(10):1403-7.
37. Helling, A. L., Tsekoura, E. K., Biggs, M., Bayon, Y., Pandit, A., Zeugolis, D. I. In vitro enzymatic degradation of tissue grafts and collagen

biomaterials by matrix metalloproteinases: Improving the collagenase assay. *ACS Biomater Sci Eng.* 2017;3(9):1922-32.

38. Jeevithan, E., Bao, B., Bu, Y., Zhou, Y., Zhao, Q., Wu, W. Type II collagen and gelatin from silvertip shark (*Carcharhinus albimarginatus*) cartilage: Isolation, purification, physicochemical and antioxidant properties. *Mar Drugs.* 2014;12(7):3852-73.

39. Kittiphattanabawon, P., Benjakul, S., Visessanguan, W., Shahidi, F. Isolation and characterization of collagen from the cartilages of brownbanded bamboo shark (*Chiloscyllium punctatum*) and blacktip shark (*Carcharhinus limbatus*). *LWT-Food Sci Technol.* 2010;43(5):792-800.

40. Calabrese, G., Forte, S., Gulino, R., Cefalì, F., Figallo, E., Salvatorelli, L., Maniscalchi, E. T., Angelico, G., Parenti, R., Gulisano, M., Memeo, L., Giuffrida, R. Combination of collagen-based scaffold and bioactive factors induces adipose-derived mesenchymal stem cells chondrogenic differentiation in vitro. *Front Physiol.* 2017;8:50.

41. Wahl, D. A., Sachlos, E., Liu, C., Czernuszka, J. T. Controlling the processing of collagen-hydroxyapatite scaffolds for bone tissue engineering. *J Mater Sci Mater Med.* 2007;18(2):201-9.

42. Katoh, K., Tanabe, T., Yamauchi, K. Novel approach to fabricate keratin sponge scaffolds with controlled pore size and porosity. *Biomaterials.* 2004;25(18):4255-62.

43. Thomas, D., Fontana, G., Chen, X., Sanz-Nogués, C., Zeugolis, D. I., Dockery, P., O'brien, T., Pandit, A. A shape-controlled tuneable microgel platform to modulate angiogenic paracrine responses in stem cells. *Biomaterials.* 2014;35(31):8757-66.

44. Bae, I., Osatomi, K., Yoshida, A., Osako, K., Yamaguchi, A., Hara, K. Biochemical properties of acid-soluble collagens extracted from the skins of underutilised fishes. *Food Chem.* 2008;108(1):49-54.

45. Ikoma, T., Kobayashi, H., Tanaka, J., Walsh, D., Mann, S. Physical properties of type I collagen extracted from fish scales of *Pagrus major* and *Oreochromis niloticus*. *Int J Biol Macromol.* 2003;32(3-5):199-204.

46. Addad, S., Exposito, J. Y., Faye, C., Ricard-Blum, S., Lethias, C. Isolation, characterization and biological evaluation of jellyfish collagen for use in biomedical applications. *Mar Drugs*. 2011;9(6):967-83.
47. Subhan, F., Ikram, M., Shehzad, A., Ghafoor, A. Marine collagen: An emerging player in biomedical applications. *J Food Sci Technol*. 2015;52(8):4703-7.
48. Kontturi, L. S., Järvinen, E., Muhonen, V., Collin, E. C., Pandit, A. S., Kiviranta, I., Yliperttula, M., Urtti, A. An injectable, in situ forming type II collagen/hyaluronic acid hydrogel vehicle for chondrocyte delivery in cartilage tissue engineering. *Drug Deliv Transl Res*. 2014;4(2):149-58.
49. Fontana, G., Thomas, D., Collin, E., Pandit, A. Microgel microenvironment primes adipose-derived stem cells towards an NP cells-like phenotype. *Adv Healthc Mater*. 2014;3(12):2012-22.
50. Ko, C. S., Huang, J. P., Huang, C. W., Chu, I. M. Type II collagen-chondroitin sulfate-hyaluronan scaffold cross-linked by genipin for cartilage tissue engineering. *J Biosci Bioeng*. 2009;107(2):177-82.
51. Estes, B. T., Guilak, F. Three-dimensional culture systems to induce chondrogenesis of adipose-derived stem cells. *Methods Mol Biol*. 2011;702:201-17.
52. Öztürk, E., Arlov, Ø., Aksel, S., Li, L., Ornitz, D. M., Skjåk-Bræk, G., Zenobi - Wong, M. Sulfated hydrogel matrices direct mitogenicity and maintenance of chondrocyte phenotype through activation of FGF signaling. *Adv Funct Mater*. 2016;26(21):3649-62.
53. Rutgers, M., Saris, D. B., Vonk, L. A., Van Rijen, M. H., Akrum, V., Langeveld, D., Van Boxtel, A., Dhert, W. J., Creemers, L. B. Effect of collagen type I or type II on chondrogenesis by cultured human articular chondrocytes. *Tissue Eng Part A*. 2013;19(1-2):59-65.
54. Jakobsen, R. B., Shahdadfar, A., Reinholt, F. P., Brinchmann, J. E. Chondrogenesis in a hyaluronic acid scaffold: Comparison between chondrocytes and MSC from bone marrow and adipose tissue. *Knee Surg Sports Traumatol Arthrosc*. 2010;18(10):1407-16.

55. Perrier, E., Ronzière, M. C., Bareille, R., Pinzano, A., Mallein-Gerin, F., Freyria, A. M. Analysis of collagen expression during chondrogenic induction of human bone marrow mesenchymal stem cells. *Biotechnol Lett.* 2011;33(10):2091-101.
56. Mahmoudifar, N., Doran, P. M. Chondrogenesis and cartilage tissue engineering: The longer road to technology development. *Trends Biotechnol.* 2012;30(3):166-76.
57. Mwale, F., Stachura, D., Roughley, P., Antoniou, J. Limitations of using aggrecan and type X collagen as markers of chondrogenesis in mesenchymal stem cell differentiation. *J Orthop Res.* 2006;24(8):1791-8.
58. Musumeci, G., Mobasher, A., Trovato, F. M., Szychlinska, M. A., Graziano, A. C., Lo Furno, D., Avola, R., Mangano, S., Giuffrida, R., Cardile, V. Biosynthesis of collagen I, II, RUNX2 and lubricin at different time points of chondrogenic differentiation in a 3D in vitro model of human mesenchymal stem cells derived from adipose tissue. *Acta Histochem.* 2014;116(8):1407-17.
59. Sekiya, I., Colter, D. C., Prockop, D. J. BMP-6 enhances chondrogenesis in a subpopulation of human marrow stromal cells. *Biochem Biophys Res Commun.* 2001;284(2):411-8.
60. Ragety, G. R., Griffon, D. J., Lee, H. B., Fredericks, L. P., Gordon-Evans, W., Chung, Y. S. Effect of chitosan scaffold microstructure on mesenchymal stem cell chondrogenesis. *Acta Biomater.* 2010;6(4):1430-6.
61. Szychlinska, M. A., Calabrese, G., Ravalli, S., Parrinello, N. L., Forte, S., Castrogiovanni, P., Pricoco, E., Imbesi, R., Castorina, S., Leonardi, R., Di Rosa, M., Musumeci, G. Cycloastragenol as an exogenous enhancer of chondrogenic differentiation of human adipose-derived mesenchymal stem cells. A morphological study. *Cells.* 2020;9(2):347.
62. Nürnberger, S., Schneider, C., Van Osch, G. V. M., Keibl, C., Rieder, B., Monforte, X., Teuschl, A. H., Mühleder, S., Holthoner, W., Schädl, B., Gahleitner, C., Redl, H., Wolbank, S. Repopulation of an auricular cartilage scaffold, AuriScaff, perforated with an enzyme combination. *Acta Biomater.* 2019;86:207-22.

63. Pelttari, K., Winter, A., Steck, E., Goetzke, K., Hennig, T., Ochs, B. G., Aigner, T., Richter, W. Premature induction of hypertrophy during in vitro chondrogenesis of human mesenchymal stem cells correlates with calcification and vascular invasion after ectopic transplantation in SCID mice. *Arthritis Rheum.* 2006;54(10):3254-66.
64. Jiang, T., Liu, W., Lv, X., Sun, H., Zhang, L., Liu, Y., Zhang, W. J., Cao, Y., Zhou, G. Potent in vitro chondrogenesis of CD105 enriched human adipose-derived stem cells. *Biomaterials.* 2010;31(13):3564-71.
65. Liu, K., Zhou, G. D., Liu, W., Zhang, W. J., Cui, L., Liu, X., Liu, T. Y., Cao, Y. The dependence of in vivo stable ectopic chondrogenesis by human mesenchymal stem cells on chondrogenic differentiation in vitro. *Biomaterials.* 2008;29(14):2183-92.
66. Porter, M. E., Beltrán, J. L., Koob, T. J., Summers, A. P. Material properties and biochemical composition of mineralized vertebral cartilage in seven elasmobranch species (Chondrichthyes). *J Exp Biol.* 2006;209(Pt 15):2920-8.
67. Sorushanova, A., Skoufos, I., Tzora, A., Mullen, A. M., Zeugolis, D. I. The influence of animal species, gender and tissue on the structural, biophysical, biochemical and biological properties of collagen sponges. *J Mater Sci Mater Med.* 2021;32(1):1-12.

Chapter 4 – The influence of bloom index, endotoxin levels and polyethylene glycol succinimidyl glutarate crosslinking on the physicochemical and biological properties of gelatin biomaterials

This chapter has been published in:

The influence of bloom index, endotoxin levels and polyethylene glycol succinimidyl glutarate crosslinking on the physicochemical and biological properties of gelatin biomaterials. **Z Wu**, SH Korntner, J Olijve, AM Mullen, DI Zeugolis. *Biomolecules* 2021

Authors' contribution: Z.W. contributed the concept, performed all the experiments (gelatin purity assessment, biomechanical and free amine assessment, resistance to enzymatic degradation assessment, macrophage viability, proliferation and metabolic activity assessment, macrophage morphology assessment), drafted figures and tables, wrote the manuscript; S.H.K. contributed the concept, reviewed and commented the manuscript; J.O. provided Rousselot® gelatin products; A.M.M. provided the funding; D.I.Z. contributed the concept, reviewed and edited the manuscript, provided the funding; all authors reviewed and approved the manuscript.

4.1. Introduction

Gelatin is attracting growing attention in the fields of tissue engineering and drug delivery due to its low antigenicity, high cell affinity, relatively easy processability and high availability at low cost (1-4). Gelatin is a mixture of peptides produced by partially acid (gelatin type A, isoelectric point of ~8) or alkaline (gelatin type B, isoelectric point of ~5) collagen hydrolysis (5, 6). Subject to the stage of the extraction, gelatin preparations are classified as low (initial stage of extraction / incomplete hydrolysis) or high (late stage of extraction / complete hydrolysis) bloom index (ranging from 50 to 300) (7). The bloom index and the concentration of the solution affect the gelling capacity and the gel strength of gelatin preparations (8, 9), which in turn affect their drug (10) and cell (11, 12) encapsulation and release capacity.

Despite the positive data that have been obtained over the years, the use of gelatin in biomedicine is somehow restricted due to its, among others, high affinity to endotoxin contamination. Endotoxins are large and complex lipopolysaccharides that are localised at the outer membrane of Gram-negative bacteria (13, 14) and are often associated with contamination of medical devices. Specifically, as endotoxins possess a high thermal stability (15) and are hard to destroy with conventional sterilisation conditions (16), residual endotoxins constitute the most significant pyrogen in parenteral drugs and medical devices (17, 18) and frequently lead to post-operative complications, such as delayed tissue regeneration and homeostasis, implant failure and septic shock (19-22). It is therefore imperative to assess residual endotoxins in medical devices and especially in natural biomaterials that are prone to endotoxin contamination (23, 24).

Herein, we ventured to assess the biophysical, biochemical and biological properties of gelatin (porcine type A and bovine type B, from two different suppliers) and gelatin-based biomaterials (hydrogels for physicochemical analysis and films for biological analysis) as a function of different levels of endotoxin content (from < 1 up to 10,370 endotoxin units per gram) and bloom

index (from 220 to 355). Gelatin hydrogels and films were crosslinked with 4-arm polyethylene glycol succinimidyl glutarate, which stabilisation and cytocompatibility efficiency have been repeatedly demonstrated in the literature (25-27).

4.2. Materials and Methods

4.2.1. Materials

Gelatin products (**Table 4.1**) were provided by Rousselot R&D Center (Belgium) or purchased from Sigma-Aldrich (Ireland). 4-arm polyethylene glycol (PEG) succinimidyl glutarate (4SG, Mw 10,000) was purchased from JenKem Technology (USA). All other materials and reagents were purchased from Sigma-Aldrich (Ireland) unless otherwise stated.

Table 4.1: Properties of gelatin samples used in this study. * The endotoxin units per gram values were provided by the supplier and were measured using the ENDONEXT™ EndoZyme® II–Recombinant Factor C (rFC) Endotoxin Detection Assay (Bernried am Starnberger See, Hyglos GmbH).

Material	Abbreviation	Bloom	Endotoxin Units per gram*
Rousselot®, type A porcine	RAP1	355	<1
Rousselot®, type A porcine	RAP80	220	80
Rousselot®, type A porcine	RAP780	285	780
Rousselot®, type A porcine	RAP4K	300	4000
Sigma G2500, type A porcine	SAP10.5K	300	10,370
Rousselot®, type B bovine	RBB9	247	9
Sigma G9382, type B bovine	SBB1.5K	225	1360

4.2.2. Purity assessment

To assess the purity of the gelatin samples, sodium dodecyl sulphate-polyacrylamide gel electrophoresis (SDS-PAGE) under non-reducing conditions was conducted (28) using a Mini-Protean 3 electrophoresis system (Bio-Rad Laboratories, UK). A 3 % running gel and a 5 % separation gel were used. Briefly, 10 % gelatin solutions were dissolved in 0.5 M acetic acid and neutralised with 1 N NaOH, followed by the addition of 5x sample buffer (bromophenol blue / SDS). The sample-buffer mixtures were heated at 95 °C for 5 mins and a 10 µl aliquot of each mixture was loaded into each well of the running gel. High purity soluble collagen type I (Symatase, France) was used as control. Electrophoresis was carried out by first applying 50 V constant voltage until the samples reached the end of the running gel (~ 30 min) and then 120 V constant voltage was applied until the samples reached the end of the separation gel (~ 60 min). The gels were stained with a silver staining kit (SilverQuest™, Invitrogen, USA) according to the manufacturer's protocol.

4.2.3. Fabrication and crosslinking of gelatin hydrogels and films

Gelatin hydrogels (250 µl final volume was used) were prepared by dissolving gelatin products in 1x phosphate buffered saline (PBS) at 50 °C to form solutions of 100 mg/ml, mixing them with 1 mM PEG-4SG and letting them assemble at 25 °C for 1 h in Ace silicone O-rings (Z504165). Gelatin films (250 µl final volume was used) were prepared by dissolving gelatin products in 1x PBS at 50 °C to form solution of 100 mg/ml, mixing them with 1 mM PEG-4SG at 25 °C in 48-well plates (Sarstedt, Germany) and allowing the liquid to evaporate overnight in a fume hood.

4.2.4. Biomechanical assessment

The mechanical properties of gelatin hydrogels were assessed via uniaxial compression using a universal tensile testing machine (Z2.5, Zwick/Roell, Germany), loaded with a 100 N static load cell. Uniaxial constant loading was

performed on gelatin hydrogels with approximately 3 mm height and 10 mm diameter. The gelatin hydrogels were placed between two loading cells and compressed until 70 % deformation, with a compression rate of 10 mm/min. Force, strain and elastic modulus were determined by plotting stress versus strain curves. Both compression strength and elastic modulus were determined on the linear area of the curves at the position of 30 % deformation and elastic modulus was calculated using the linear equation of trend-lines at the position of 30 % of the deformation (29).

4.2.5. Free amines assessment

Crosslinking efficiency was quantified using the 2,4,6-trinitrobenzene sulfonic acid (TNBSA) assay (Thermo Fisher Scientific, Ireland) (28). Briefly, gelatin hydrogels (~ 500 mg) were incubated with TNBSA at 37 °C for 2 h. The reaction was stopped by adding 10 % SDS and 1 M hydrochloric acid. The mixtures were subsequently heated at 95 °C for 15 min in order to hydrolyse the gelatin hydrogel samples. The absorbance was read at 335 nm (Varioskan Flash Multimode Reader, Thermo Scientific, Ireland) and values were normalised to the standard curve, which has been generated with a series of known glycine concentrations (0.005, 0.01, 0.02, 0.03, 0.04 and 0.05 mg/ml).

4.2.6. Resistance to enzymatic degradation assessment

Enzymatic stability of the gelatin hydrogels was quantified with the collagenase assay (30). Briefly, gelatin hydrogels were weighed and then incubated for 2 h in 0.1 M Tris-HCl and 50 mM CaCl₂ at pH 7.4. Subsequently, the hydrogels were digested with 50 U/ml bacterial collagenase type II (MMP-8; 17101-015, Gibco, Ireland). After 3 h, 6 h, 9 h, 12 h and 24 h of digestion at 37 °C, centrifugation was carried out at 10,000 g for 5 min, the supernatant was removed and the remaining gelatin hydrogels were weighed. The degree of enzymatic degradation was quantified using the following equation: $[(W_o - W_t) / W_o] \times 100$, where W_o is the original weight and W_t is the remaining weight.

4.2.7. Cell culture

In vitro inflammatory response was assessed using human-derived leukemic monocyte cells (THP-1, ATCC, USA) (31). Cells were grown in RPMI-1640 medium supplemented with 10 % foetal bovine serum and 1 % penicillin-streptomycin at 37 °C in 95 % humidified atmosphere of 5 % CO₂. Cells were seeded on gelatin films and tissue culture plastic (TCP) at an initial density of 26,000 cells/cm² and cultured in RPMI-1640 medium for 6 h to enable cell attachment. A mature macrophage-like state was induced through treatment with phorbol 12-myristate 13-acetate (PMA) at 100 ng/ml for 6 h, as has been described previously. Subsequently, human macrophages were washed with Hank's Balanced Salt Solution (HBSS) and incubated with RPMI-1640 medium at 37 °C in 95 % humidified atmosphere of 5 % CO₂ for 1 and 2 days.

4.2.8. Cell viability assessment

Cell viability was analysed using the Live/Dead[®] assay (Life Technologies, Ireland) as per manufacturer's protocol. Briefly, at the end of each timepoint, the gelatin films were washed three times with HBSS and incubated with calcein AM and ethidium homodimer 1 solution (4 µM calcein-AM and 2 µM ethidium homodimer-1) in HBSS at 37 °C and 5 % CO₂ humidified atmosphere for 30 min. The gelatin films were washed with fresh HBSS to remove excess dye. Images were then acquired using an inverted fluorescence microscope (IX 51, Olympus Corporation, Japan). Live (green: FITC, ~495 nm) and dead (red: TexasRed, ~589 nm) cells were analysed using ImageJ software (NIH, USA).

4.2.9. Cell proliferation assessment

Cell proliferation was assessed using the Quant-iT[™] PicoGreen[®] dsDNA kit (Invitrogen, Ireland), according to the manufacturer's guidelines. Gelatin films were washed three times with HBSS at each timepoint, 200 µl DNase free water was added and frozen at -80 °C until analysis. Gelatin films were freeze-thawed at least three times in order to lyse the cells. Subsequently, PicoGreen[®] working

solution was added to the gelatin films and incubated at room temperature for 5-10 min, protected from light. Fluorescence was measured at excitation and emission wavelengths of 480 nm and 520 nm, respectively, using a Varioskan™ Flash Multimode Reader (Thermo Fisher Scientific, Ireland). The obtained values were normalised to the standard curve, which was generated with a series of known DNA stock solutions at different concentrations (0, 5, 10, 25, 50, 100, 500 and 1,000 ng/ml).

4.2.10. Cell metabolic activity assessment

Cell metabolic activity was analysed using the alamarBlue® assay (Invitrogen, Ireland), as per manufacturer's protocol. Briefly, gelatin films were washed three times with HBSS at the end of each time point, 10 % alamarBlue® was added to each gelatin film and incubated at 37 °C and 5 % CO₂ humidified atmosphere for 3 h. Absorbance was measured at excitation and emission wavelengths of 570 nm and 600 nm, respectively, using a Varioskan™ Flash Multimode Reader (Thermo Fisher Scientific, Ireland).

4.2.11. Cell morphology assessment

At the end of each timepoint, gelatin films were washed three times with HBSS and cell morphology was analysed using a brightfield microscope (Olympus Corporation, Japan). The levels of macrophage fusion on gelatin films were analysed by measuring cell numbers on different gelatin films using ImageJ software (NIH, USA).

4.2.12. Statistical analysis

Numerical data are expressed as mean ± standard deviation. Statistical analysis was performed using SPSS. Analysis was performed using One-way analysis of variance (ANOVA) for multiple comparisons and 2-sample t-test for pair wise comparisons were employed after confirming the following assumptions: the

distribution from which each of the samples was derived was normal (Shapiro-Wilk normality test) and the variances of the population of the samples were equal to one another (Levene's test for equal variances). Nonparametric statistics were used when either or both of the above assumptions were violated and consequently Kruskal-Wallis test for multiple comparisons and Mann-Whitney test for 2-samples were carried out. Statistical significance was accepted at $p < 0.05$.

4.3. Results

4.3.1. Purity assessment

SDS-PAGE (**Figure 4.1**) revealed typical electrophoretic mobility of gelatin for all samples, characterised by the presence of α -, β - and γ - bands, as well as other bands of variable molecular weight.

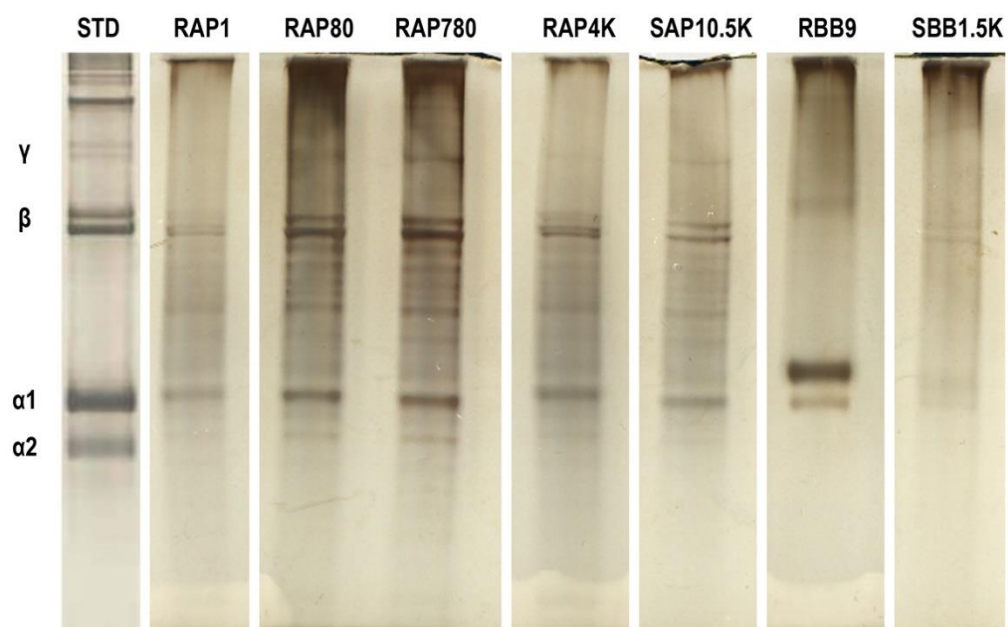


Figure 4.1: SDS-PAGE analysis of gelatin samples used in this study. It revealed typical electrophoretic mobility of gelatin, characterised by the presence of α -, β - and γ - bands, as well as other bands of variable molecular weight.

4.3.2. Biomechanical and free amine assessment

Among the different gelatin preparations, the RAP80 and SBB1.5K resulted in hydrogels with the lowest ($p < 0.05$) stress and modulus values in both non-crosslinked and crosslinked state; the SBB1.5K resulted in hydrogels with the highest % free amines in both non-crosslinked ($p < 0.05$) and crosslinked state ($p < 0.05$); and for all gelatin preparations, crosslinking significantly ($p < 0.05$) increased stress and modulus values and decreased % free amines (**Table 4.2**).

Table 4.2: Mechanical properties and free amine content of non-crosslinked (-PEG-4SG) and crosslinked (+PEG-4SG) gelatin samples used in this study. *: Indicates lowest ($p < 0.05$) mechanical properties and highest ($p < 0.05$) free amine content among non-crosslinked and crosslinked gelatin samples used in this study. #: Indicates higher ($p < 0.05$) mechanical properties and lower ($p < 0.05$) free amine content between non-crosslinked and crosslinked gelatin samples used in this study.

	RAP1		RAP80		RAP780		RAP4K		SAP10.5K		RBB9		SBB1.5K	
	-PEG- 4SG	+PEG- 4SG	-PEG- 4SG	+PEG- 4SG	-PEG- 4SG	+PEG- 4SG	-PEG- 4SG	+PEG- 4SG	-PEG- 4SG	+PEG- 4SG	-PEG- 4SG	+PEG- 4SG	-PEG- 4SG	+PEG- 4SG
Stress	21.7 ±	28.8 ±	12.5 ±	15.4 ±	21.0 ±	28.8 ±	22.1 ±	27.5 ±	22.8 ±	29.5 ±	21.8 ±	30.2 ±	10.2 ±	16.0 ±
(kPa)	1.2	1.6#	0.6*	0.2*#	2.9	3.2#	1.9	1.8#	2.5	3.0#	1.3	3.1#	2.0*	2.8*#
Modulus	72.4 ±	95.5 ±	41.8 ±	51.3 ±	70.0 ±	95.2 ±	73.8 ±	91.6 ±	75.8 ±	97.8 ±	72.8 ±	100.6	34.0 ±	53.3 ±
(kPa)	4.1	5.0#	1.9*	0.4*#	9.4	10.6#	6.3	6.0#	8.1	10.4#	4.3	±	6.5*	9.2*#
												10.1#		
Free	1.6 ±	0.6 ±	1.9 ±	0.8 ±	1.7 ±	0.6 ±	1.7 ±	0.7 ±	1.6 ±	0.8 ±	1.8 ±	0.8 ±	2.4 ±	1.8 ±
Amines	0.2	0.2#	0.1	0.1#	0.3	0.1#	0.1	0.3#	0.1	0.1#	0.1#	0.1#	0.1*	0.1*#
(%)														

4.3.3. Resistance to enzymatic degradation assessment

Collagenase digestion analysis (**Figure 4.2**) revealed that all non-crosslinked samples were completely degraded within 6 h of exposure to collagenase. Crosslinking significantly ($p < 0.05$) increased resistance to collagenase digestion, as crosslinked samples had at least > 35 % remaining mass after 6 h and were completely digested after 12 h of exposure to collagenase. Among the non-crosslinked groups, the SBB1.5K group exhibited the lowest ($p < 0.05$) resistance to collagenase digestion and no significant ($p > 0.05$) differences were observed between the other groups at 3 h of collagenase digestion. Among the crosslinked groups, the SBB1.5K group followed by the RAP80 group, exhibited significantly ($p < 0.05$) lower resistance to collagenase digestion than the other groups and no significant ($p > 0.05$) differences were observed between the other groups at 9 h of collagenase digestion.

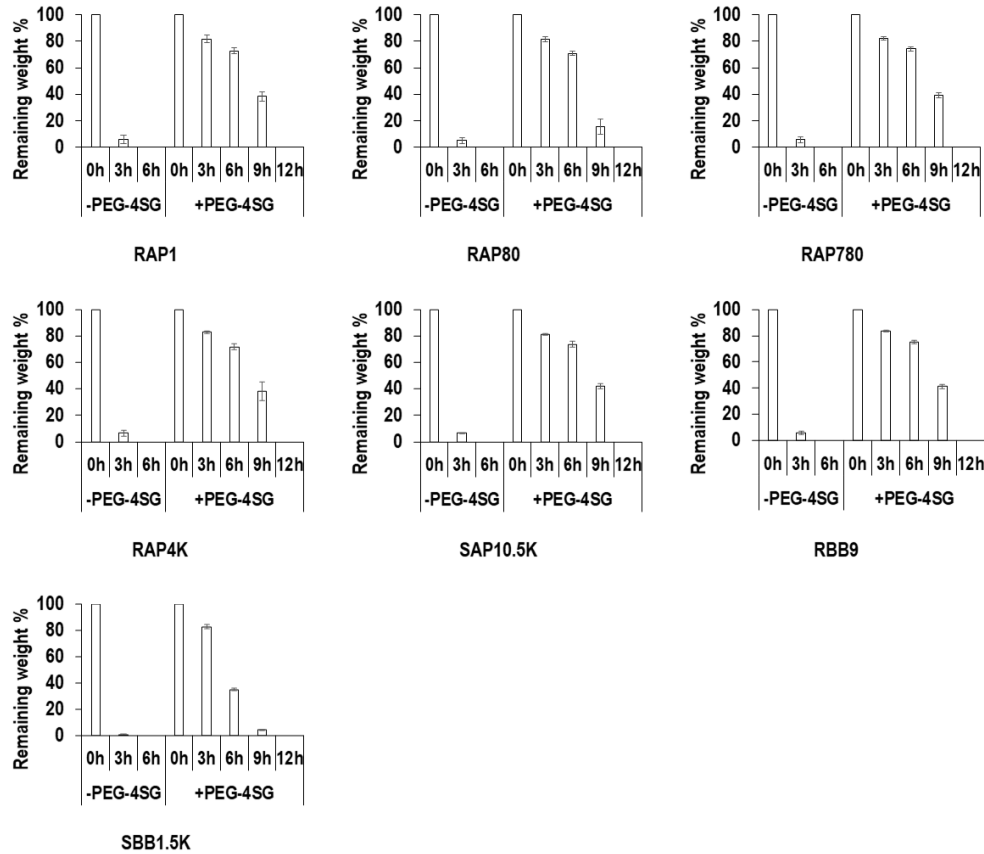


Figure 4.2: Resistance to enzymatic degradation analysis of non-crosslinked (-PEG-4SG) and crosslinked (+PEG-4SG) gelatin samples used in this study. Crosslinking significantly ($p < 0.05$) increased the resistance to collagenase digestion of each group. The SBB1.5K group exhibited the lowest resistance to collagenase digestion within the non-crosslinked ($p < 0.05$) and crosslinked groups ($p < 0.05$).

4.3.4. Macrophage viability, proliferation and metabolic activity assessment

Qualitative (**Figure 4.3A**) and quantitative (**Figure 4.3B**) cell viability and quantitative DNA concentration (**Figure 4.3C**) and metabolic activity (**Figure 4.3D**) analyses revealed no significant ($p > 0.05$) differences between the groups at any timepoint, apart from the SBB1.5K group, which exhibited the lowest ($p < 0.05$) cell viability at day 2 and the lowest ($p < 0.05$) metabolic activity at day 1 and day 2.

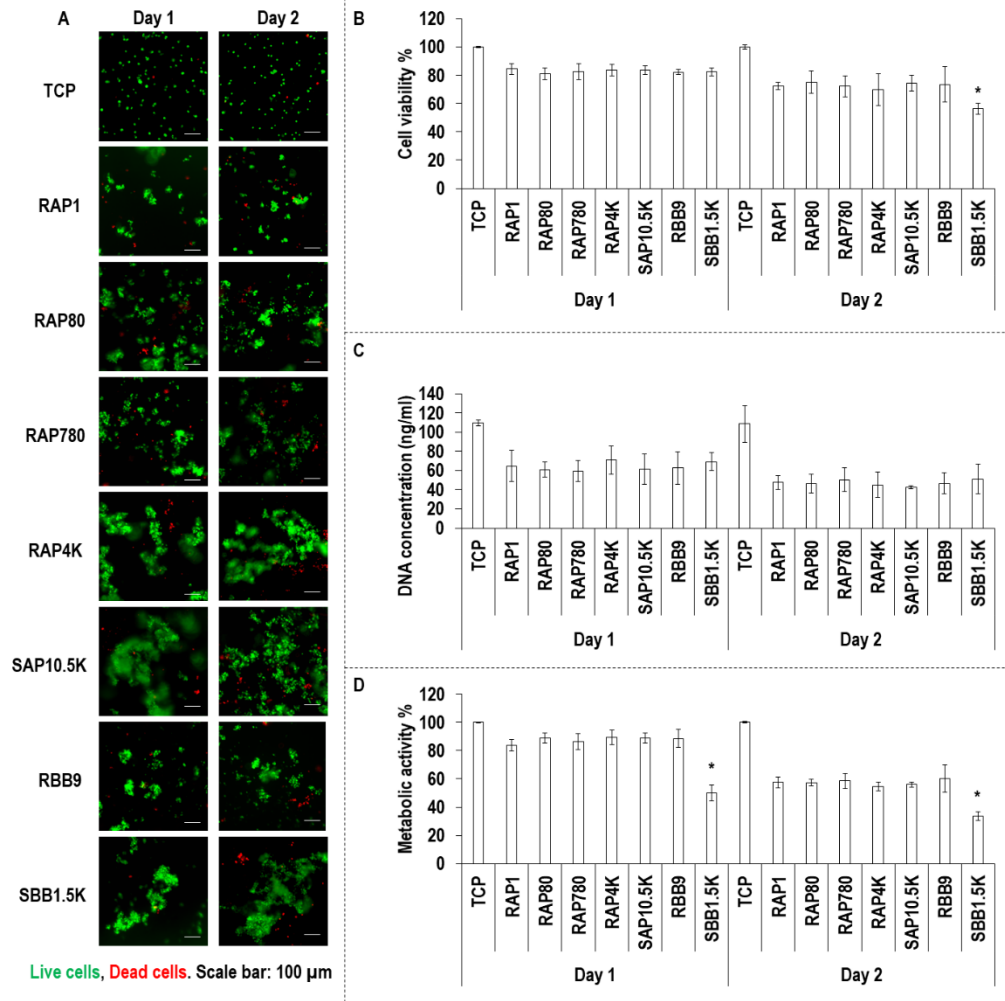


Figure 4.3: Macrophage viability (**A**, **B**), DNA concentration (**C**) and metabolic activity (**D**) analyses. The analyses revealed no significant ($p > 0.05$) differences between the groups, apart from the SBB1.5K group, which induced the lowest ($p < 0.05$) cell viability at day 2 and the lowest ($p < 0.05$) metabolic activity at day 1 and day 2. * indicates statistically significant difference ($p < 0.05$) between the gelatin groups.

4.3.5. Macrophage morphology assessment

Macrophage morphology (**Figure 4.4A**) and fusion (**Figure 4.4B**) assessment revealed that macrophages were of round morphology on all groups and formed the least ($p < 0.05$) number of clusters on TCP, RAP1, RAP80, RAP780 and RBB9 at both timepoints, respectively.

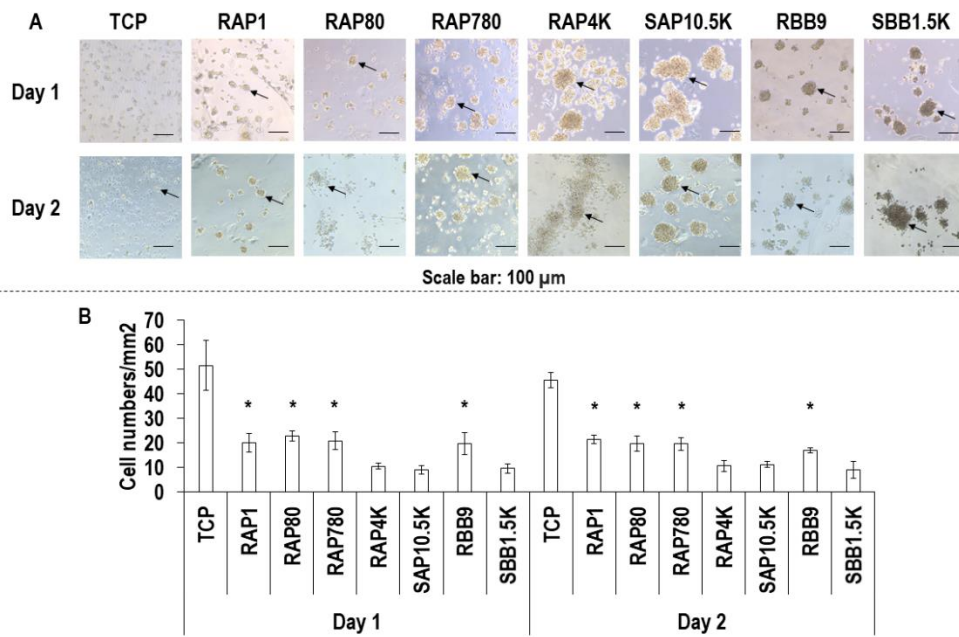


Figure 4.4: Macrophage morphology (**A**) and cell number (**B**) analyses. Cell clusters are indicated using black arrows. On all groups, macrophages exhibited a round morphology and on RAP4K, SAP10.5K and SBB1.5K, they formed the highest number ($p < 0.05$) of clusters. TCP: Tissue culture plastic. * indicates statistically significant difference ($p < 0.005$) between the gelatin groups.

4.4. Discussion

Gelatin, the hydrolysed derivative of collagen, is extensively used in food, pharma and medical device sectors (32-35). In medical device development, bloom index, a unit that measures extent of hydrolysis, is an important parameter that should be assessed as it affects the gelling capacity, gel strength and cell response of gelatin preparations. Another crucial factor in medical device development is residual endotoxin levels, as endotoxins are considered to be the most significant pyrogens and associated with post-operative complications, including implant failure. Herein, we assessed the physiochemical and biological properties of gelatin-based biomaterials and we correlated them to their bloom index and amount of endotoxins present in the original raw materials.

Starting with SDS-PAGE assessment, all gelatin preparations were comprised of α -, β - and γ - bands, as well as other bands of variable molecular weight. This is in agreement with previous publications, considering that gelatin is a mixture of water-soluble protein fragments, obtained by the destruction of collagen, with a molecular weight distribution ranging from 10 kDa to 400 kDa (36). Variable number and intensity of bands was observed between the different gelatin preparations, which we attribute to the origin and the manufacturing process of the respective gelatin preparations (37-41), as has also been observed previously for collagen preparations (28, 31, 42, 43).

With respect to mechanical properties, resistance to enzymatic degradation and free amine content, crosslinking increased mechanical properties and resistance to enzymatic degradation and decreased free amine content. Within the different gelatin preparations, the RAP80 and SBB1.5K groups exhibited the lowest compression stress and elastic modulus values, the highest free amine content (only the SBB1.5K was statistically significant) and the lowest resistance to enzymatic degradation (i.e. the crosslinked groups at 9 h of degradation). We attribute this low mechanical resilience / high free amine content / low resistance to enzymatic degradation to the low bloom strength of these gelatin preparations. In agreement with our observations, previous studies have shown that high bloom

rate results in gelatin scaffolds with high ultimate strength, rigidity and Young's modulus (11, 44-46). With respect to free amines and resistance to enzymatic degradation, high % of free amines and low resistance to enzymatic degradation are related to less crosslinked materials, as has been shown repeatedly for gelatin (47-49) and collagen (26, 28, 43) scaffolds.

With respect to cell shape, on all substrates the cells exhibited a round morphology, whilst cells have been reported to be of round morphology on low bloom index hydrogels and of elongated morphology on high bloom index hydrogels (50-52). We attribute this indifference in cell shape between the different gelatin preparations to residual endotoxins. Indeed, biological analysis with macrophages made apparent that high levels of residual endotoxins (> 1.5 K units/g) were responsible for cell fusion. It has been well-established in the literature that endotoxins are associated with macrophage activation (53, 54) and macrophage aggregation is indicative of foreign body response (55-57). Further, high endotoxin levels in gelatin preparations have been shown to significantly increase synthesis of TNF- α and CCL2 (58), notorious pro-inflammatory cytokines (59-61). To reduce the burden of endotoxin activated immune response, functionalisation strategies have been recommended (e.g. gelatin preparations functionalised with desaminotyrosine or desaminotyrosyl tyrosine resulted in reduced expression of IL6 and TNF- α (62)).

4.5. Conclusions

In this study, we evaluated the influence of bloom index and endotoxin level on the physicochemical and biological properties of gelatin biomaterials. Our data suggest that low endotoxin and high bloom index gelatin preparations should be used in medical device sector, unless fast degradation is required, in which case, low endotoxin and low bloom index gelatin preparations should be used.

4.6. References

1. Su, K., Wang, C. Recent advances in the use of gelatin in biomedical research. *Biotechnol Lett.* 2015;37(11):2139-45.
2. Afewerki, S., Sheikhi, A., Kannan, S., Ahadian, S., Khademhosseini, A. Gelatin - polysaccharide composite scaffolds for 3D cell culture and tissue engineering: Towards natural therapeutics. *Bioeng Transl Med.* 2019;4(1):96-115.
3. Echave, M. C., Hernandez-Moya, R., Iturriaga, L., Pedraz, J. L., Lakshminarayanan, R., Dolatshahi-Pirouz, A., Taebnia, N., Orive, G. Recent advances in gelatin-based therapeutics. *Expert Opin Biol Ther.* 2019;19(8):773-9.
4. Echave, M. C., Saenz Del Burgo, L., Pedraz, J. L., Orive, G. Gelatin as biomaterial for tissue engineering. *Curr Pharm Des.* 2017;23(24):3567-84.
5. Aramwit, P., Jaichawa, N., Ratanavaraporn, J., Srichana, T. A comparative study of type A and type B gelatin nanoparticles as the controlled release carriers for different model compounds. *Mater Express.* 2015;5(3):241-8.
6. Yeh, M. Y., Zhao, J. Y., Hsieh, Y. R., Lin, J. H., Chen, F. Y., Chakravarthy, R. D., Chung, P. C., Lin, H. C., Hung, S. C. Reverse thermo-responsive hydrogels prepared from Pluronic F127 and gelatin composite materials. *RSC Adv.* 2017;7(34):21252-7.
7. Bello, A. B., Kim, D., Kim, D., Park, H., Lee, S. H. Engineering and functionalization of gelatin biomaterials: From cell culture to medical applications. *Tissue Eng Part B Rev.* 2020;26(2):164-80.
8. Mad-Ali, S., Benjakul, S., Prodpran, T., Maqsood, S. Characteristics and gel properties of gelatin from goat skin as influenced by alkaline-pretreatment conditions. *Asian-Australas J Anim Sci.* 2016;29(6):845-54.
9. Gupta, D., Santoso, J. W., McCain, M. L. Characterization of gelatin hydrogels cross-linked with microbial transglutaminase as engineered skeletal muscle substrates. *Bioengineering (Basel).* 2021;8(1):6.

10. Chou, S. F., Luo, L. J., Lai, J. Y., Ma, D. H. On the importance of bloom number of gelatin to the development of biodegradable in situ gelling copolymers for intracameral drug delivery. *Int J Pharm.* 2016;511(1):30-43.
11. Lai, J. Y. The role of bloom index of gelatin on the interaction with retinal pigment epithelial cells. *Int J Mol Sci.* 2009;10(8):3442-56.
12. Lai, J. Y., Lin, P. K., Hsiue, G. H., Cheng, H. Y., Huang, S. J., Li, Y. T. Low bloom strength gelatin as a carrier for potential use in retinal sheet encapsulation and transplantation. *Biomacromolecules.* 2009;10(2):310-9.
13. Cavaillon, J. M. Exotoxins and endotoxins: Inducers of inflammatory cytokines. *Toxicon.* 2018;149:45-53.
14. Bertani, B., Ruiz, N. Function and biogenesis of lipopolysaccharides. *EcoSal Plus.* 2018;8(1):10.1128/ecosalplus.ESP-0001-2018.
15. Townsend, S., Caubilla Barron, J., Loc-Carrillo, C., Forsythe, S. The presence of endotoxin in powdered infant formula milk and the influence of endotoxin and *Enterobacter sakazakii* on bacterial translocation in the infant rat. *Food Microbiol.* 2007;24(1):67-74.
16. Gorbet, M. B., Sefton, M. V. Endotoxin: The uninvited guest. *Biomaterials.* 2005;26(34):6811-7.
17. Gorbet, M. B., Sefton, M. V. Biomaterial-associated thrombosis: Roles of coagulation factors, complement, platelets and leukocytes. *Biomaterials.* 2004;25(26):5681-703.
18. Borton, L. K., Coleman, K. P. Material-mediated pyrogens in medical devices: Applicability of the in vitro monocyte activation test. *ALTEX.* 2018;35(4):453-63.
19. Li, Y., Fujita, M., Boraschi, D. Endotoxin contamination in nanomaterials leads to the misinterpretation of immunosafety results. *Front Immunol.* 2017;8:472.
20. Wang, G., Zhang, P., Zhao, J. Endotoxin contributes to artificial loosening of prostheses induced by titanium particles. *Med Sci Monit.* 2018;24:7001.

21. Lieder, R., Petersen, P. H., Sigurjónsson, Ó. E. Endotoxins—The invisible companion in biomaterials research. *Tissue Eng Part B Rev.* 2013;19(5):391-402.
22. Munford, R. S. Endotoxemia—Menace, marker, or mistake? *J Leukoc Biol.* 2016;100(4):687-98.
23. Li, Y., Boraschi, D. Endotoxin contamination: A key element in the interpretation of nanosafety studies. *Nanomedicine (Lond).* 2016;11(3):269-87.
24. Dullah, E. C., Ongkudon, C. M. Current trends in endotoxin detection and analysis of endotoxin–protein interactions. *Crit Rev Biotechnol.* 2017;37(2):251-61.
25. Collin, E. C., Grad, S., Zeugolis, D. I., Vinatier, C. S., Clouet, J. R., Guicheux, J. J., Weiss, P., Alini, M., Pandit, A. S. An injectable vehicle for nucleus pulposus cell-based therapy. *Biomaterials.* 2011;32(11):2862-70.
26. Delgado, L. M., Fuller, K., Zeugolis, D. I. Collagen cross-linking: Biophysical, biochemical, and biological response analysis. *Tissue Eng Part A.* 2017;23(19-20):1064-77.
27. Wang, J., Zhang, F., Tsang, W. P., Wan, C., Wu, C. Fabrication of injectable high strength hydrogel based on 4-arm star PEG for cartilage tissue engineering. *Biomaterials.* 2017;120:11-21.
28. Capella-Monsonís, H., Coentro, J. Q., Graceffa, V., Wu, Z., Zeugolis, D. I. An experimental toolbox for characterization of mammalian collagen type I in biological specimens. *Nat Protoc.* 2018;13(3):507.
29. Oliveira, S. M., Ringshia, R. A., Legeros, R. Z., Clark, E., Yost, M. J., Terracio, L., Teixeira, C. C. An improved collagen scaffold for skeletal regeneration. *J Biomed Mater Res A.* 2010;94(2):371-9.
30. Helling, A. L., Tsekoura, E. K., Biggs, M., Bayon, Y., Pandit, A., Zeugolis, D. I. In vitro enzymatic degradation of tissue grafts and collagen biomaterials by matrix metalloproteinases: Improving the collagenase assay. *ACS Biomater Sci Eng.* 2017;3(9):1922-32.

31. Delgado, L. M., Shologu, N., Fuller, K., Zeugolis, D. I. Acetic acid and pepsin result in high yield, high purity and low macrophage response collagen for biomedical applications. *Biomed Mater.* 2017;12(6):065009.
32. Ramos, M., Valdes, A., Beltran, A., Garrigós, M. C. Gelatin-based films and coatings for food packaging applications. *Coatings.* 2016;6(4):41.
33. Jaipan, P., Nguyen, A., Narayan, R. J. Gelatin-based hydrogels for biomedical applications. *MRS Commun.* 2017;7(3):416.
34. Klotz, B. J., Gawlitta, D., Rosenberg, A. J. W. P., Malda, J., Melchels, F. P. W. Gelatin-methacryloyl hydrogels: Towards biofabrication-based tissue repair. *Trends Biotechnol.* 2016;34(5):394-407.
35. Ali, E., Sultana, S., Hamid, S. B. A., Hossain, M., Yehya, W. A., Kader, A., Bhargava, S. K. Gelatin controversies in food, pharmaceuticals, and personal care products: Authentication methods, current status, and future challenges. *Crit Rev Food Sci Nutr.* 2018;58(9):1495-511.
36. Mariod, A. A., Fadul, H. Gelatin, source, extraction and industrial applications. *Acta Sci Pol Technol Aliment.* 2013;12(2):135-47.
37. Zhou, P., Mulvaney, S. J., Regenstein, J. M. Properties of Alaska pollock skin gelatin: A comparison with tilapia and pork skin gelatins. *J Food Sci.* 2006;71(4):C313-C21.
38. Zhang, Z., Li, G., Shi, B. Physicochemical properties of collagen, gelatin and collagen hydrolysate derived from bovine limed split wastes. *J Soc Leather Technol Chem.* 2006;90(1):23-8.
39. Cole, C. G. B., Roberts, J. J. Changes in the molecular composition of gelatine due to the manufacturing process and animal age, as shown by electrophoresis. *J Soc Leather Technol Chem.* 1996;80(5):136-41.
40. Ahmad, M., Benjakul, S. Characteristics of gelatin from the skin of unicorn leatherjacket (*Aluterus monoceros*) as influenced by acid pretreatment and extraction time. *Food Hydrocoll.* 2011;25(3):381-8.
41. Tukiran, N. A., Amin, I., Man, Y. Differentiation of bovine and porcine gelatins in processed products via sodium dodecyl sulphate-polyacrylamide gel

electrophoresis (SDS-PAGE) and principal component analysis (PCA) techniques. *Int Food Res J.* 2012;19(3):1175-80.

42. Soroushanova, A., Delgado, L. M., Wu, Z., Shologu, N., Kshirsagar, A., Raghunath, R., Mullen, A. M., Bayon, Y., Pandit, A., Raghunath, M., Zeugolis, D. I. The collagen suprafamily: From biosynthesis to advanced biomaterial development. *Adv Mater.* 2019;31(1):e1801651.

43. Soroushanova, A., Skoufos, I., Tzora, A., Mullen, A. M., Zeugolis, D. I. The influence of animal species, gender and tissue on the structural, biophysical, biochemical and biological properties of collagen sponges. *J Mater Sci Mater Med.* 2021;32(1):1-12.

44. Usta, M., Piech, D. L., MacCrone, R. K., Hillig, W. B. Behavior and properties of neat and filled gelatins. *Biomaterials.* 2003;24(1):165-72.

45. Netter, A. B., Goudoulas, T. B., Germann, N. Effects of bloom number on phase transition of gelatin determined by means of rheological characterization. *LWT.* 2020;132:109813.

46. Bigi, A., Panzavolta, S., Rubini, K. Relationship between triple-helix content and mechanical properties of gelatin films. *Biomaterials.* 2004;25(25):5675-80.

47. Siqueira, N. M., Paiva, B., Camassola, M., Rosenthal-Kim, E. Q., Garcia, K. C., Dos Santos, F. P., Soares, R. M. Gelatin and galactomannan-based scaffolds: Characterization and potential for tissue engineering applications. *Carbohydr Polym.* 2015;133:8-18.

48. Jetbumpenkul, P., Amornsudthiwat, P., Kanokpanont, S., Damrongsakkul, S. Balanced electrostatic blending approach—an alternative to chemical crosslinking of Thai silk fibroin/gelatin scaffold. *Int J Biol Macromol.* 2012;50(1):7-13.

49. Kishan, A. P., Nezarati, R. M., Radzicki, C. M., Renfro, A. L., Robinson, J. L., Whitely, M. E., Cosgriff-Hernandez, E. M. In situ crosslinking of electrospun gelatin for improved fiber morphology retention and tunable degradation. *J Mater Chem B.* 2015;3(40):7930-8.

50. Rens, E. G., Merks, R. M. H. Cell shape and durotaxis explained from cell-extracellular matrix forces and focal adhesion dynamics. *iScience*. 2020;23(9):101488.
51. Gupta, M., Doss, B. L., Kocgozlu, L., Pan, M., Mège, R. M., Callan-Jones, A., Voituriez, R., Ladoux, B. Cell shape and substrate stiffness drive actin-based cell polarity. *Phys Rev E*. 2019;99(1):012412.
52. Tee, S. Y., Fu, J., Chen, C. S., Janmey, P. A. Cell shape and substrate rigidity both regulate cell stiffness. *Biophys J*. 2011;100(5):L25-L7.
53. Foey, A. D., Crean, S. Macrophage subset sensitivity to endotoxin tolerisation by *Porphyromonas gingivalis*. *PLoS One*. 2013;8(7):e67955.
54. Blunck, R., Scheel, O., Müller, M., Brandenburg, K., Seitzer, U., Seydel, U. New insights into endotoxin-induced activation of macrophages: Involvement of a K⁺ channel in transmembrane signaling. *J Immunol*. 2001;166(2):1009-15.
55. Yahyouché, A., Zhidao, X., Czernuszka, J. T., Clover, A. J. Macrophage-mediated degradation of crosslinked collagen scaffolds. *Acta Biomater*. 2011;7(1):278-86.
56. Collier, T. O., Anderson, J. M., Brodbeck, W. G., Barber, T., Healy, K. E. Inhibition of macrophage development and foreign body giant cell formation by hydrophilic interpenetrating polymer network. *J Biomed Mater Res A*. 2004;69(4):644-50.
57. Mori, K., Nishimura, M., Tsurudome, M., Ito, M., Nishio, M., Kawano, M., Kozuka, Y., Yamashita, Y., Komada, H., Uchida, A., Ito, Y. The functional interaction between CD98 and CD147 in regulation of virus-induced cell fusion and osteoclast formation. *Med Microbiol Immunol*. 2004;193(4):155-62.
58. Groen, W. M. G. a. C., Utomo, L., Castilho, M., Gawlitta, D., Malda, J., Weeren, P. R. V., Levato, R., Korthagen, N. M. Impact of endotoxins in gelatine hydrogels on chondrogenic differentiation and inflammatory cytokine secretion in vitro. *Int J Mol Sci*. 2020;21(22):8571.
59. Varfolomeev, E., Vucic, D. Intracellular regulation of TNF activity in health and disease. *Cytokine*. 2018;101:26-32.

60. Zuckerman, S. H., Evans, G. F., Snyder, Y. M., Roeder, W. D. Endotoxin-macrophage interaction: Post-translational regulation of tumor necrosis factor expression. *J Immunol.* 1989;143(4):1223-7.
61. Cerri, C., Genovesi, S., Allegra, M., Pistillo, F., Püntener, U., Guglielmotti, A., Perry, V. H., Bozzi, Y., Caleo, M. The chemokine CCL2 mediates the seizure-enhancing effects of systemic inflammation. *J Neurosci.* 2016;36(13):3777-88.
62. Roch, T., Pierce, B. F., Zaupa, A., Jung, F., Neffe, A. T., Lendlein, A. Reducing the endotoxin burden of desaminotyrosine - and desaminotyrosyl tyrosine-functionalized gelatin. *Macromol Symp.* 2011;309(1):182-9.

Chapter 5 – Conclusions and future studies

5.1. Conclusions

Articular cartilage is a specialised connective tissue of joints, with limited self-repair capacity renders its regeneration a formidable challenge. Collagen type I biomaterials have demonstrated limited regeneration capacity in long term clinical studies. Although the use of collagen type II in cartilage engineering has been advocated as it is the main constituent of cartilage tissue, its optimal source still remains elusive. The aim of this study was to assess the chondrogenic differentiation of human adipose derived stem cells in chondrogenic media using mammalian (porcine; male and female; and articular, tracheal and auricular cartilage tissues were used) derived collagen type II sponges (**Chapter 2**) and marine (lesser spotted dogfish, thorn back ray, cuckoo ray and blonde ray chondrichthyan tissues were used) derived collagen type II sponges (**Chapter 3**). Data obtained from **Chapter 2** (porcine tissues) advocate the use of male / female articular cartilage (as opposed to tracheal and auricular cartilage) derived collagen type II scaffolds for cartilage engineering applications, as judged by resistance to enzymatic degradation, biomechanical properties and chondrogenic differentiation potential. Data obtained from **Chapter 3** (marine tissues) advocate the use of lesser spotted dogfish (as opposed to thorn back ray, cuckoo ray and blonde ray) derived collagen type II scaffolds for cartilage engineering applications, as judged by enzymatic degradation, biomechanical properties and chondrogenic differentiation potential. In both (mammalian and marine collagen sponges) cases, the presence of collagen type I appeared to reduce the chondrogenic differentiation of human adipose derived stem cells, further advocating the notion that collagen type I scaffolds are not suitable for cartilage engineering. In **Chapter 4**, it was demonstrated that the bloom index modulates the physicochemical properties and the endotoxin content regulates the biological response of gelatin biomaterials. For various reasons, the chondrogenic potential of gelatin preparations was not assessed.

5.2. Future studies

5.2.1. Engineering and assessing an optimally functionalised collagen type II sponge

This study very clearly illustrated the potential of collagen type II scaffolds to induce chondrogenic phenotype to human adipose derived stem cells. Although plausible, it would be naïve to assume that collagen type II alone will be enough to induce hyaline cartilage in preclinical and clinical setting. To this end, it is proposed to appropriate functionalise collagen type II scaffolds with molecules that have been shown to induce chondrogenesis *in vitro* and *in vivo* (e.g. glycosaminoglycans, such as hyaluronic acid (1-4) and chondroitin sulphate (5, 6); hormones, such as thyroxine (7) and parathyroid hormone (8); genes, such as SOX trio (9, 10) and RUNX2 (11); growth factors, such as TGF- β 1 (12, 13), TGF- β 3 (14, 15) and BMP-7 (16); and small molecules, such as kartogenin (17, 18)) and to assess the optimal combination(s) in an appropriate preclinical model.

5.2.2. Engineering and assessing an optimally functionalised gelatin material

This study very clearly illustrated that the bloom index modulates the physicochemical properties and the endotoxin content regulates the biological response of gelatin biomaterials. The next logical step is to fabricate appropriately crosslinked (finetune mechanical properties, degradation and cytocompatibility) and functionalised (see above) gelatin-based scaffolds (e.g. hydrogels, bioprinted materials, electrospun fibres) for cartilage engineering. After all, the potential of gelatin in cartilage engineering has already been shown ((19-23)), without however taking into consideration bloom index and endotoxin level.

5.3. References

1. Allemann, F., Mizuno, S., Eid, K., Yates, K. E., Zaleske, D., Glowacki, J. Effects of hyaluronan on engineered articular cartilage extracellular matrix gene expression in 3-dimensional collagen scaffolds. *J Biomed Mater Res.* 2001;55(1):13-9.
2. Tang, S., Spector, M. Incorporation of hyaluronic acid into collagen scaffolds for the control of chondrocyte-mediated contraction and chondrogenesis. *Biomed Mater.* 2007;2(3):S135-S41.
3. Matsiko, A., Levingstone, T. J., O'Brien, F. J., Gleeson, J. P. Addition of hyaluronic acid improves cellular infiltration and promotes early-stage chondrogenesis in a collagen-based scaffold for cartilage tissue engineering. *J Mech Behav Biomed Mater.* 2012;11:41-52.
4. Murphy, C. M., Matsiko, A., Haugh, M. G., Gleeson, J. P., O'Brien, F. J. Mesenchymal stem cell fate is regulated by the composition and mechanical properties of collagen–glycosaminoglycan scaffolds. *J Mech Behav Biomed Mater.* 2012;11:53-62.
5. Chen, W. C., Wei, Y. H., Chu, I. M., Yao, C. L. Effect of chondroitin sulphate C on the in vitro and in vivo chondrogenesis of mesenchymal stem cells in crosslinked type II collagen scaffolds. *J Tissue Eng Regen Med.* 2013;7(8):665-72.
6. Recha-Sancho, L., Semino, C. E. Chondroitin sulfate-and decorin-based self-assembling scaffolds for cartilage tissue engineering. *PLoS One.* 2016;11(6):e0157603.
7. Whitney, G. A., Kean, T. J., Fernandes, R. J., Waldman, S., Tse, M. Y., Pang, S. C., Mansour, J. M., Dennis, J. E. Thyroxine increases collagen type II expression and accumulation in scaffold-free tissue-engineered articular cartilage. *Tissue Eng Part A.* 2018;24(5-6):369-81.
8. Dutra, E. H., O'Brien, M. H., Chen, P. J., Wei, M., Yadav, S. Intermittent parathyroid hormone [1-34] augments chondrogenesis of the mandibular condylar cartilage of the temporomandibular joint. *Cartilage.* 2019.

9. Im, G. I., Kim, H. J., Lee, J. H. Chondrogenesis of adipose stem cells in a porous PLGA scaffold impregnated with plasmid DNA containing SOX trio (SOX-5,-6 and-9) genes. *Biomaterials*. 2011;32(19):4385-92.
10. Ikeda, T., Kamekura, S., Mabuchi, A., Kou, I., Seki, S., Takato, T., Nakamura, K., Kawaguchi, H., Ikegawa, S., Chung, U. I. The combination of SOX5, SOX6, and SOX9 (the SOX trio) provides signals sufficient for induction of permanent cartilage. *Arthritis Rheum*. 2004;50(11):3561-73.
11. Kim, S. M., Yi, S. W., Kim, H. J., Park, J. S., Kim, J. H., Park, K. H. Co-delivery of RUNX2-targeting miRNAs and shRNAs using nanoparticles composed of dexamethasone and PEI induces chondrogenesis of human mesenchymal stem cells. *J Biomed Nanotechnol*. 2019;15(1):113-26.
12. Chiang, C. S., Chen, J. Y., Chiang, M. Y., Hou, K. T., Li, W. M., Chang, S. J., Chen, S. Y. Using the interplay of magnetic guidance and controlled TGF- β release from protein-based nanocapsules to stimulate chondrogenesis. *Int J Nanomedicine*. 2018;13:3177-88.
13. Defail, A. J., Chu, C. R., Izzo, N., Marra, K. G. Controlled release of bioactive TGF- β 1 from microspheres embedded within biodegradable hydrogels. *Biomaterials*. 2006;27(8):1579-85.
14. Mahmoudi, Z., Mohammadnejad, J., Razavi Bazaz, S., Abouei Mehrizi, A., Saidijam, M., Dinarvand, R., Ebrahimi Warkiani, M., Soleimani, M. Promoted chondrogenesis of hMCSs with controlled release of TGF- β 3 via microfluidics synthesized alginate nanogels. *Carbohydr Polym*. 2020;229:115551.
15. Almeida, H. V., Liu, Y., Cunniffe, G. M., Mulhall, K. J., Matsiko, A., Buckley, C. T., O'brien, F. J., Kelly, D. J. Controlled release of transforming growth factor- β 3 from cartilage extracellular matrix derived scaffolds to promote chondrogenesis of human joint tissue derived stem cells. *Acta Biomater*. 2014;10(10):4400-9.
16. Crecente-Campo, J., Borrajo, E., Vidal, A., Garcia-Fuentes, M. New scaffolds encapsulating TGF- β 3/BMP-7 combinations driving strong chondrogenic differentiation. *Eur J Pharm Biopharm*. 2017;114:69-78.

17. Sun, X., Wang, J., Wang, Y., Zhang, Q. Collagen-based porous scaffolds containing PLGA microspheres for controlled kartogenin release in cartilage tissue engineering. *Artif Cells Nanomed Biotechnol.* 2018;46(8):1957-66.
18. Cai, G., Liu, W., He, Y., Huang, J., Duan, L., Xiong, J., Liu, L., Wang, D. Recent advances in kartogenin for cartilage regeneration. *J Drug Target.* 2019;27(1):28-32.
19. Choi, S. M., Lee, K. M., Ryu, S. B., Park, Y. J., Hwang, Y. G., Baek, D., Choi, Y., Park, K. H., Park, K. D., Lee, J. W. Enhanced articular cartilage regeneration with SIRT1-activated MSCs using gelatin-based hydrogel. *Cell Death Dis.* 2018;9(9):866.
20. Xu, Y., Wang, Z., Hua, Y., Zhu, X., Wang, Y., Duan, L., Zhu, L., Jiang, G., Xia, H., She, Y., Zhou, G. Photocrosslinked natural hydrogel composed of hyaluronic acid and gelatin enhances cartilage regeneration of decellularized trachea matrix. *Mater Sci Eng C Mater Biol Appl.* 2021;120:111628.
21. Li, Q., Xu, S., Feng, Q., Dai, Q., Yao, L., Zhang, Y., Gao, H., Dong, H., Chen, D., Cao, X. 3D printed silk-gelatin hydrogel scaffold with different porous structure and cell seeding strategy for cartilage regeneration. *Bioact Mater.* 2021;6(10):3396-410.
22. Shi, C., Yao, Y., Wang, L., Sun, P., Feng, J., Wu, G. Human salivary histatin-1-functionalized gelatin methacrylate hydrogels promote the regeneration of cartilage and subchondral bone in temporomandibular joints. *Pharmaceuticals (Basel).* 2021;14(5):484.
23. Semitela, Â., Girão, A. F., Fernandes, C., Ramalho, G., Pinto, S. C., Completo, A., Marques, P. a. a. P. Boosting in vitro cartilage tissue engineering through the fabrication of polycaprolactone-gelatin 3D scaffolds with specific depth-dependent fiber alignments and mechanical stimulation. *J Mech Behav Biomed Mater.* 2021;117:104373.

Appendices: protocols and research outputs

A. Protocols

Table A.1: List of reagents and respective suppliers

Reagents	Suppliers
4-arm PEG Succinimidyl Glutarate MW 10,000 (4S-StarPEG)	Jenkem Technology, China
2,4,6-Trinitrobenzene sulfonic acid	Sigma Aldrich, Ireland
Tissue culture plastics	SARSTEDT, Ireland NUNC, Ireland
Acrylamide/bis-acrylamide 30 % solution	Sigma Aldrich, Ireland
α -Minimum Essential Medium GlutaMAX™	Life Technologies, Ireland
alamarBlue®	Invitrogen, USA
Alcian blue solution	Sigma Aldrich, Ireland
Absolute ethanol	Lennox, Ireland
Ammonium persulphate (APS)	Sigma Aldrich, Ireland
Ambion® RNA Storage Solution	Thermo Fisher Scientific, Ireland
Blyscan™ sGAG assay kit	Biocolor, UK
Bovine serum albumin	Sigma Aldrich, Ireland
Bromophenol blue	Bio-Rad, UK
Calcium chloride	Sigma Aldrich, Ireland
Calcein AM	Invitrogen, USA
Collagen type I	Symatase Biomateriaux, France
Collagenase type II from <i>Clostridium histolyticum</i>	Thermo Fisher Scientific, Ireland
Chloroform	Sigma Aldrich, Ireland
Dulbecco's Modified Eagle's Medium – high glucose	Sigma Aldrich, Ireland
Dexamethasone	Sigma Aldrich, Ireland
Dimethyl sulfoxide (DMSO)	Sigma Aldrich, Ireland

Dibutylphthalate polystyrene xylene (DPX)	Sigma Aldrich, Ireland
Eosin	Carl Roth, Germany
Ethidium homodimer-1	Sigma Aldrich, Ireland
Foetal bovine serum (FBS)	Sigma Aldrich, Ireland
Glycerol	Sigma Aldrich, Ireland
Glycine	Fisher Chemicals, Ireland
Glacial acetic acid	Thermo Fisher Scientific, Ireland
GlycoBlue™ coprecipitant	Thermo Fisher Scientific, Ireland
Gelatine, porcine, type A	Sigma Aldrich, Ireland
Gelatin, bovine, type B	Sigma Aldrich, Ireland
Gelatin, porcine, type A	Rousselot, Belgium
Gelatin, bovine, type B	Rousselot, Belgium
Hank's Balanced Salt Solution (HBSS)	Sigma Aldrich, Ireland
Hydrochloric acid 37 %	Sigma Aldrich, Ireland
Isopropanol	Sigma Aldrich, Ireland
ITS liquid media supplement	Sigma Aldrich, Ireland
iScript™ reverse transcription supermix	BioRad, UK
L-ascorbic acid 2-phosphate	Sigma Aldrich, Ireland
Mayer's Haematoxylin	Carl Roth, Germany
N,N,N',N'-Tetramethylethylenediamine (TEMED)	Bio-Rad, UK
Nuclear fast red solution	Sigma Aldrich, Ireland
Nuclease free water	Sigma Aldrich, Ireland
Optimal cutting temperature compound (OCT compound)	Thermo Fisher Scientific, Ireland
Phosphate buffered saline (PBS)	Thermo Fisher Scientific, Ireland

Penicillin streptomycin	Sigma Aldrich, Ireland
Pepsin from porcine gastric mucosa 3,200-4,500 units/mg protein	Sigma Aldrich, Ireland
Papain from papaya latex	Sigma Aldrich, Ireland
Phorbol 12-myristate 13-acetate (PMA)	Sigma Aldrich, Ireland
Paraformaldehyde (PFA)	Sigma Aldrich, Ireland
Quant-iT™ PicoGreen® dsDNA Assay Kit	Invitrogen, USA
Roswell Park Memorial Institute (RPMI)-1640 medium	Sigma Aldrich, Ireland
Recombinant Human TGF-β3	R&D Systems
RiboSafe RNase inhibitor	Bioline, Ireland
Sucrose	Sigma Aldrich, Ireland
Sodium bicarbonate	Sigma Aldrich, Ireland
SilverQuest™ Silver staining kit	Invitrogen, USA
Sodium chloride	Sigma Aldrich, Ireland
Sodium dodecyl sulphate (SDS)	Sigma Aldrich, Ireland
Sodium hydroxide	Sigma Aldrich, Ireland
Tris-base	Fisher Chemicals, Ireland
Trypsin/EDTA	Sigma Aldrich, Ireland
TRI-Reagent®	Sigma Aldrich, Ireland
TaqMan® Primer Probe Assays	IDT-Integrated DNA Technologies
TaqMan® Gene Expression MasterMix	Fisher Scientific, Ireland
Xylene	Sigma Aldrich, Ireland
Dibutylphthalate polystyrene xylene (DPX)	Sigma Aldrich, Ireland

A.1. Collagen type II isolation

Materials and equipment

- Frozen porcine and marine tissues
- Sodium hydroxide
- Absolute ethanol
- Glacial acetic acid
- Sodium chloride
- Pepsin (3200-4500 units/mg protein)
- CryoMill (SPEX SamplePrep 6870, Germany).
- Sieve
- Filter mesh (100 μm in diameter).
- Centrifuge, 500 ml centrifuge bottles.
- Dialysis tubing cellulose membrane

Methods

1. Thaw porcine and marine tissues at room temperature and dissect cartilage from surrounding tissue using a surgical scalpel.
2. Incubate cartilage samples into 0.2 M NaOH solution for 12 h and wash with absolute ethanol.
3. Cut cartilage samples into small pieces, homogenise in liquid nitrogen using a CryoMill.
4. Suspend homogenised cartilage samples in 1 M acetic acid at a ratio of 1 to 1 (g/l) under stirring for 48 h at 4 °C.
5. Add pepsin at tissue to pepsin ratio of 10 to 1 (w/w) at room temperature.
6. Keep the solutions under constant stirring for 48 h at 4 °C.
7. Filter the collagen solutions with sieve and filter mesh, discard the insoluble residues.
8. Add 0.9 M NaCl to the collected collagen solution and manually gently stir the collagen solution every 2 h for three times to generate collagen precipitates.

9. After salt precipitation, collect collagen precipitates through centrifugation using 500 ml centrifuge bottles (20 min, 8,000 rpm, 4-8 °C).
10. Resuspend collagen precipitates in 1 M acetic acid at a ratio of 1.5 to 1 (g/ml) under stirring for 48 h at 4 °C and repeat salt precipitation.
11. Add minimal amount of 1 M acetic acid into collagen precipitates to obtain highly concentrated collagen solution.
12. dialyse highly concentrated collagen solution against 0.001 M acetic acid using dialysis tubing cellulose membrane.
13. Dialyse collagen solution against 0.001 M acetic acid for 48 h at 4 °C.
14. The final collagen solution was stored at 4 °C until use.

A.2. Collagen sponge fabrication and crosslinking

Materials and equipment

- 1x PBS
- 4-arm PEG Succinimidyl Glutarate, MW 10,000
- 48 well-plate
- Centrifuge
- -80 °C freezer
- Freeze-dryer

Methods

1. Dissolve collagen in 0.05 M acetic acid to make 5 mg/ml collagen solution at 4 °C (Falcon tubes can be used to prepare collagen solution).
2. Prepare crosslinking agent (4-arm PEG Succinimidyl Glutarate MW 10,000) in 1x PBS to make stock solution of 10 mM.
3. Mix collagen solution with crosslinking agent to reach the final crosslinking concentration of 1 mM.
4. Add 200 µl of non-crosslinked and crosslinked collagen solution into each well of 48 well-plate.
5. Freeze collagen solutions in -80 °C freezer for 12 h.

6. Freeze dry frozen collagen solutions in freeze-dryer for 24 h.
7. All the collagens were produced on the same day and under the same freeze-drying conditions.

A.3. Gelatin hydrogel fabrication and crosslinking

Materials and equipment

- 1x PBS
- 4arm PEG Succinimidyl Glutarate, MW 10,000
- Ace silicone O-rings (Z504165)
- Water bath
- Centrifuge

Methods

1. Dissolve gelatin products in 1x PBS at 50°C in water bath to make 100 mg/ml gelatin solution (Falcon tubes can be used to prepare gelatin solution).
2. Prepare crosslinking agent (4-arm PEG Succinimidyl Glutarate MW 10,000) in 1x PBS to make stock solution of 10 mM.
3. Mix gelatin solution with crosslinking agent to reach the final crosslinking concentration of 1 mM.
4. Centrifuge at 3,000 rpm for 20 sec to remove bubbles.
5. Add 250 µl of the crosslinked gelatin solution to each Ace silicone O-ring.
6. Incubate at 25 °C (or room temperature) for 1 hour to fabricate gelatin hydrogel.

A.4. Gelatin film fabrication and crosslinking

Materials and equipment

- 1x PBS
- 4-arm PEG Succinimidyl Glutarate, MW 10,000

- 48 well-plate
- Water bath
- Centrifuge

Methods

1. Dissolve gelatin products in 1x PBS at 50 °C in water bath to make 100 mg/ml gelatin solution (Falcon tubes can be used to prepare gelatin solution).
2. Prepare crosslinking agent (4-arm PEG Succinimidyl Glutarate MW 10,000) in 1x PBS to make stock solution of 10 mM.
3. Mix gelatin solution with crosslinking agent to reach the final crosslinking concentration of 1 mM.
4. Centrifuge at 3,000 rpm for 20 sec to remove bubbles.
5. Add 250 µl of the crosslinked gelatin solution to each well of the 48 well-plate.
6. Incubate at 25 °C (or room temperature) for 1 h.
7. Allow the liquid to evaporate overnight in a fume hood to fabricate gelatin films.

A.5. Sodium dodecyl sulphate-polyacrylamide gel electrophoresis

Materials and equipment

- 1.875 M Tris Base pH 8.8
- 1.25 M Tris-HCl pH 6.8
- 5x sample buffer
- 5x running buffer
- Glacial acetic acid
- Absolute ethanol
- Glycerol
- Bromophenol blue
- TEMED

- 30 % Acrylamide/Bis
- 100 mg/ml Ammonium Persulphate (APS)
- 10 % SDS
- Benchtop vortex
- Mini-Protean 3 electrophoresis system (Bio-Rad Laboratories, UK)

Methods

Reagents and collagen / gelatin samples preparation

1. Prepare 1.875 M Tris Base pH 8.8: Dissolve 22.70 g Tris-base in 80 ml ddH₂O, add 2 ml of concentrated HCl (37 %), leave it overnight to equilibrate and then adjust pH to 8.8 with concentrated HCl. Fill it up to 100 ml with ddH₂O. Store it at 4-8 °C.
2. Prepare 1.25 M Tris-HCl pH 6.8: Dissolve 15.14 g Tris-base in 70 ml ddH₂O, add 7 ml of concentrated HCl (37 %), leave it overnight to equilibrate and then adjust pH to 6.8 with concentrated HCl. Fill it up to 100 ml with ddH₂O. Store it at 4-8 °C.
3. Prepare 5x sample buffer: Dissolve 0.25 g SDS in 0.625 ml 1.25 M Tris-HCl, pH 6.8 and 2 ml ddH₂O. Leave it overnight for the foam to settle. Fill with glycerol to 5 ml. Add 2.5 mg bromophenol blue per 10 ml buffer.
4. Prepare 5x running buffer: Dissolve 15.1 g Tris-base, 72 g glycine and 5 g SDS in 1 L of ddH₂O. Store at 4 °C. To run the gel, 1x running buffer should be prepared by diluting 5x running buffer in ddH₂O.
5. Dissolve freeze-dried collagen samples and collagen type I (Symatase Biomateriaux, France) in 0.5 M acetic acid to make 1 mg/ml collagen solution.
6. Dissolve gelatin products and collagen type I (Symatase Biomateriaux, France) in 0.5 M acetic acid to make 10 % gelatin solutions and 1 mg/ml collagen solution.
7. Collagen / gelatin sample preparation:
 - 4 µl collagen / gelatin samples

- 4 μ l 1 M NaOH
 - 34 μ l ddH₂O
 - 18 μ l 5x sample buffer
8. Vortex the samples and centrifuge them briefly.
 9. Denature the samples at 95 °C for 5 min.
 10. Vortex the samples and centrifuge them briefly.
 11. Load the samples in Mini gel (for 10-well: 15 μ l and for 15-well: 10 μ l).

Gel preparation

1. Clean glass plates with 100 % ethanol and dry with tissue papers.
2. Prepare the separating gel according to **Table 2** below.
Note: Add the APS and the TEMED last, immediately prior to pouring the gels.
3. Vortex the gel mixture and pour it to reach about 1 cm from the top of the glass.
4. Overlay the separating gel with 10 % (vol/vol) ethanol to cut off oxidation.
5. When the separating gel mixture is polymerised (approximately 30 min), remove the ethanol.
6. Prepare the stacking gel mixture according to **Table 3** below.
Note: Add the APS and the TEMED last, immediately prior to pouring the gels.
7. Vortex the gel mixture and pour it on of the polymerised separating gel.
8. Insert the comb into the stacking gel.
Note: Avoid trapping air bubbles while inserting the comb.
9. Remove the comb after the gel is polymerised (~30 min).
10. Assemble the Mini-Protean 3 electrophoresis system, fit the gel plates on the electrode bar and fit the set into the inner chamber and clamp them.
11. Fill the upper/inner chamber with 1x running buffer.

Collagen / gelatin samples loading

1. Load an aliquot of collagen / gelatin samples (for 10-well: 15 μ l and for 15-well: 10 μ l) and standards into each well of the stacking gel.
2. Put the upper chamber on the main chamber, close the lid and run the gel.
3. Run the gel at constant voltage: 50 V until the front reaches the end of the stacking gel (~30-40 min), then 120 V until the front reaches the end of the separation gel (~1 h).
4. Remove the glass using the wonder wedge and release the gel slowly into 1x running buffer.
5. Proceed with Silver staining.

Table A.2: 5 % separating gel for 1mm thickness mini gel (Protean II Bio-Rad).

Reagents	Volume for 1 gel
30 % Acrylamide/Bis (37.5:1)	830 μ l
1.875 M Tris-HCl pH 8.8	1000 μ l
10 % SDS	50 μ l
ddH ₂ O	3070 μ l
APS (100 mg/ml)	42 μ l
TEMED	5 μ l
Total	5000 μ l

Table A.3: 3 % stacking gel for 1mm thickness mini gel (Protean II Bio-Rad).

Reagents	Volume for 1 gel
30 % Acrylamide/Bis (37.5:1)	200 μ l
1.25 M Tris-HCl pH 6.8	200 μ l
10 % SDS	33 μ l
ddH ₂ O	1550 μ l
APS (100 mg/ml)	17 μ l
TEMED	3 μ l
Total	2000 μ l

A.6. Silver staining of SDS-PAGE gels

Adapting the manufacturer instructions for the SilverQuest™ Silver Staining Kit, the method is briefly described in the following **Table 4**.

Table A.4: Silver staining method step by step. Volumes are indicated per gel.

Step	Reagent	Incubation time
Fix	Ethanol 10 ml Acetic acid 2.5 ml Water up to 25 ml	20 mins
Wash	Ethanol 7.5 ml Water up to 25 ml	10 mins
Sensitize	Ethanol 7.5 ml Sensitizer 2.5 ml Water up to 25 ml	10 mins
First wash	Ethanol 7.5 ml Water up to 25 ml	10 mins
Second wash	Water 25 ml	10 mins
Stain	Stainer 0.25 ml Water up to 25 ml	15 mins
Wash	Water 25 ml	1 min

Step	Reagent	Incubation time
Develop	Developer 2.5 ml Developer enhancer 1 drop Water up to 25 ml	4-8 mins
Stop	Stopper 10 ml (add directly to developing solution)	10 mins
Wash	Water 25 ml	10 mins

A.7. TNBSA assay

Materials and equipment

- Glycine
- Glacial acetic acid
- Sodium hydroxide
- Hydrochloric acid
- Sodium dodecyl sulphate (SDS)
- Sodium bicarbonate
- 2,4,6-Trinitrobenzene sulfonic acid (TNBSA)
- 96 well-plate
- Benchtop vortex
- Block heater (optional)

Methods

1. Place ~ 3 mg collagen sponges / ~ 500 mg gelatin hydrogels in 1.5 ml microtubes and add 500 μ l of 0.1 M sodium bicarbonate solution.
2. Prepare standard curve solutions of 0, 0.005, 0.01, 0.02, 0.03, 0.04 and 0.05 mg/ml glycine in 0.1 M sodium bicarbonate solution.
3. Add 500 μ l of each standard glycine curve solution to a 1.5 ml microtube.
4. Add 250 μ l of 0.01 % TNBSA to each sample and standard curve point solution. Mix the samples well using benchtop vortex.
5. Incubate the samples and standard curve point solution in a 37 °C incubator for 2 h.
6. Add 250 μ l of 10 % SDS and 125 μ l of 1 M hydrochloric acid to stop the reaction.
Note: (Optional) If the samples are not completely dissolved at this stage, hydrolyse the samples by incubating them in a block heater at 95 °C for 15 min.
7. Transfer 100 μ l of sample solution to each well of 96-well plate and measure the absorbance at 335 nm.

A.8. Collagenase

Materials and equipment

- 0.1 M Tris-HCl pH 7.4
- 50 mM CaCl₂
- 50 U/ml bacterial collagenase type II; MMP-8

Methods

1. Place ~ 1.0-1.5 mg collagen sponges / ~ 500 mg gelatin hydrogels in 1.5 ml microtubes.
2. Prepare the buffer: 0.1 M Tris-HCl pH 7.4 + 50 mM CaCl₂.
3. Incubate the samples in 500 μ l of 0.1 M Tris-HCl pH 7.4 / 50 mM CaCl₂ buffer for 2 h.
4. Prepare a 50 U/ml collagenase solution in the buffer.

5. Add 500 μ l of reconstituted collagenase solution into the samples.
6. Incubate the samples with reconstituted collagenase solution at 37 °C for different time points.
7. Centrifuge at 10,000 rpm for 5 min.
8. Remove the supernatants, the remaining collagen sponges were freeze-dried and weighed and the remaining gelatin hydrogels were weighed.
9. The degree of enzymatic degradation was quantified using the weight difference approach $[(W_o - W_t) / W_o] \times 100$, where W_o is the original weight and W_t is the remaining weight.

A.9. Scanning electron microscopy (SEM)

Materials and equipment

- Carbon disk
- Hitachi S-4700 scanning electron microscope
- Emitech K-550X sputtering system

Methods

1. Collagen sponges were sectioned in the dry state to expose the inner porous structure and mounted onto a carbon disk.
2. Place collagen sample and carbon disk into the gold sputtering system.
3. Gold coating using Emitech K-550X sputtering system for 2 min.
4. Put the sample stage into sample chamber and turn on the pumps.
5. Capture the SEM images of collagen sponges.
6. SEM images were analysed using ImageJ software.

A.10. Denaturation temperature assessment

Materials and equipment

- 1x PBS
- Filter paper

- Differential scanning calorimeter (DSC, DSC-60, Shimadzu, Japan)

Methods

1. Hydrate collagen sponges in 1x PBS for 12 h at 4 °C.
2. After hydration, remove excess PBS by blotting with filter paper.
3. Place hydrated collagen sponges (10-15 mg for each sample) into aluminum crucibles, spread it out at the bottom of the crucible and record its weight.
4. Place the lid on the aluminium crucible and seal it.
5. Use an empty aluminium crucible as a reference crucible.
6. Carry out a constant temperature ramp at 10 °C/min with a temperature range of 20-100 °C.
7. Record the peak temperature as the denaturation temperature.

A.11. Biomechanical assessment – Compression test

Materials and equipment

- 10 N loading cell
- 100 N loading cell
- Material testing machine (Z2.5, Zwick/Roell, Germany)

Methods

1. Measure the height and diameter of collagen sponges / gelatin hydrogels.
2. Place collagen sponges between two 10 N loading cells.
Note: Place gelatin hydrogels between two 100 N loading cells.
3. Perform uniaxial constant loading on the samples and compress until 70 % deformation was reached, with a compression rate of 10 mm/min.
4. Force, strain and elastic modulus were determined by plotting stress versus strain curves.

A.12. Cell thawing and expansion, freezing (human adipose derived stem cells)

Note: The entire protocol should be performed in aseptic conditions. All materials should be sprayed with 70 % ethanol before putting into the biological safety cabinet.

Materials and equipment

- Alpha – Minimum Essential Medium with GlutaMax™ (alpha-MEM)
- Fetal bovine serum (FBS)
- Penicillin streptomycin
- Trypsin/EDTA
- Hank's balanced salt solution (HBSS)
- Neubauer chamber
- Dimethyl sulfoxide (DMSO)
- Mr. Frosty™ freezing container
- Liquid nitrogen container
- Cell culture flasks

Cell thawing and expansion

1. Prepare cell expansion medium: alpha-MEM with GlutaMax™; 10 % FBS; 1 % penicillin streptomycin.
2. Remove vials from the liquid nitrogen container.
3. Thaw the vial by gentle agitation in water bath at 37 °C. Keep the O-ring and cap out of the water to reduce potential contamination.
4. Transfer cell suspension to culture flask of appropriate size and add pre-warmed cell expansion medium.
5. Change medium every 2-3 days and monitor cell proliferation with a phase contrast microscope.
6. When cells cover more than 80 % of the culture flask, remove culture medium, wash cell layer with HBSS and add 5 ml of trypsin/EDTA.

7. Incubate cells with trypsin/EDTA at 37 °C for 5 min until cells start detaching.
8. Add 5 ml of expansion medium to neutralise the action of trypsin/EDTA and transfer cell suspension into a falcon tube and centrifuge at 1200 rpm for 5 min.
9. Discard the supernatant and resuspend cells in the medium.
10. Count cells using Neubauer chamber and seed them at 5000 cells/cm² in desired amount of cell expansion medium.
11. Incubate the cells in an incubator at 37 °C, 5% CO₂ and 95 % relative humidity.

Cell freezing

1. Aspirate culture medium and wash cell layer with HBSS.
2. Add trypsin/EDTA and incubate at 37 °C for 5 min.
3. Add expansion medium to neutralise the action of trypsin, collect cell suspension into a tube and centrifuge at 1200 rpm for 5 min.
4. Resuspend cells in 1 ml of expansion medium and count cells using a Neubauer chamber.
5. Resuspend cells in desired amount of freezing medium (90 % expansion medium with 10 % dimethyl sulfoxide) to have 1 million cell per ml of medium.
6. Transfer 1 ml of cell suspension per cryogenic vial.
7. Place vials into a Mr. Frosty™ freezing container and freeze overnight at -80 °C.
8. Move the vials to liquid nitrogen for long term storage.

A.13. Cell seeding and differentiation in collagen sponges (human adipose derived stem cells)

Materials and equipment

- Dulbecco's Modified Eagle's Medium (DMEM) – high glucose
- Dexamethasone

- Bovine serum albumin
- Transforming growth factor beta 3 (TGF- β 3)
- L-ascorbic acid 2-phosphate
- ITS liquid media supplement
- 48 well-plate

Methods

1. Prepare chondrogenic differentiation medium: DMEM – high glucose; 100 nM dexamethasone; 50 mg/ml bovine serum albumin; 10 ng/ml transforming growth factor beta 3 (TGF- β 3); 50 μ g/ml L-ascorbic acid 2-phosphate; 5 ml ITS liquid media supplement.
2. At passages 5, resuspend cells in fresh expansion medium.
3. Seed 100 μ l of cell suspension to each collagen sponge at a density of 200,000 cells/sponge and culture collagen sponges in 48 well-plate.
4. Culture cells on tissue culture plastic (TCP) at 50,000 cells/cm² as a negative control.
5. Incubate the collagen sponges containing cells at 37°C, 5% CO₂ and 95 % relative humidity for 2 h for cells attachment.
6. Add fresh expansion medium into collagen sponges and incubate overnight.
7. Change expansion medium into chondrogenic medium the next day.
8. Culture cells for 7, 14 and 21 days at 37°C, 5% CO₂ and 95 % relative humidity and change medium every 2 days.

A.14. Cell expansion and differentiation (human THP-1 monocytes)

Materials and equipment

- Roswell Park Memorial Institute (RPMI) 1640 medium
- FBS
- Penicillin/streptomycin
- Phorbol 12-myristate 13-acetate (PMA)

- Dimethyl sulfoxide (DMSO)

Cell expansion

1. Prepare cell expansion medium: RPMI 1640 medium; 10 % FBS; 1 % penicillin streptomycin.
2. Culture human THP-1 monocytes at 300,000 cells/ml.
3. Top up with fresh media every second day or when cell concentration reaches 800,000 cells/ml (Do not allow the cell concentration to exceed 1,000,000 cells/ml).

Cell differentiation

1. Use THP-1 monocytes when their density reaches 800,000-1,000,000 cells/ml.
2. Dilute PMA in DMSO at 5µg/ml.
3. Add 100 µl PMA for each 50 ml supplemented RPMI 1640 medium to prepare differentiation medium.
4. Resuspend the cells in differentiation medium.
5. Adjust the cell density at 100,000 cells/ml.
6. Seed cells on gelatin films and TCP at cell density 26,000 cells/cm².
7. Incubate cells at 37°C, 5% CO₂ and 95 % relative humidity for 6 h to enable cell attachment.
8. Check the differentiation by observation at the microscope. If there are floating cells (undifferentiated cells), incubate for 6 h more.
9. Remove the medium and replace it with fresh RPMI 1640 medium.
10. Incubate the cells at 37 °C, 5 % CO₂ and 95 % relative humidity for 1 and 2 days.

A.15. Cell metabolic activity assay using alamarBlue™

Materials

- alamarBlue®
- HBSS
- 96-well plate

Methods

1. Prepare a 10 % alamarBlue® solution in HBSS.
2. Remove culture medium from collagen sponges / gelatin films and wash three times with HBSS.
3. Add 0.4 ml of alamarBlue® in each well and a negative control of 10% alamarBlue® alone.
4. To obtain the background absorbance, add HBSS to empty wells.
5. Incubate for 3 h at 37°C, 5 % CO₂ and 95 % relative humidity.
6. Transfer 200 µl of each well in a clear 96-well plate.
7. Measure the absorbance at the wavelength of 570 nm and 600 nm.
8. Subtract the absorbance value of HBSS to the absorbance value of alamarBlue® alone to obtain the absorbance of alamarBlue®. For 570 nm this value is called absorbance of the oxidised form at lower wavelength (AOLW) and for 600 nm it is called absorbance of the oxidised form at higher wavelength (AOHW).
9. Calculate correlation factor: $RO = AOLW / AOHW$
10. Calculate the percentage of alamarBlue® reduced (AR) by the cells using the following equation: $AR = AOLW - (AOHW * Ro) * 100$.

A.16. Cell proliferation assay using Quant-it™ Picogreen®

Materials and equipment

- HBSS
- Quant-it™ PicoGreen® dsDNA Reagent and Kits
- 96-well plate

Methods

1. Remove culture medium from collagen sponges / gelatin films and wash three times with HBSS.
 2. Add 200 μ l of DNase free water into each well.
 3. Repeatedly freeze-thaw cells at -80 °C at least three times to lyse the cells.
 4. Prepare a 1X TE buffer from the 20X stock solution.
 5. Prepare PicoGreen[®] working solution: 9ml 1X TE buffer; 45 μ l concentrated PicoGreen.
- Note:** If more reactions are required, scale up appropriately.
6. Add 100 μ l PicoGreen[®] working solution to the collagen sponges / gelatin films and incubate at room temperature for 5-10 min, protect the reaction from light.
 7. Prepare a standard curve of DNA solution (0, 5, 10, 25, 50, 100, 500 and 1,000 ng/ml) using DNase free water as described in the following **Table 5**.
 8. Transfer 100 μ l of each sample and DNA standard curve solution into a 96-well plate.
 9. Measure the fluorescent at excitation and emission wavelengths of 480 nm and 520 nm.

Table A.5: Detailed preparation of the DNA standard curve.

Final DNA concentration (ng/ml)	Water volume (μ l)	Volume of 2 μ g/ml DNA stock (μ l)	Volume of 50 ng/ml DNA stock (μ l)
1000	200	200	0
500	300	100	0
100	380	20	0
50	0	0	400
25	200	0	200
10	320	0	80
5	360	0	40
0	400	0	0

A.17. Cell viability assay using Live/Dead staining

Materials

- HBSS
- Calcein AM
- Ethidium homodimer-1

Methods

1. Prepare staining solution by diluting calcein AM to 4 μ M and ethidium homodimer-1 to 2 μ M in HBSS.
2. Remove culture medium from collagen sponges / gelatin films and wash three times with HBSS.
3. Add staining solution to the samples (enough volume to cover the sample completely).
4. Incubate at 37 °C, 5 % CO₂ and 95 % relative humidity for 30 min and protect the reaction from light.
5. Remove staining solution and wash cells with HBSS to remove excess dye.
6. Stained samples are visualised using a confocal laser microscope (for collagen sponges) / an inverted fluorescence microscope (for gelatin films):
 - Calcein AM: fluorescein isothiocyanate (FITC) filter.
 - Ethidium homodimer-1: texas red filter.

A.18. Fixation and embedding of collagen sponges

Materials and equipment

- 1x PBS
- Paraformaldehyde (PFA)
- Sucrose-PBS
- Optimal cutting temperature compound (OCT)
- Liquid nitrogen
- Cryostat

- Adhesion glass slide

Methods

1. Remove culture medium from the collagen sponges and wash three times with 1x PBS.
2. Fix collagen sponges in 4 % PFA for 30 min at 4 °C.
3. Wash collagen sponges once with 1x PBS at 4 °C.
4. Cryoprotection (for cryo-embedding):
 - First step: Incubate collagen sponges in 15 % sucrose-PBS at 4 °C overnight.
 - Second step: Incubate collagen sponges in 30 % sucrose-PBS at 4 °C overnight.
5. Embed collagen sponges in fresh OCT and snap freeze with liquid nitrogen and store at -80 °C.
6. Cryosection collagen sponges using a Cryostat at 5-10 µm in thickness and collect on adhesion glass slides.
7. Let slides air dry at room temperature for at least 1 h.
8. Store slides at -20 °C.

Note: Avoid freeze-thaw cycles during the storage of slides.

A.19. Alcian blue staining

Materials and equipment

- Glacial acetic acid
- 1x PBS
- Alcian blue solution (pH 2.5)
- Nuclear fast red solution
- Graded ethanol solution (70%, 90%, 100% I, 100% II)
- Xylene
- Dibutylphthalate polystyrene xylene (DPX)

Methods

1. Take collagen sponges cryosection slides out from -20 °C freezer and let them dry at room temperature for 10-20 min.
2. Rehydrate the slides in 1x PBS for 5 min.
3. Incubate the slides in 1 % acetic acid for 3 min.
4. Stain with Alcian blue solution pH 2.5 for 30 min.
5. Stop staining reaction in 1 % acetic acid.
6. Rinse slides briefly in distilled water.
7. Counterstain with 0.1 % nuclear fast red solution for 5 min.
8. Rinse slides briefly in distilled water.
9. Dehydrate rapidly in grades of 70%, 90%, 100% I, 100% II ethanol, each for 30 sec to 1 min.
10. Clean the slides with xylene twice until mounting.
11. Mount the slides with DPX.
Note: Process Step 10 and 11 in fume hood to avoid the toxicity of xylene and DPX.
12. Air dry the slides in fume hood for at least 12 h.
13. Capture images under a light microscope.

A.20. Haematoxylin & Eosin staining

Materials and equipment

- 1x PBS
- Mayer's Haematoxylin
- Eosin Y solution (50 % of ethanol and 0.15 % of eosin)
- 0.5 % HCl-ethanol
- 1 % acetic acid
- Graded ethanol solution (70%, 90%, 100% I, 100% II)
- Xylene

- Dibutylphthalate polystyrene xylene (DPX)

Methods

1. Take collagen sponges cryosection slides out from -20 °C freezer and let them dry at room temperature for 10-20 min.
2. Rehydrate the slides in 1x PBS for 5 min.
3. Stain with Mayer's Haematoxylin for 5 min.
4. wash slides in 0.5 % HCl-ethanol for 1-3 sec to destain the connective tissue.
5. Stop reaction in 1 % acetic acid.
6. Bluing under running tap water for 10 min (colour change: red to blue).
7. Counterstain with eosin Y solution for 30 sec.
8. Stop the reaction in 1 % acetic acid.
9. Dehydrate rapidly in grades of 70%, 90%, 100% I, 100% II ethanol, each for 30 sec to 1 min.
10. Clean the slides with xylene twice until mounting.
11. Mount the slides with DPX.
Note: Process Step 10 and 11 in fume hood to avoid the toxicity of xylene and DPX.
12. Air dry the slides in fume hood for at least 12 h.
13. Capture images under a light microscope.

A.21. Sulphated glycosaminoglycan (sGAG) assessment

Materials and equipment

- 1x PBS
- Papain extraction reagent
- Blyscan™ sGAG assay kit
- 96-well plate

Methods

1. Remove the medium and wash collagen sponges three times with 1x PBS.
2. Transfer collagen sponges to 1.5 ml microtubes.
3. Add 200 μ l papain extraction reagent to each sample.
4. Incubate for 3 h at 65 °C with occasional mixing.
5. Prepare Glycosaminoglycan standard curve using aliquots containing 1, 2, 3, 4 and 5 μ g of the reference standard. The standards and the reagent blank (0 μ g) are used to produce a calibration curve.
6. Add 1 ml Blyscan dye reagent to each sample and incubate under gently shaking for 30 min.
Note: During this time period, a sulphated glycosaminoglycan-dye complex will form and precipitate out from the soluble unbound dye.
7. Centrifuge the samples at 17,000 g for 10 min.
8. Carefully drain the unbound dye solution. Any remaining droplets can be removed from the tubes by gently tapping the inverted tube on a paper tissue.
Note: Do not attempt to physically remove any fluid that is in close contact to the deposit.
9. Add 0.5 ml dissociation reagent to the remaining sGAG droplets to release the bound dye into the solution.
10. When all the bound dye has been dissolved, centrifuge at 12,000 rpm for 5 min to remove foam.
11. Transfer 200 μ l of each sample to a 96-well plate and measure the absorbance at 656 nm.

A.22. RNA isolation

Materials and equipment

- 75% ethanol
- Isopropanol (2-propanol, isopropyl alcohol)
- TRI-Reagent®
- Chloroform
- Glycoblue

- Ambion® RNA Storage Solution
- RiboSafe RNase inhibitor
- NanoDrop 2000c Spectrophotometer

Methods

Note: Store 75% ethanol, isopropanol and Ambion® RNA storage solution on ice.

1. Collagen sponges were homogenised using surgical scalpels.
2. Add TRI-Reagent® to collagen samples.
3. Incubate collagen samples at room temperature for 5 min under vortex to allow the complete dissociation of nucleoprotein complexes.
4. Add 100 µl of chloroform per 1 ml TRI-Reagent® used in Step 2, shake vigorously for at least 15 sec and incubate for 5 min at room temperature.
5. Centrifuge at 12,000 g for 15 min at 4°C to generate 3 phases: upper, colourless aqueous phase; white interphase; lower, red organic phase.
6. Transfer the colourless aqueous phase solution to a new RNase-free tube without disturbing the interphase.

Note: Repeat Steps 4, 5, 6 to get purer RNA.

7. Add 1 (actual) volume of Isopropanol (2-propanol, isopropyl alcohol) into colourless aqueous phase solution and add 1 µl Glycoblue, mix thoroughly and incubate for 30 min at -20°C.
8. Centrifuge at 12,000 g for 30 min at 4°C. The RNA will appear as a blue pellet.
9. Carefully discard the supernatant without destroying the RNA pellet.
10. Wash the RNA pellet by adding 1 ml of 75 % ethanol for every 1 ml of TRI-Reagent® used in Step 2.

Note: Air dry the RNA pellet for no longer than 5 min to avoid the decrease in the solubility of pellet.

11. Resuspend the pellet in the Ambion® RNA storage solution, supplemented with 0.5 µl RiboSafe RNase Inhibitor.
12. Measure RNA integrity with NanoDrop 2000c Spectrophotometer.

Note: OD 260/280 should be between 1.9 ~ 2.0.

13. Store RNA samples at -80 °C for long term storage. Or reverse-transcribe RNA into cDNA immediately.

Note: Avoid freeze-thaw cycles of RNA.

A.23. cDNA synthesis

Materials and equipment

- iScript™ reverse transcription supermix
- Nuclease-free water
- Thermal cycler

Methods

Note: 1 µg of total RNA is suggested for cDNA synthesis.

1. Prepare cDNA synthesis reaction as described in the following **Table 6**.
2. Mix cDNA synthesis reactions thoroughly by pipetting up and down several times.
3. Incubate the complete reaction mix in a thermal cycler using the following steps:
 - Priming: 5 min at 25 °C.
 - Reverse transcription: 20 min at 46 °C.
 - RT inactivation: 1 min at 95 °C.
4. Store cDNA samples at -20 °C for long term storage.

Table A.6: Reaction setup for a single cDNA synthesis reaction.

Component	Volume (µl)
iScript reverse transcription supermix	4

RNA sample (1 µg total RNA)	Variable (volume calculated based on RNA concentration)
Nuclease-free water	Variable (volume can be adjusted based on RNA volume)
Total volume	20

A.24. Quantitative real-time PCR

Materials and equipment

- cDNA (1-5 ng/µl): stored at -20 °C, keep on ice, vortex and spin down before use.
- TaqMan® Primer Probe Assays: stored at -20 °C, thaw on ice, protect from light and spin down before use.
- TaqMan® Gene Expression MasterMix, stored at 4 °C.
- Nuclease-free water
- DNAzap
- 10 % bleach
- 70 % ethanol
- 96-well PCR plate
- Adhesive films

Methods

Note: Clean all surfaces with 10% bleach, DNAzap and 70% ethanol. Keep all reagents clean.

1. Thaw TaqMan® Primer Prober Assays on ice and protect from light.
2. Prepare TaqMan® Gene Expression MasterMasterMix for target genes as described in the following **Table 7**.
3. Place the 96-well PCR plate on ice and put 1 µl of cDNA in each well.

4. Add the respective TaqMan® Gene Expression MasterMasterMix to each well.
5. Seal the plate properly with the adhesive film.
6. Centrifuge the plate briefly to remove the air bubble.
7. Run the qPCR using Applied Biosystems (Ireland) StepOnePlus™ Real Time PCR System.
8. Default amplification conditions: 50 °C for 2 min, 95 °C for 10 min, followed by 40 cycles of 95 °C for 15 sec and 60 °C for 1 min.

Table A.7: TaqMan® Gene Expression MasterMasterMix setup for a 15 μ l qPCR run

Component	Volume (μ l)
TaqMan® Gene Expression MasterMix	7.5
TaqMan® Primer Probe Assay	0.75
Nuclease free water	5.75
cDNA	1
Total volume	15

Note: cDNA is not added to the TaqMan® Gene Expression MasterMasterMix. cDNA is added to each well of 96-well PCR plate.

B. Research outputs

B.1. Published manuscripts

1. **Wu, Z.**, Korntner, S. H., Olijve, J., Mullen, A. M., & Zeugolis, D. I. (2021). The Influence of Bloom Index, Endotoxin Levels and Polyethylene Glycol Succinimidyl Glutarate Crosslinking on the Physicochemical and Biological Properties of Gelatin Biomaterials. *Biomolecules*, 11(7), 1003.
2. **Wu, Z.**, Korntner, S. H., Mullen, A. M., & Zeugolis, D. I. (2021). In the quest of the optimal chondrichthyan for the development of collagen sponges for articular cartilage. *Journal of Science: Advanced Materials and Devices*.
3. **Wu, Z.**, Korntner, S. H., Mullen, A. M., Skoufos, I., Tzora, A., & Zeugolis, D. I. (2021). In the quest of the optimal tissue source (porcine male and female articular, tracheal and auricular cartilage) for the development of collagen sponges for articular cartilage. *Biomedical Engineering Advances*, 1, 100002.
4. Capella-Monsonís, H., Coentro, J. Q., Graceffa, V., **Wu, Z.**, & Zeugolis, D. I. (2018). An experimental toolbox for characterization of mammalian collagen type I in biological specimens. *Nature protocols*, 13(3), 507.

5. Soroushanova, A., Delgado, L. M., **Wu, Z.**, Shologu, N., Kshirsagar, A., Raghunath, R., ... & Zeugolis, D. I. (2019). The collagen suprafamily: from biosynthesis to advanced biomaterial development. *Advanced materials*, 31(1), 1801651.

B.2. Submitted manuscripts

1. **Z Wu**, SH Korntner, AM Mullen, DI Zeugolis. Collagen type II: From biosynthesis to advanced biomaterials for cartilage engineering. Submitted to *Biomaterials and Biosystems*

B.3. Book chapters

1. Coentro, J. Q., Capella-Monsonís, H., Graceffa, V., **Wu, Z.**, Mullen, A. M., Raghunath, M., & Zeugolis, D. I. (2017). Collagen quantification in tissue specimens. In *Fibrosis* (pp. 341-350). Humana Press, New York, NY.

B.4. Conferences podium presentations

1. **Wu, Z.**, Korntner, S. H., Mullen, A. M., Skoufos, I., Tzora, A., & Zeugolis, D. I. Assessing the properties of collagen type II scaffolds as a function of species, tissue and gender. European Orthopaedic Research Society, EORS 2018, 25.09.-28.09.2018, Galway, Ireland.
2. **Wu, Z.**, Korntner, S. H., Mullen, A. M., Skoufos, I., Tzora, A., & Zeugolis, D. I. Biophysical, biochemical and biological properties of pepsin soluble type II collagen from mammalian and marine tissue sources for cartilage regeneration. European Federation of National Associations of Orthopaedics and Traumatology, EFORT 2018, 30.05.-01.06.2018, Barcelona, Spain.
3. **Wu, Z.**, Korntner, S. H., Mullen, A. M., Skoufos, I., Tzora, A., & Zeugolis, D. I. Biophysical, biochemical and biological properties of pepsin soluble type II collagen from mammalian and marine tissue sources for cartilage

regeneration. Future Investigators of Regenerative Medicine, FIRM 2017, 25.09.-28.09.2017, Girona, Spain.

4. **Wu, Z.**, Korntner, S. H., Mullen, A. M., Skoufos, I., Tzora, A., & Zeugolis, D. I. Isolation and characterization of pepsin soluble type II collagen from porcine cartilage and cartilaginous fishes for cartilage repair. European Orthopaedic Research Society, EORS 2017, 13.09.-15.09.2017, Munich, Germany
5. **Wu, Z.**, Korntner, S. H., Mullen, A. M., Skoufos, I., Tzora, A., & Zeugolis, D. I. Isolation and characterization of pepsin soluble type II collagen from porcine cartilage and cartilaginous fishes for cartilage repair. Bioengineering in Ireland, BINI 2016, 22.01.-23.01.2016, Galway, Ireland

B.5. Conferences poster presentations

1. **Wu, Z.**, Korntner, S. H., Mullen, A. M., Skoufos, I., Tzora, A., & Zeugolis, D. I. Biophysical, biochemical and biological properties of pepsin soluble type II collagen from mammalian and marine tissue sources for cartilage regeneration. Matrix Biology Ireland, MBI 2017, 30.11.-01.12.2017, Dublin, Ireland.
2. **Wu, Z.**, Korntner, S. H., Mullen, A. M., Skoufos, I., Tzora, A., & Zeugolis, D. I. Isolation and characterization of pepsin soluble type II collagen from porcine cartilage and cartilaginous fishes for cartilage repair. TERMIS European Chapter Meeting 2017, 26.06.-30.06.2017, Davos, Switzerland.
3. **Wu, Z.**, Korntner, S. H., Mullen, A. M., Skoufos, I., Tzora, A., & Zeugolis, D. I. Isolation and characterization of pepsin soluble type II collagen from porcine cartilage and cartilaginous fishes for cartilage repair. Matrix Biology Ireland, MBI 2016, 16.11.-18.11.2016, Galway, Ireland.
4. **Wu, Z.**, Korntner, S. H., Mullen, A. M., Skoufos, I., Tzora, A., & Zeugolis, D. I. Isolation and characterization of pepsin soluble type II collagen from porcine cartilage and cartilaginous fishes for cartilage repair. SFI-ISCA

Ireland-Japan Biomaterials & Tissue Engineering Meeting, 22.06.-23.06.2016, Galway, Ireland.

5. **Wu, Z.**, Korntner, S. H., Mullen, A. M., Skoufos, I., Tzora, A., & Zeugolis, D. I. Isolation and characterization of pepsin soluble type II collagen from porcine cartilage and cartilaginous fishes for cartilage repair. World Biomaterials Congress, WBC 2016, 17.05.-22.05.2016, Montreal, Canada.
6. **Wu, Z.**, Korntner, S. H., Mullen, A. M., Skoufos, I., Tzora, A., & Zeugolis, D. I. Isolation and characterization of pepsin soluble type II collagen from porcine cartilage and cartilaginous fishes for cartilage repair. European materials research society 2016 spring, 02.05.-06.05.2016, Lille, France.